3. PHYSICS AND CHEMISTRY OF PARTICULATE MATTER

3.1 INTRODUCTION

3.1.1 Overview

Atmospheric particles originate from a variety of sources and possess a range of morphological, chemical, physical, and thermodynamic properties. Examples include combustion-generated particles such as diesel soot or fly ash, photochemically produced particles such as those found in urban haze, salt particles formed from sea spray, and soil-like particles from resuspended dust. Some particles are liquid, some are solid; others contain a solid core surrounded by liquid. Atmospheric particles contain inorganic ions and elements, elemental carbon, organic compounds, and crustal compounds. Some atmospheric particles are hygroscopic and contain particle-bound water. The organic fraction is especially complex, containing hundreds of organic compounds.

Particle diameters span more than four orders of magnitude, from a few nanometers to one hundred micrometers. Combustion-generated particles, such as those from power generation, from automobiles, and in tobacco smoke, can be as small as 0.003 µm and as large as 1 µm. Particles produced in the atmosphere by photochemical processes range in diameter from 0.003 to 2 µm. Fly ash produced by coal combustion ranges from 0.1 to 50 µm or more. Wind-blown dust, pollens, plant fragments, and cement dusts are generally above 2 µm in diameter. Particles as small as a few nanometers (Covert et al., 1992; Clarke, 1992) and as large as 100 µm have been measured in the atmosphere (Lin et al., 1993).

Particles are ubiquitous in the atmosphere. The lowest concentrations are found in background marine environments, where particle number concentrations range from 100/cm^3 to 400/cm^3. In background continental environments, particle concentrations vary from 100/cm^3 to 5,000/cm^3; while in urban areas of the United States concentrations may be as high as 4,000,000/cm^3 (Willeke and Whitby, 1975; Whitby and Sverdrup, 1980). Particles account for a mass of a few µg/m^3 near the surface over dry continental areas to several hundred µg/m^3 in polluted urban areas.

The composition and behavior of airborne particles are fundamentally linked with those of the surrounding gas. Aerosol is defined as a suspension of solid or liquid particles in air and includes both the particles and all vapor or gas phase components of air. However, the term aerosol is often used to refer to the suspended particles only. Particles may be solid or liquid or a mixture of both phases. Particulate is an adjective and should only be used as a modifier, as in particulate matter.

Particulate material can be primary or secondary. Primary particles are composed of material emitted directly into the atmosphere. This includes material emitted in particulate form such as wind-blown dust, sea salt, road dust, mechanically generated particles and combustion-generated particles such as fly ash and soot. It also includes particles formed from the condensation of high temperature vapors such as those formed during combustion. The concentration of primary particles depends on their emission rate, transport and dispersion, and removal rate from the atmosphere.

Secondary particles form from condensable vapors formed by chemical reaction involving gas-phase precursors or by other processes involving chemical reactions of free, adsorbed, or dissolved gases. Secondary formation processes can result in either the formation of new particles (Wiedensohler et al., 1994; Covert et al., 1992; Clarke et al., 1991, 1993; Frick and Hoppel, 1993; Hoppel et al., 1994; Weber et al., 1995) or the addition of particulate material to preexisting particles (Andreae et al., 1986; Wall et al., 1988; Wu and Okada, 1994). Most atmospheric sulfate particles are formed from atmospheric oxidation of sulfur dioxide. Atmospheric nitrate is also essentially secondary. Oxides of nitrogen react in the atmosphere to form nitric acid vapor which in turn may react with ammonia gas to form particulate ammonium nitrate. Nitric acid may also react with particles containing sodium chloride or calcium carbonate, releasing hydrochloric acid or carbon dioxide, and forming sodium nitrate or calcium nitrate which remains in the particle. A portion of the organic aerosol is also attributed to secondary processes (Hildemann et al., 1994a,b; Turpin and Huntzicker, 1991; Mylonas et al., 1991; Pickle et al., 1990; Gray et al., 1986). Secondary aerosol formation can depend on concentrations of other gaseous reactive species such as ozone, hydroxyl radical, or hydrogen peroxide; atmospheric conditions including solar radiation and relative humidity; and the interactions of precursors and preexisting particles within cloud or fog droplets (Meng and Seinfeld, 1994; McMurry

and Wilson, 1983; Hoppel and Frick, 1990). As a result, it is considerably more difficult to relate ambient concentrations of secondary species to sources of precursor emissions than it is to identify the sources of primary particles.

Airborne particulate matter can be anthropogenic or natural in origin. Both anthropogenic and natural particulate material can occur from either primary or secondary processes. Anthropogenic refers to particulate matter which is directly emitted, or formed from precursors which are emitted, as a result of human activity. Primary anthropogenic sources include fossil fuel combustion, fireplace emissions, and road dust. Secondary anthropogenic particulate material can be generated photochemically from anthropogenic SO_2, NO_x, or organic gases. Primary natural sources include wind blown dust from soil undisturbed by man, sea-salt, natural forest fires and biogenic sources such as pollen, mold spores, leaf waxes and fragments from plants (Simoneit and Mazurek, 1982). In addition, plants emit gaseous species such as terpenes (Lamb et al., 1987). Terpenes are photochemically reactive. In the presence of ozone or hydroxyl radicals they react to form secondary organic particles (Kamens et al., 1981; Pandis et al., 1991, 1993).

Volatilization and sorption processes also affect concentrations and compositions of airborne particles. Some aerosol constituents are semivolatile and exist in both gas and particle phases. Their gas-particle distribution depends on atmospheric conditions such as temperature, the concentrations of other aerosol species including water vapor, and the vapor pressure of the constituent. Some inorganic compounds such as ammonium nitrate (Stelson and Seinfeld, 1982a,b; Bassett and Seinfeld, 1983, 1984) and organic compounds, including many polycyclic aromatic hydrocarbons (Yamasaki et al., 1982; Ligocki and Pankow, 1989; Pankow, 1987, 1994a,b), are semivolatile. Diurnal temperature fluctuations can cause substantial changes in the particle-phase concentrations of semivolatile constituents as a result of gas-particle redistribution. Evidence exists suggesting that this volatilization-sorption cycle results in the redistribution of semivolatile material among particles of differing origins (Venkataraman and Hildemann, 1994).

A complete description of the atmospheric aerosol would include an accounting of the chemical composition, morphology, and size of each particle and the relative abundance of each particle type as a function of particle size (Friedlander, 1970). However, most often the physical and chemical characteristics of particles are measured separately. Number size

distributions are often determined by physical means, such as electrical mobility or light-scattering. Chemical composition is determined by analysis of collected samples. The mass size distribution and the average chemical composition of the aerosol as a function of size can be determined by collection of size-segregated samples (Countess et al., 1980; Hering and Friedlander, 1982; John et al., 1990; Sloane et al., 1991). Recent developments in single particle analysis techniques coupled with multivariate classification methods (Van Grieken and Xhoffer, 1992; Germani and Buseck, 1991; Mansoori et al., 1994) are bringing the description envisioned by Friedlander closer to reality. This introductory section describes some of the measurements that have been made on atmospheric particles, and the insights thus provided on the nature, origins, and atmospheric processes that affect particle composition.

3.1.2 Atmospheric Aerosol Size Distributions

Size is one of the most important parameters in determining the properties, effects and fate of atmospheric particles. The atmospheric deposition rates of particles, and therefore, their residence time in the atmosphere, are a strong function of particle size. Size also influences deposition patterns of particles within the lung. Light scattering is strongly dependent on particle size. Particle size distributions, therefore, have a strong influence on atmospheric visibility and through their effect on radiative balance on climate.

Atmospheric size distributions for averaged continental background, urban-influenced background, averaged urban, and freeway-influenced urban aerosols are shown in Figures 3-1. (Whitby and Sverdrup, 1980). Figure 3-1 describes the number of particles as a function of particle diameter. For the same data, the particle volume distribution is shown in Figures 3-2. Note that for the particle number distribution both the diameter and the number of particles are shown on a logarithmic scale. For the volume distribution, the volume is shown on an arithmetic scale and the distribution is plotted such that the volume of particles in a specified size range is proportional to the corresponding area under the curve. These distributions show that most of the particles are quite small, below 0.1 μm, while most of the particle volume (and therefore most of the mass) is found in particles > 0.1.

An important feature of atmospheric aerosol size distributions is their multimodal nature. Volume distributions, measured in ambient air in the United States, are almost

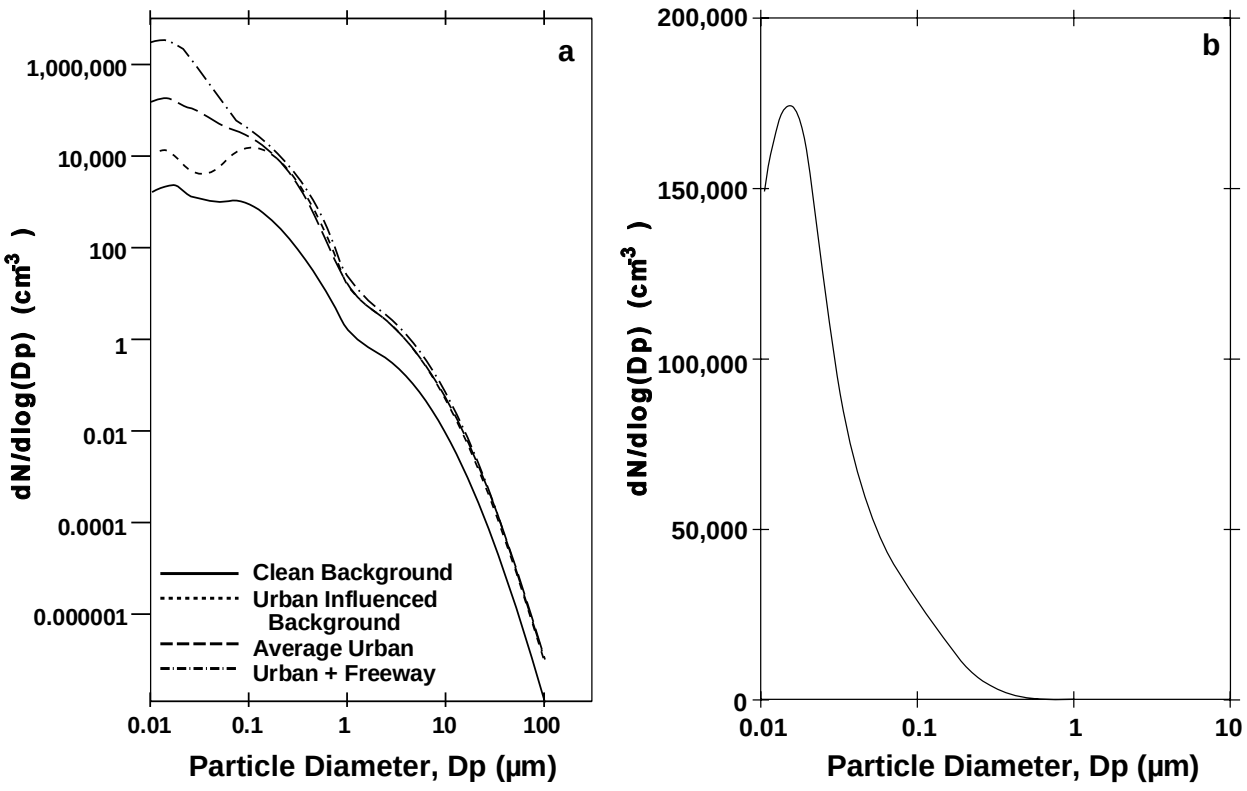

Figure 3-1. Number of particles as a function of particle diameter: (a) data are shown on a logarithmic scale to display the wide range in number concentrations from different sites; (b) averaged urban distribution are shown on a linear scale for which the area under the curve is proportional to particle number.

Source: Whitby and Sverdrup (1980).

always found to be bimodal, with a minimum between 1.0 and 3 µm. The distribution of particles that are mostly larger than the minimum is termed "coarse". The distribution of particles that are mostly smaller than the minimum is termed "fine". Whitby and Sverdrup (1980) and Willeke and Whitby (1975) identified three modes: nuclei, accumulation, and coarse. The three modes are most apparent in the freeway-influenced size distribution of Figure 3-2b. The smallest mode, corresponding to particles below about 0.1 µm, is the nuclei mode. The middle mode, from 0.1 to 1 or 2 µm, is the accumulation mode. Fine particles include both the accumulation and the nuclei modes. The largest mode, containing particles larger than 1 or 2 μm, is the coarse particle mode. Whitby and coworkers observed

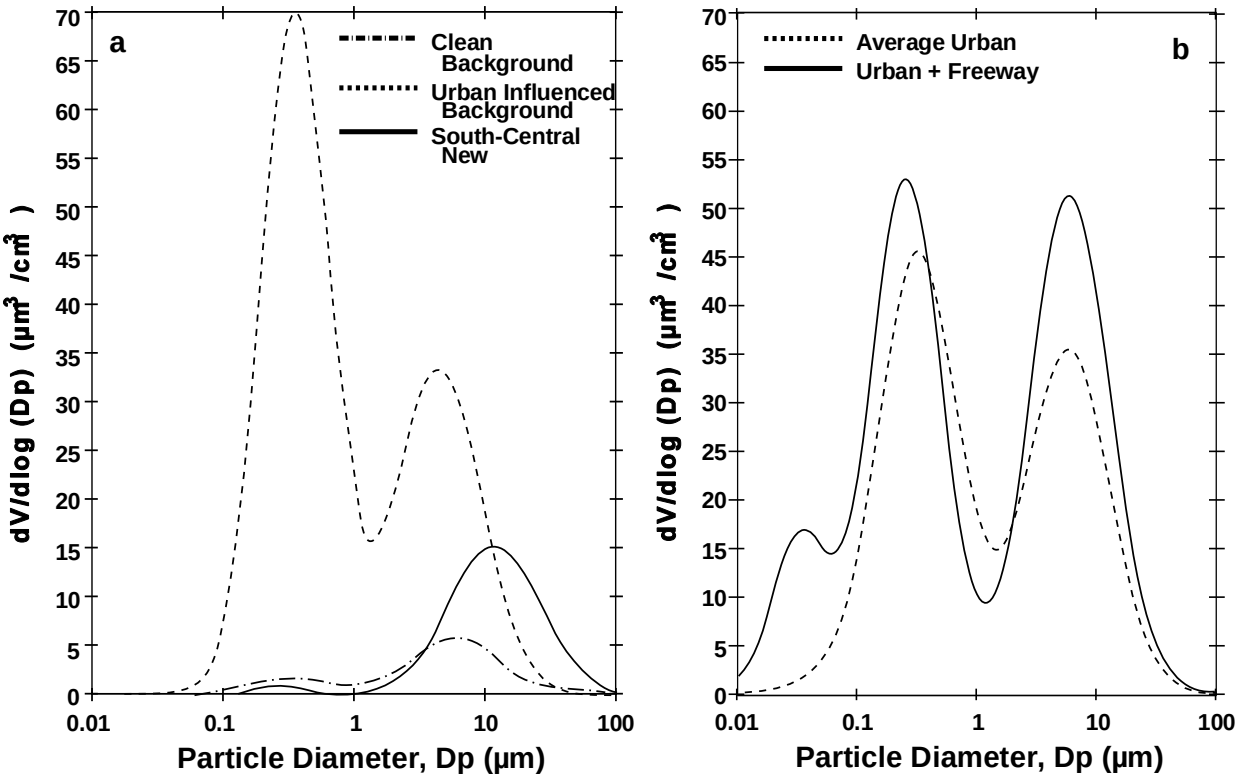

Figure 3-2. Particle volume distribution as a function of particle diameter: (a) for the averaged background and urban-influenced background number distributions shown in Figure 3-1 and a distribution from south central New Mexico, and (b) for the averaged urban and freeway-influenced urban number distributions shown in Figure 3-1.

Source: Whitby and Sverdrup (1980) and Kim et al. (1993c).

that continental background aerosols not influenced by sources have a small accumulation mode and no nuclei mode. For urban aerosols, the accumulation and coarse particles modes are comparable in volume. The nuclei mode is small in volume but, as discussed further in Section 6.8, dominates the number distributions of urban aerosols.

Many measurements indicate that the chemical compositions of coarse and fine particles are distinct. The processes that affect the formation and removal of these two size fractions of atmospheric aerosols are also distinct. Coarse particles are generated by mechanical processes and consist of soil dust, fly ash, sea spray, plant fragments, particles from tire wear, and emissions from rock-crushing operations. These particles are removed primarily by impaction and settling. Nuclei and accumulation mode particles contain primary particles

from combustion sources and secondary particles that result from condensation of low-volatility vapors formed from chemical reactions. Particles in the nuclei mode may be transferred into the accumulation mode by coagulation. Cloud coalescence and transformations in cloud droplets, followed by evaporation, are other processes that are important in atmospheric formation of accumulation mode particles. Accumulation mode particles do not ordinarily grow into the coarse mode, because number concentrations are too low for coagulation to be effective. Nuclei are readily removed by diffusion to surfaces. However, accumulation mode particles are not easily removed from the airstream. They have long atmospheric lifetimes and are able to penetrate deep into the lungs. The nuclei and accumulation modes are fairly independent of the coarse mode, both in formation and removal (Willeke and Whitby, 1975; Whitby and Sverdrup, 1980).

Fine and coarse particles are best differentiated by their formation mechanism (Wilson and Suh, 1996). Fine particles are formed by nucleation with gases while coarse particles are formed by mechanical processes from larger particles or bulk materials. The most appropriate size cut for separating fine from coarse particles is in the range of 1 to 3 μm in particle diameter; however, a precise size cut cannot be determined because of some size overlap between the fine and coarse particle modes.

3.1.3 Definitions

3.1.3.1 Definitions of Particle Diameter

The diameter of a particle may be determined geometrically, from optical or electron microscopy; by light scattering and Mie theory, or by its behavior, such as its electrical mobility, its settling velocity, or its aerodynamic behavior. Although atmospheric particles are often not spherical, their diameters are described by an "equivalent" diameter, that of a sphere which would have the same physical behavior. Two parameters that are often used are the Stokes diameter and the aerodynamic diameter. The Stokes diameter, D_p, describes particle size based on the aerodynamic drag force imparted on a particle when its velocity differs from that of the surrounding fluid. For a smooth, spherically shaped particle, D_p exactly equals the physical diameter of the particle. For irregularly shaped particles, D_p is the diameter of an equivalent sphere that would have the same aerodynamic resistance. Particles of equal Stokes diameters that carry the same electric charge will have the same

electrical mobility. Particles of equal density and equal Stokes diameter have the same settling velocity.

Aerodynamic diameter, D_a, depends on particle density and is defined as the diameter of a spherical particle with equal settling velocity but a material density of 1 g/cm^3. Particles with the same physical size and shape but different densities will have the same Stokes diameter but different aerodynamic diameters. For particles greater than about 0.5 µm, the aerodynamic diameter is generally the quantity of interest because it is the parameter that is important to particle transport, collection, and respiratory tract deposition. Respirable, thoracic, and inhalable particle sampling are based on particle aerodynamic diameter.

Aerodynamic diameter, D_a, is related to the Stokes diameter, D_p, by:

$$D_a = \left(\frac{\rho C}{C_a} \right)^{1/2} D_p \qquad (3\text{-}1)$$

where ρ is the particle density, and C and C_a are the Cunningham slip factors evaluated for the particle diameters D_p and D_a respectively. The slip factor is a function of the ratio between particle diameter and mean free path of the suspending gas; it is given by the expression (Hinds, 1982):

$$C = 1 + \frac{\lambda}{D_p} \{2.514 + 0.800 \exp(-0.55 \frac{D_p}{\lambda})\} \qquad (3\text{-}2)$$

where λ is the mean free path of the air. C is an empirical factor that accounts for the reduction in the drag force on particles due to the "slip" of the gas molecules at the particle surface. It is important for particles less than 1 µm in diameter, for which the surrounding air cannot be modeled by a continuous fluid. At normal atmospheric conditions (temperature = 20 °C, pressure = 1 atmosphere) λ = 0.066 µm. For large particles (D_p > 5 µm) C = 1; while for smaller particles C > 1.

For particles with diameters greater than the mean free path, the aerodynamic diameter given by equation (3-1) is approximated by:

$$D_a = (\rho)^{1/2} D_p \qquad (D_p \gg \lambda) \qquad (3\text{-}3)$$

This expression, which shows that aerodynamic diameter is directly proportional to the square root of the particle density, is often used for particles as small as 0.5 μm. For particles with diameters much smaller than the mean free path, the slip factor must be taken into account. In this case the aerodynamic diameter is directly proportional to the particle density [$D_a = (\rho) D_p$ for $D_p < \lambda$].

3.1.3.2 Definitions of Particle Size Fractions

In the preceding discussion several subdivisions of the aerosol size distribution were identified. The aerosol community uses three different approaches or conventions in the classification of particles by size: (1) modes, based on the observed size distributions and formation mechanisms; (2) dosimetry, based on the entrance into various compartments of the respiratory system; and (3) cut point, based on the 50% cut point of the specific sampling device.

Modal

The modal classification was first proposed by Whitby (1978). An idealized version is shown in Figure 3-3. A number of actual distributions are shown in Section 3.7. The observed modal structure is frequently approximated by several log-normal distributions.

Coarse Mode: The distribution of particles with diameters mostly greater than the minimum in the particle mass distribution, which generally occurs between 1 and 3 μm. These particles are usually mechanically generated.

Fine Mode: The distribution of particles with diameters mostly smaller than the minimum in the particle mass distribution, which generally occurs between 1 μm and 3 μm. These particles are usually formed from gases.

Accumulation Mode: That portion of the fine particle fraction with diameters above about 0.1 μm. Secondary particulate matter, formed from chemical reactions in the atmosphere, often "accumulates" in this size range. Accumulation-mode particles normally do not grow into the coarse mode.

Nuclei Mode: That portion of the fine particle fraction with diameters below about 0.1 μm. The nuclei mode can be observed as a separate mode only in clean or remote

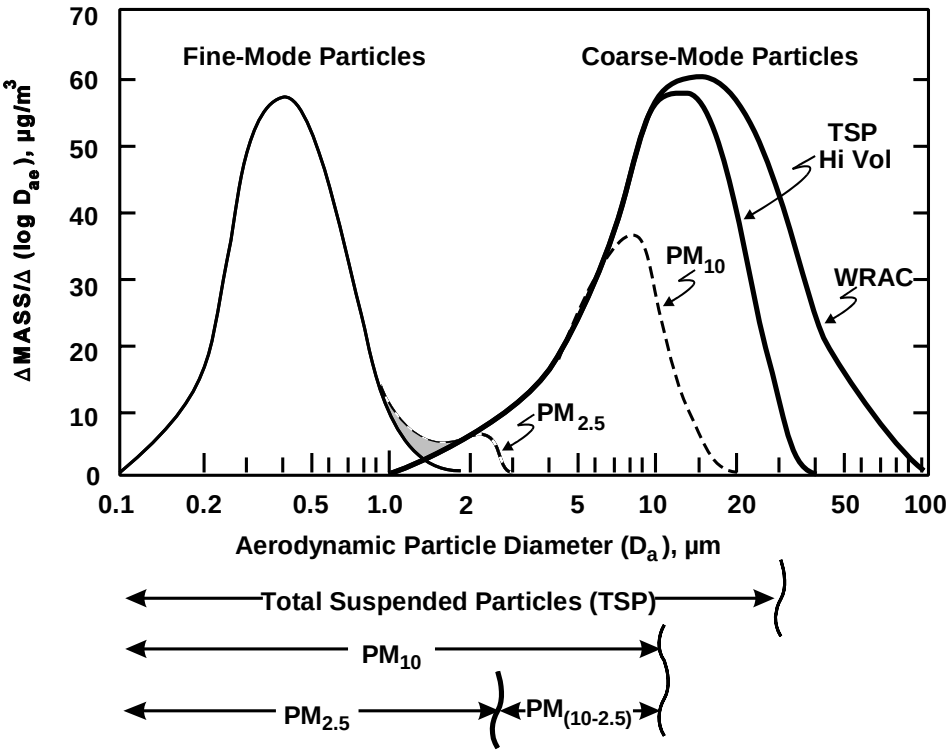

Figure 3-3. An idealized distribution of ambient particulate matter showing fine-mode particles and coarse-mode particles and the fractions collected by size-selective samplers.

Source: Adapted from Wilson and Suh (1996).

areas or near sources of new particle formation by nucleation. Nuclei-mode particles rapidly grow into the accumulation mode.

Over the years, the terms fine and coarse, as applied to particle sizes, have lost the precise meaning given in Whitby's (1978) definition. In any given article, therefore, the meaning of fine and coarse must be inferred from the author's usage. In this document, the term mode is used with fine and coarse when it is desired to specify the distribution of fine-mode particles or coarse-mode particles as shown in Figure 3-3.

Modes Within the Accumulation Mode: Aqueous-phase reactions may occur within cloud droplets, fog droplets or particles at very high relative humidity. The partial drying out of these particles may lead to a mode which is larger than the accumulation mode formed under drier conditions. This has been called the *droplet* mode. A smaller mode, perhaps

formed from non-hygroscopic material or formed after the relative humidity has decreased, may also be observed. This has been called the *condensation* mode (Hering and Friedlander, 1982; John et al., 1990). This phenomenon is discussed in greater detail in Section 3.7.

Modes Within the Nuclei Mode: Measurements over clean, remote areas (Hoppel et al., 1986; Hoppel and Frick, 1990; Covert et al., 1992; Wiedensohler et al., 1994) indicate that under some conditions two modes may be observed within the nuclei mode. Aerosol physicists distinguish these as:

> *Aitken Nuclei*: That portion of the nuclei mode which exhibits a local maximum in the number distribution above 15 nm; and the
>
> *Ultra-fine Nuclei*: That portion of the nuclei mode which exhibits a local maximum in the number distribution below 15 nm.

Ultra-fine Particles in a Biological Context: In the terminology of health scientists ultrafine is often used to characterize any size distribution, natural or laboratory-generated, which, under dry conditions, has a mass median diameter below about 0.1 μm. One hypothesis holds that such particles may cause inflammation and other health effects due to their physical size in addition to any chemically-induced effects (Oberdöster, 1995). Ultrafine particles, in the health effects usage, are closely related to the nuclei mode. In this document ultrafine will be used in the biological context and may include particles from the minimum size of about 3 nm to about 100 nm (100 nm = 0.1 μm).

Dosimetry

In a second approach, size fraction definitions are based on human health significance. This convention classifies particles into inhalable, thoracic, and respirable particles according to their entrance into the various compartments of the respiratory system. In a general sense, inhalable particles refer to those that enter the respiratory tract, including the head airways region. Thoracic particles refer to particles that reach the lung airways and the gas-exchange region of the lung, and respirable particles are those that reach the gas-exchange region. In the past exact definitions of these terms have varied among organizations. As of 1993 a unified set of definitions was adopted by the American Conference of Governmental Industrial Hygienists (ACGIH) (1994), the International Standards Organization (ISO), and the European Standardization Committee (CEN).

Sampler Cut Point

Another set of definitions of particle size fractions arises from considerations of size-selective sampling. Size-selective sampling refers to the collection of particles below or within a specified aerodynamic size range, usually defined by the 50% cut point size, and has arisen in an effort to measure particle size fractions with some special significance, e.g., health, visibility, source apportionment, etc. The PM_{10} standard set by the U.S. Environmental Protection Agency in 1987 is an example of size-selective sampling (Federal Register, 1987). The PM_{10} size cut was designed to focus regulatory concern on those particles small enough to enter the thoracic region. PM_{10} samplers, as defined in Appendix J to 40 Code of Federal Regulations (CFR) Part 50 (Federal Register, 1988), collect all of the fine particles and part of the coarse particles. The upper cut point is defined as having a 50% collection efficiency at 10±0.5 μm diameter. The slope of the collection efficiency curve is defined in amendments to 40 CFR, Part 53. The curve which defines PM_{10}, and the curves which define inhalable, thoracic, and respirable particles, are shown in Figure 3-4.

Prior to the establishment of the PM_{10} standard, the particulate matter standard was based on total suspended particulate matter (TSP). TSP is defined by the design of the High Volume Sampler (hivol) which collects all of the fine particles but only part of the coarse particles. The upper cut off size of the hivol depends on the wind speed and direction, and may vary from 25 to 40 μm. Heroic measures, such as were undertaken with the Wide Range Aerosol Classifier (WRAC), are required to collect the entire coarse mode (Lundgren and Burton, 1995). Samplers with upper cut-points of 3.5, 2.5, 2.1 and 1.0 μm are also in use. Dichotomous samplers split the particles into smaller and larger fractions, which may be collected on separate filters.

An idealized distribution showing the normally observed division of ambient aerosols into fine-mode particles and coarse-mode particles, and the size fractions collected by TSP, PM_{10}, $PM_{2.5}$ and $PM_{(10-2.5)}$ samplers, is shown in Figure 3-3.

In an analysis reported in 1979, EPA scientists endorsed the need to measure fine and coarse particles separately (Miller et al., 1979). Based on the availability of a dichotomous sampler with a separation size of 2.5 μm, they recommended 2.5 μm as the cut point between fine and coarse particles. Because of the wide use of this cut point, the $PM_{2.5}$ fraction is frequently referred to as "fine" particles. However, while the $PM_{2.5}$ sample

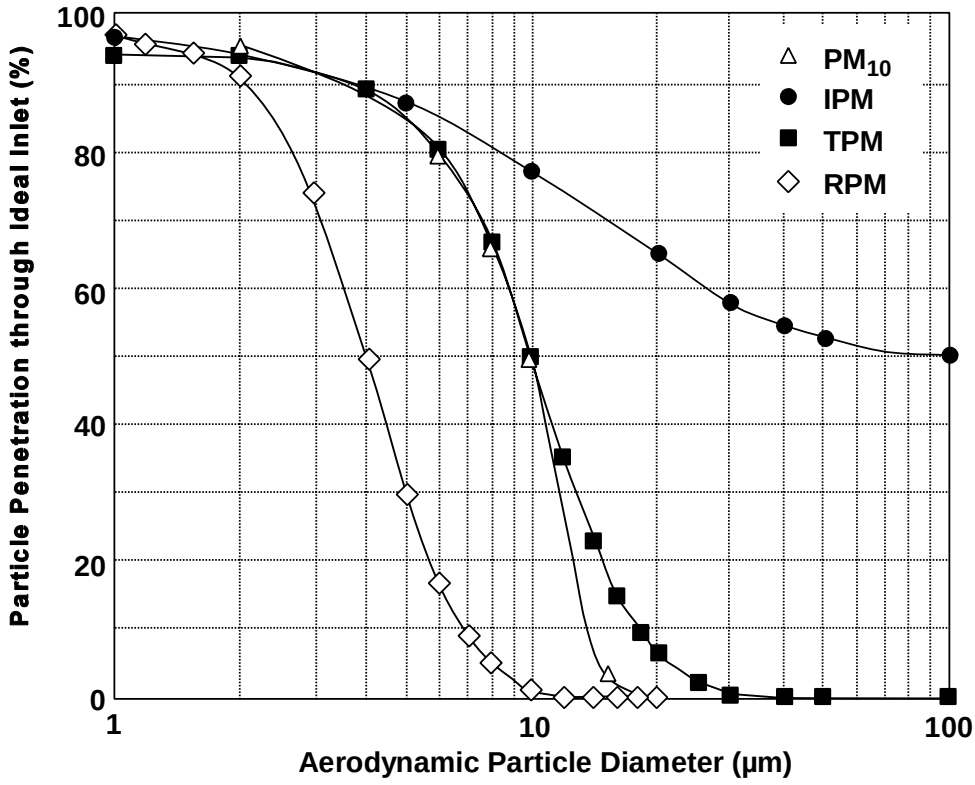

Figure 3-4. Specified particle penetration through an ideal inlet for four different size-selective sampling criteria. PM_{10} is defined in the Federal Register (1988). Curves for inhalable particulate matter (IPM), thoracic particulate matter (TPM) and respirable particulate matter (RPM) size cuts are computed from definitions given by American Conference of Governmental Industrial Hygienists (1994).

contains all of the fine particles it may, especially in dry areas or during dry conditions, collect a small fraction of the coarse particles. A PM_{10}-$PM_{2.5}$ size fraction may be obtained from a dichotomous sampler or by subtracting the mass on a $PM_{2.5}$ sampler from the mass on a PM_{10} sampler. The resulting PM_{10}-$PM_{2.5}$ mass, or $PM_{(10-2.5)}$, is sometimes called "coarse" particles. However, it would be more correct to call $PM_{2.5}$ an indicator of fine-mode particles, PM_{10} an indicator of thoracic particles, and PM(10-2.5) an indicator of the thoracic component of coarse-mode particles.

3.1.3.3 Other Terminology

Other terminology that has been introduced in this section is summarized below:

Primary Particles: material emitted into the atmosphere, either directly as particles or a vapor which rapidly forms particles by nucleation and/or condensation, from either natural sources or sources derived from human activity;

Secondary Particulate Material: material formed in the atmosphere as the result of chemical conversion of precursor gaseous species;

Internal Mixture: an aerosol for which the chemical composition of each individual particle is the same, that is, equal to the bulk composition;

External Mixture: an aerosol for which different chemical species comprise separate particles;

Anthropogenic: derived from human activities;

Biogenic: derived from plants;

Bioaerosols: airborne microorganisms and aeroallergens;

Fossil: derived from fossil fuel combustion; and

Contemporary carbon: derived from non-fossil fuel sources such as plants, wood burning, and cooking oils.

3.1.4 Major Chemical Constituents

The major constituents of atmospheric aerosol are sulfates, nitrates, carbonaceous compounds, water, hydrogen ions, ammonium ions, and materials of crustal origin. Average compositions vary with particle size, geographic location and season. Inorganic ions, including sulfate and nitrate, are typically analyzed by ion chromatography. Crustal elements are analyzed by x-ray fluorescence and/or proton-induced x-ray emission. The equilibrium models for inorganic ions predict that water is an important constituent of atmospheric particles, but measurements of particle-associated water are limited. McMurry and coworkers (McMurry and Stolzenburg, 1989; Zhang et al., 1993) measured the sensitivity of particle size to relative humidity for Los Angeles and Grand Canyon aerosols. They found that atmospheric particles of a single size exhibited two distinct hygroscopicities. These were described as "more" and "less" hygroscopic, as shown in Figure 3-5. For example, the diameters of more hygroscopic 0.2 μm particles humidified to approximately 90% relative

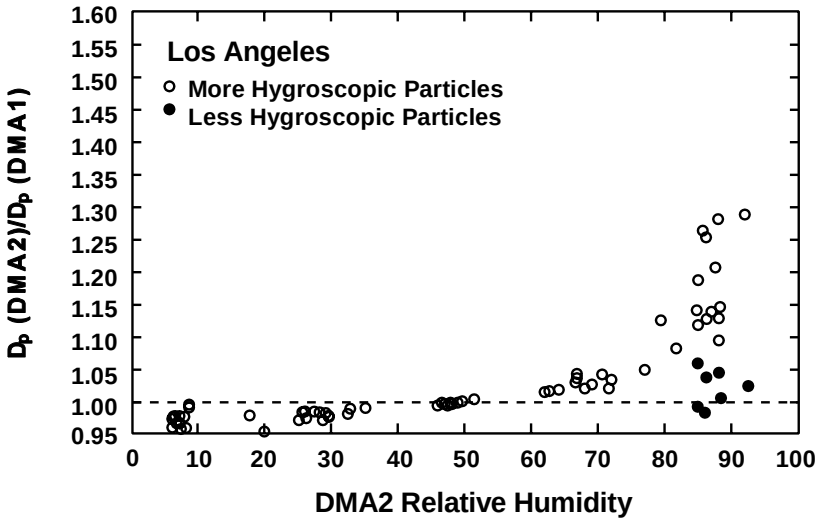

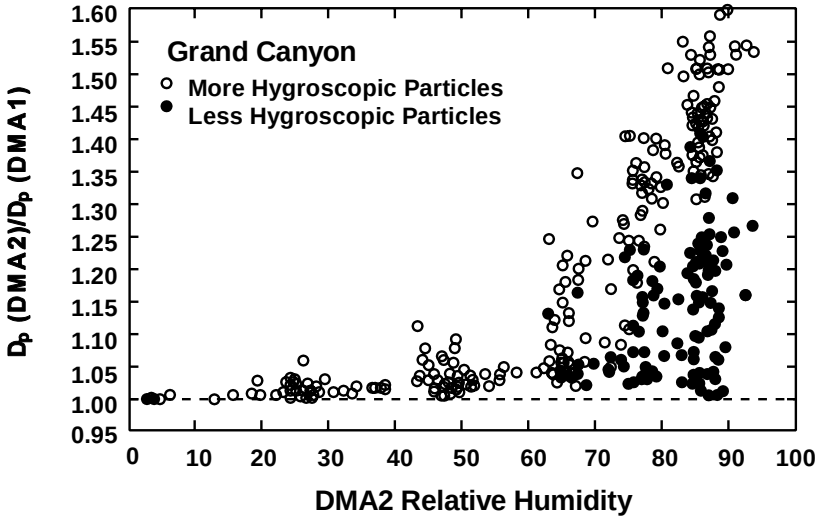

Figure 3-5. Particle size related to relative humidity.

Source: Zhang et al. (1993).

humidity increased by factors of 1.23 ± 0.08 and 1.49 ± 0.11 for Los Angeles and Grand Canyon particles, respectively. For relative humidities above 85 or 90%, water was the most abundant particulate species both in Los Angeles and at the Grand Canyon.

Because of the multitude of carbonaceous compounds present in atmospheric aerosols, carbonaceous material is often categorized as either organic carbon or elemental carbon.

Most measurements of aerosol carbon are made using one of a variety of thermal techniques that report particulate organic and elemental carbon concentrations (Johnson et al., 1981; Huntzicker et al., 1982; Mueller et al., 1982; Turpin et al., 1990). The split between organic and elemental carbon is somewhat operationally defined, but the term elemental generally refers to the nonvolatile,optically absorbing (black) portion of the carbon aerosol. Elemental carbon is associated with soot emissions from combustion. The remaining, more volatile portion is termed organic. Various methods of further classifying the organic fraction include: selective solvent extraction (Lioy and Daisey, 1986), functional group identification (Allen et al., 1994; Gordon et al., 1988), and division into neutral and acidic fractions (Hildemann et al., 1994a). Radiocarbon dating techniques have been used to distinguish fossil and contemporary carbon (Currie et al., 1994; Kaplan and Gordon, 1994; Hildemann et al., 1994a).

3.1.5 Chemical Composition and Its Dependence on Particle Size

Since the work of Whitby (1978), many studies have been conducted that provide chemical or elemental composition data on the coarse and fine fractions of the atmospheric aerosol. This has been done in several ways. The dichotomous sampler collects a $PM_{2.5}$ and a PM_{10}-$PM_{2.5}$ or coarse faction of PM_{10}. Alternately, a PM_{10} and a $PM_{2.5}$ sample may be collected and the $PM_{2.5}$ composition subtracted from the PM_{10} composition. Results from many such studies are presented in Section 6-6. More detailed information may be obtained by analysis of smaller size fractions obtained with cascade impactors (Figures 3-6, 20, Section 6-9). Studies conducted in most parts of the U.S. indicate that sulfate, ammonium, and hydrogen ions; elemental carbon and secondary organic carbon; and certain transition metals are found predominantly in the fine particles. Crustal materials such as calcium, aluminum, silicon, magnesium, and iron are found predominately in the coarse particles. Some organic material such as pollen, spores, and plant and animal debris is also found predominantly in the coarse mode. Some components such as potassium and nitrate may be found in both fine and coarse particles but from different sources or mechanisms. Potassium in coarse particles comes from soil, and in fine particles, comes from combustion of wood. Nitrate in fine particles comes primarily from the reaction of gas-phase nitric acid with gas-phase ammonia to form particulate ammonium nitrate. Nitrate in coarse particles comes primarily from the reaction of gas-phase nitric acid with pre-existing coarse particles.

In the presence of cloud or fog droplets, or when sodium chloride particles from ocean spray or other sources are present, a mechanism is available for sulfate, nitrate, and ammonium ions to occur in the coarse mode. Detailed size distributions of the inorganic ions in Los Angeles are shown in Figure 3-6 (Wall et al., 1988; John et al., 1990). These data show two modes for sulfate and nitrate aerosols between 0.1 and 1 μm. Similar results for sulfate aerosols were reported by Hering and Freidlander (1982). The smaller mode, corresponding to particles near 0.2 μm in diameter, is attributed to gas-phase formation of condensible species and is referred to as the condensation mode. The larger mode has a peak near 0.6 μm and is called the droplet mode (Hering and Freidlander, 1982). Its existence is attributed to secondary formation through heterogeneous, aqueous-phase transformations. McMurry and Wilson (1983) found 0.6 μm sulfate particles in power plant plumes and attributed their existence to formation by heterogeneous processes. Further analysis of the data by Meng and Seinfeld (1994) indicates that these aqueous reactions most likely occur in cloud or fog droplets.

The data of Figure 3-6 in Los Angeles show that particulate nitrate is found in both coarse and fine particles. Nitrate near the coast was predominantly in the coarse mode. Coarse mode nitrate was less prominent for inland sites. Several investigators (Wall et al., 1988; John et al., 1990; Andreae et al., 1986) proposed that the coarse particle nitrate results from the heterogeneous reaction of nitric acid with sea salt. On the basis of single particle analysis by electron microscopy-energy dispersive XRF spectroscopy, Wu and Okada (1994) concluded that coarse-particle nitrate in a coastal region of Japan formed on sea salt. Coarse nitrate collected at an inland site was associated with soil dust. These data suggest that a heterogeneous chemical reaction on the surface of a mechanically generated, primary particle may provide a mechanism for adding secondary material to the coarse particle mode. They also show that secondary particulate material can be formed by the interaction of a natural constituent (sea salt) with a species derived from anthropogenic emissions (nitric acid).

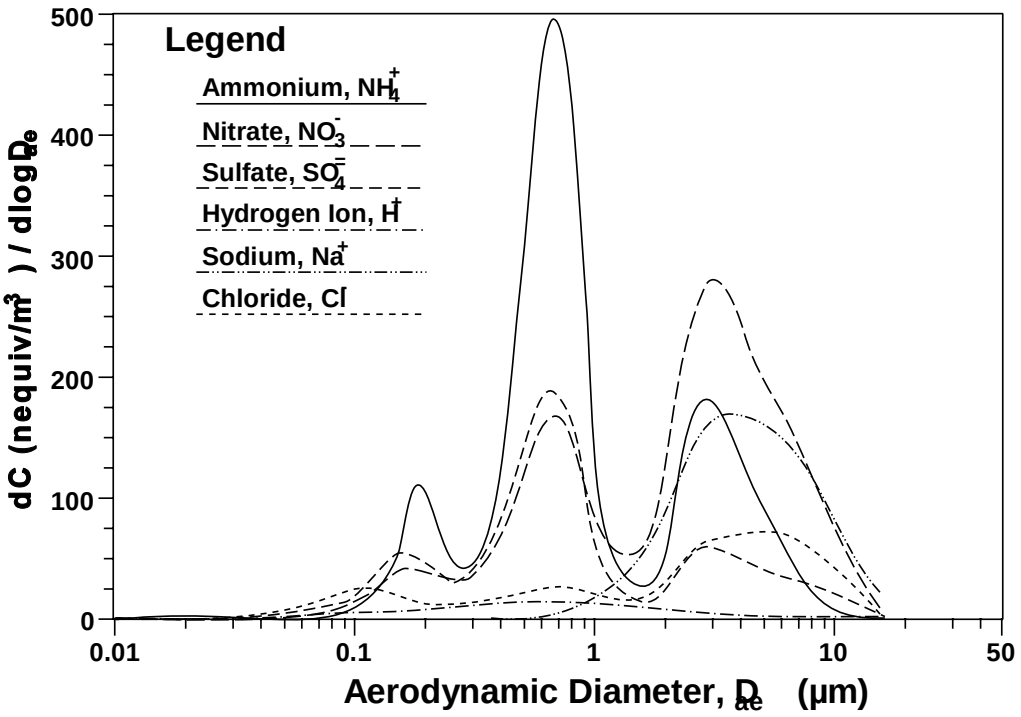

Figure 3-6. Ion concentration as a function of particle size, measured in Claremont, CA.

Source: Wall et al. (1988).

3.1.6 Particle-Vapor Partitioning

Several atmospheric aerosol species, such as ammonium nitrate and certain organic compounds, are semivolatile and are found in both gas and particle phases. The gas-particle distribution of semivolatile organic compounds depends on compound vapor pressure, total particle surface area, particle composition, and atmospheric temperature (Pankow, 1987; Junge, 1977; Bidleman, 1988). Junge (1977) modeled this relationship using a linear form of a Langmuir adsorption isotherm. Measurements of semivolatile organic compounds show that gas-particle distributions are highly correlated with total suspended particulate matter, temperature, and the sub-cooled liquid vapor pressure of the pure compound (Foreman and Bidleman, 1990; Ligocki and Pankow, 1989; Yamasaki et al., 1982). Yamasaki et al. (1982) used this information to model an empirical relationship between the gas-particle distribution, total suspended particulate matter and temperature. Pankow showed that the expressions of

Junge (1977) and Yamasaki et al. (1982) are consistent and continued the theoretical development of equilibrium gas-particle partitioning (Pankow, 1987; 1991; 1994a,b).

Although it is generally assumed that the gas-particle partitioning of semivolatile organics is in equilibrium in the atmosphere, the kinetics of redistribution are not well understood. Gerde and Scholander (1989) and Rounds and Pankow (1990) predicted that redistribution in the ambient air could take minutes to hours. Since changes in atmospheric conditions (i.e., temperature) will drive redistribution, it is not clear whether equilibrium conditions are maintained. However, the gas and particle data agree reasonably well with equilibrium theories. Hampton et al. (1983) report that the gas-particle partitioning of semi-volatile hydrocarbons from motor vehicle emissions can be described by Raoult's Law, i.e, the hydrocarbon species behave as solutes. The development of an understanding of gas-particle partitioning of semivolatile organic compounds is hampered by the difficulty associated with measuring the multitude of compounds, all present in small concentrations. Diurnal temperature fluctuations, which cause gas-particle partitioning to be dynamic on a time scale of a few hours, add to the measurement problems.

Stelson and Seinfeld (1982a) developed a thermodynamic model to predict the temperature and relative humidity dependence of the ammonium nitrate equilibrium dissociation constant. The model is supported by ambient data at inland sites in the Los Angeles Basin (Hildemann et al., 1984; Doyle et al., 1979). Bassett and Seinfeld extended the equilibrium model to include sulfates (1983) and the effect of particle size (1984). With the inclusion of sodium chloride in the equilibrium model, Pilinis and Seinfeld (1987) were able to predict observations at coastal sites. Atmospheric models based on equilibrium considerations have been successful in accounting for the gas-particle partitioning of inorganic species measured in Phoenix, Arizona (Watson et al., 1994a), and Uniontown, Pennsylvania (Saxena et al., 1993). Wexler and Seinfeld (1992) found that under some atmospheric conditions, such as cool, cold, or very clean air, the size distributions of ammonium ion and nitrate are not accurately predicted by equilibrium considerations alone, and that transport kinetics can be important. The dynamic changes in gas-particle partitioning, caused by changes in temperature or total concentration, both in the atmosphere and after collection, cause sampling problems which are discussed in Chapter 4.

3.1.7 Single Particle Characteristics

The "mixing characteristics" of the aerosol describes the distribution of chemical species among particles. An aerosol in which all particles contain the same homogeneous blend of chemical species is internally mixed. In an externally mixed aerosol each chemical species is found in a distinct set of particles. Experiments measuring atmospheric aerosol properties for single-particle size ranges (Hering and McMurry, 1991; Covert et al., 1990; Zhang et al., 1993) and single-particle analyses (De Bock et al., 1994; Sheridan et al., 1993; Van Borm et al., 1989; Anderson et al., 1988) indicate that atmospheric aerosols are to some degree both internally and externally mixed. Single particle analyses provide descriptions of individual particle compositions. These are then categorized either manually or through multivariate methods such as cluster analysis (Kim and Hopke, 1988) to give an accounting of the relative number of particles of each chemically defined particle type. Morphological information can also be included in particle type definitions.

Single-particle composition and morphology provide insights into the sources and atmospheric processes affecting airborne particles. For example, a priori one expects that particles emitted from different sources would in fact be distinct. However, Andreae et al. (1986) observed that over remote ocean areas between 80 and 90% of silicon-rich particles (presumably originating from silicate mineral particles) were also rich in sodium, chlorine, and variable amounts of potassium, magnesium, calcium, and sulfur (attributed to sea salt particles). The internal mixing of silicates with sea salt, particles originating from different sources and externally mixed when emitted into the atmosphere, suggested the processing of aerosol particles within clouds (see Section 3.2.2.5). The hypothesis was that a single cloud droplet could take up two or more particles and that these particles would remain together after droplet evaporation. Other mechanisms of particle coalescence, such as differential settling, Brownian coagulation, and electrostatic attraction, were considered too slow to account for the large fraction of internal mixing observed. Andreae et al. (1986) also found enrichment of sulfur (presumably sulfate) on sea salt particles. This also was attributed to the interaction of clouds with particles. Gas-to-particle conversion in cloud droplets or by condensation can also lead to mixtures of aerosol species.

Particle morphology has many effects on atmospheric particle properties and processes. Chain agglomerates, for example, have much larger surface areas on which adsorption and

chemical reactions can take place than spherical particles of identical volumes. In addition, the atmospheric lifetime is longer, and the optical absorption per unit mass is greater for chain agglomerates than for more compact particles. Combustion-generated soot particles are often chain agglomerates composed of a large number of small primary spherules. Laboratory experiments conducted by Huang et al. (1994) and Colbeck et al. (1990) demonstrated that condensation-evaporation processes can cause chain agglomerates to become more compact. Colbeck et al. (1990) also showed that the collapse of the soot aggregates resulting from humidification results in a decrease in both the optical scattering and extinction of the particles.

3.1.8 Dry Deposition

Dry deposition is the process whereby, in the absence of precipitation, airborne gases and particles are transported down to the surface of the earth where they are removed. Atmospheric turbulent mixing continually brings airborne gases and particles into close proximity to the earth's surface, where they may diffuse across a thin layer of stagnant air to the surface itself. Actual removal at the surface depends on the affinity between the airborne substance and the surface element (ground, body of water, vegetation surface, etc.). Dry deposition is a complex process but it is represented as occurring in three steps: (1) transport down to the vicinity of the earth by turbulent mixing processes; (2) diffusion across a thin quasi-laminar layer of air; and (3) attachment to the surface itself. Dry deposition of particles is a strong function of particle size, atmospheric conditions and terrain physiography. For large particles (e.g., above 10 μm in diameter), gravitation also contributes significantly to the overall dry deposition process.

3.1.9 Atmospheric Scavenging or Wet Deposition

Atmospheric gases are scavenged directly by absorption in droplets and by chemical reactions in clouds. The direct absorption of gases in falling droplets depends on the solubility of the gas in water, and may be affected by the presence of other species in solution (Seinfeld, 1986). Particles are scavenged in clouds when they serve as nuclei for the formation of cloud droplets (cloud condensation nuclei). This process is especially important for fine particles. Particles are also scavenged below clouds when they are intercepted by falling hydrometeors, e.g., rain, snow, etc. This process is more important for coarse particles than fine particles. Because fine particles tend to follow air motions, they move out of the way and are not impacted

by falling rain drops. The wet removal of particles depends on the air trajectories through clouds, the supersaturation to which the air mass is exposed, and the time for which droplets are present before arriving at the ground.

3.2 PHYSICAL PROPERTIES AND PROCESSES

3.2.1 Aerosol Size Distributions

3.2.1.1 Particle Size Distribution Functions

The distribution of particles with respect to size is perhaps the most important physical parameter governing their behavior. The concentration of the number of particles as a function of their diameter is given by a particle number distribution.

Because atmospheric particles cover several orders of magnitude in particle size, size distributions are often expressed in terms of the logarithm of the particle diameter, on the X-axis, and the differential concentration on the Y-axis: $dN/d(\log D_p)$ = the number of particles per cm^3 of air having diameters in the size range from $\log D_p$ to $\log(D_p + dD_p)$. It is not proper formally to take the logarithm of a dimensional quantity. However, one can think of the distribution as a function of $\log(D_p/D_{p0})$, where the reference diameter D_{p0} = 1 μm is not explicitly stated. If $dN/d(\log D_p)$ is plotted on a linear scale, the number of particles between D_p and $D_p + dD_p$ is proportional to the area under the curve of $dN/d(\log D_p)$ versus $\log D_p$. Similar considerations apply to distributions of surface, volume, and mass.

3.2.1.2 Log-Normal Size Distributions

Under some conditions, atmospheric aerosol size distributions may be approximated by a sum of log-normal distributions. Although such log-normal representations are not always an accurate description of the actual aerosol size distributions, they have been found, in many cases, to be convenient mathematical constructs to represent aerosol size distributions. The use of log-normal approximations to aerosol size distributions was first introduced by Foitzik (1950) and later expanded to a wide range of atmospheric data by Whitby and

co-workers (e.g., Whitby and Sverdrup, 1980; Willeke and Whitby, 1975). A log-normal distribution is a specific form of the size distribution function for which the population of particles follows a Gaussian distribution function with respect to the logarithm of the particle diameter. The logarithm of the geometric standard deviation, σ_g, is the standard deviation of the quantity $\log D_p$ and defines the width of the distribution. For a monodisperse aerosol, that is, one for which all particles are the same diameter, $\sigma_g = 1$. For polydisperse aerosols, $\sigma_g > 1$. Typical values for one of the modes of the atmospheric aerosol, such as the accumulation mode discussed above, are $1.8 < \sigma_g < 2.8$. For log-normal distributions, 84.1% of the particles are below the size $\sigma_g \cdot D_{gn}$, 84.1% lie above the size D_{gn}/σ_g, and 95% of the particles lie within two standard deviations of the mean, that is, the range from $D_{gn}/2\sigma_g$ to $D_p \cdot 2\sigma_g$.

One of the properties of the log-normal distribution is that if the number distribution is log-normal, the surface and volume distributions are also log-normal, and their geometric standard deviation σ_g is the same as for the number distribution.

3.2.1.3 Ambient Aerosol Size Distributions

Log-normal parameters which describe ambient aerosol size distributions are listed in Table 3-1. These parameters are the geometric number mean diameter, D_{gn}, geometric standard deviation, σ_g, and number concentration, N, for each mode. Also given are the parameters of the lognormal volume distributions, geometric mean diameters, D_{gv}, and the corresponding total particle volume for each mode, V. The tables include data from Sverdrup and Whitby (1980) and results from more recent measurements in a nonurban area of New Mexico (Kim et al., 1993c). Note that the volume geometric mean diameters for the accumulation mode vary from 0.2 μm to 0.4 μm and those for the coarse mode from 5 to 12 μm. The standard deviations for the coarse particle mode tend to be larger than for the accumulation mode.

3.2.1.4 Coagulation of Spherical Particles

Many processes affect the size distribution of an aerosol, including addition of volume by gas-to-particle conversion, and losses by deposition. Even without these processes, under conditions in which the total volume of an aerosol is conserved, the number of particles will

TABLE 3-1. LOGNORMAL PARAMETERS FOR AMBIENT AEROSOLS

A. Parameters of the Number Distribution

Site of Measurement	Nuclei Mode Num. (cm^3)	Nuclei Mode Dgn (μm)	Nuclei Mode σ_g	Accumulation Mode Num. (cm^3)	Accumulation Mode Dgn (μm)	Accumulation Mode σ_g	Coarse Mode Num. (cm^3)	Coarse Mode Dgn (μm)	Coarse Mode σ_g	Reference
Clean continental background	N: 1,000	0.016	1.6	800.00	0.067	2.1	0.72	0.93	2.2	(1)
Average continental background	N: 6,400	0.015	1.7	2,300.00	0.076	2.0	3.2	1.02	2.16	(1)
Urban influenced background	N: 6,600	0.014	1.6	9,600.00	0.120	1.84	7.2	0.83	2.12	(1)
Urban average	N: 106,000	0.014	1.8	32,000.00	0.054		5.4	0.86	2.25	(1)
Urban and freeway	N: 2,120,000	0.013	1.74	37,000.00	0.032	1.98	4.9	1.08	2.13	(1)
South central NM - February 1989	N: not reported			706.00	0.13	1.72	0.42	2.45	1.91	(2)
South central NM - July 1989	N: not reported			253.00	0.13	1.71	0.72	1.59	2.27	(2)

B. Parameters of the Volume Distribution

Site of Measurement	Nuclei Mode Volume ($\mu m^3\ cm^3$)	Nuclei Mode Dgv (μm)	Nuclei Mode σ_g	Accumulation Mode Volume ($\mu m^3\ cm^3$)	Accumulation Mode Dgv (μm)	Accumulation Mode σ_g	Coarse Mode Volume ($\mu m^3\ cm^3$)	Coarse Mode Dgv (μm)	Coarse Mode σ_g	Reference
Clean continental background	V: 0.01	0.030	1.6	1.50	0.35	2.1	5.0	6.0	2.0	(1)
Average continental background	V: 0.04	0.034	1.7	4.45	0.32	2.0	25.9	6.04	2.16	(1)
Urban influenced background	V: 0.03	0.028	1.6	44.00	0.36	1.84	27.4	4.51	2.12	(1)
Urban average	V: 0.63	0.038	1.8	38.40	0.32	2.16	30.8	5.7	2.25	(1)
Urban and freeway	V: 9.20	0.032	1.74	37.50	0.25	1.98	42.7	6.0	2.13	(1)

Sources: (1) Whitby and Sverdrup (1980), (2) Kim et al. (1993c).

decrease by coagulation while the average volume per particle increases. The coalescence of two particles always reduces the total surface area and therefore is favored thermodynamically. Thus, in this sense, aerosols are inherently unstable. In some cases coagulation leads to the formation of chain agglomerates, such as for soot and some metals.

3.2.2 Particle Formation and Growth

A significant portion of the fine atmospheric aerosol is secondary, i.e., material added to the particle phase as the result of gas-to-particle conversion processes. For example, fine sulfate and nitrate particles are mostly formed by secondary processes. One mechanism of gas-to-particle conversion is homogeneous gas-phase chemical reactions to form a condensible species, such as the oxidation of sulfur dioxide to form sulfuric acid. Condensible species can either nucleate to form a new particle (nucleation), or can condense onto the surface of an existing particle (condensation). Another important class of gas-to-particle conversion mechanisms is heterogeneous chemical reactions, which are chemical reactions involving both gas-phase and particle-phase constituents. Transformation on the surface of particles, such as the uptake of nitric acid on the surface of calcium carbonate particles to produce calcium nitrate, is one type of heterogeneous reaction. Aqueous-phase chemical reactions, such as the dissolution of sulfur dioxide into a hygroscopic particle or fog or cloud droplet, followed by oxidation of the dissolved sulfur dioxide to sulfate and evaporation of the fog or cloud droplets back to aerosol size, provide an important mechanism for conversion of gases to particles. Heterogeneous reactions lead to addition of aerosol material to existing particles. Nucleation results in an increase in particle number as well as an increase in particle mass. Condensation leads only to an increase of aerosol mass and surface area, but does not affect the total number of particles. In this section the physical aspects of these gas-to-particle conversion mechanisms, and their effects on the particle size distribution, are discussed.

3.2.2.1 Equilibrium Vapor Pressures

An important parameter in particle nucleation and in particle growth by condensation is the saturation ratio S, defined as the ratio of the partial pressure of a species, p, to its equilibrium vapor pressure above a flat surface, p_o: $S = p/p_o$. For either condensation or

nucleation to occur, the species vapor pressure must exceed its equilibrium vapor pressure. For particles, the equilibrium vapor pressure is not the same as p_o. Two effects are important: (1) the Kelvin effect, which is an increase in the equilibrium vapor pressure above the surface due to its curvature; thus very small particles have higher vapor pressures and will not be stable to evaporation until they attain a critical size and (2) the solute effect, which is a decrease in the equilibrium vapor pressure due to the presence of other compounds.

For an aqueous solution of a nonvolatile salt, the presence of the salt decreases the equilibrium vapor pressure of the drop. This effect is in the opposite direction as the Kelvin effect, which increases the equilibrium vapor pressure above a droplet because of its curvature.

3.2.2.2 New Particle Formation

When the vapor concentration of a species exceeds its equilibrium concentration (expressed as its equilibrium vapor pressure), it is considered condensible. Condensible species can either condense on the surface of existing particles or can form new particles. The relative importance of nucleation versus condensation depends on the rate of formation of the condensible species and on the surface area of existing particles. An analytical relation for the relative importance of each pathway is dependent on the ratio of the square of the available surface area to the rate of formation (McMurry and Friedlander, 1979). In urban environments, the available particle surface area is sufficient to rapidly scavenge the newly formed condensible species. New particle formation is usually not important except near sources of condensible species. Wilson et al. (1977) report observations of the nuclei mode in traffic. New particle formation can also be observed in cleaner, remote regions. Bursts of new particle formation in the atmosphere under clean conditions correspond to low aerosol surface area concentrations (Covert et al., 1992). The highest concentrations of volatile ultrafine particles occur in regions corresponding to the lowest particle mass concentrations, indicating that new particle formation is inversely related to the available aerosol surface area (Clarke, 1992). In contrast to continental aerosols, where sulfate particles are the result of conversion of sulfur dioxide, the sulfate particles over the oceans

are the result of the conversion of dimethylsulfide emitted by phytoplankton (Charlson et al., 1987).

3.2.2.3 Particle Growth

When material is added to the particle phase by condensation or by particle-phase chemical reactions, particles of different sizes may grow at different rates, depending on the mechanism involved. Condensational growth can have a different effect on the size distribution of the aerosol than the effect of heterogeneous conversion through chemical reactions within a droplet. The relative rates at which the size of particles change depend on whether the rate-limiting step in the growth process is transport to the particle, chemical reactions at the surface of the particle, or chemical reactions within the particle. These are referred to as transport-limited, surface-reaction rate-limited or volume-reaction rate-limited. These different physical mechanisms give rise to a different form of the growth law for the particle. Growth laws are the expressions for $d\upsilon/dt$ or dD_p/dt as a function of particle size (where υ is single particle volume and D_p is particle diameter).

For condensational growth, the rate-limiting step relevant to the rate at which particles of different size grow is transport of condensible species to the particle surface. For particles much smaller than the mean free path of air (free molecule regime), transport is governed by single molecular bombardment of the surface, and the volume (or mass) of these particles grows in proportion to their surface area. For particles larger than the mean free path (continuum regime), transport is governed by diffusion. In this regime the loss of diffusing species at the surface of the particle causes a gradient in the concentration of the diffusing species near the surface of the particle such that the volume of the particle grows in proportion to particle diameter rather than surface area.

For heterogeneous chemical reactions, the rate limiting step for growth may not be the transport of the reacting species to the particle, but the rate of reaction on or within the particle. For reactions at the surface of the particle, the rate of growth is controlled by the particle surface area; for droplet-phase reactions, it depends on the volume of the particle. In summary, the aerosol growth laws show that in the continuum regime the particle size dependence of the rate of change of particle volume varies from a dependence on D_p for condensation by diffusion, to D_p^2 for surface reactions, to D_p^3 for droplet reactions.

Condensation by diffusion varies as D_p^2 in the free molecule regime, in the transition regime, intermediate between the free molecule and continuum regimes, condensation by diffusion varies between a dependence on D_p^2 for small particles to a dependence on D_p for larger particles.

3.2.2.4 Equilibria with Water Vapor

The principal equilibrium of concern pertinent to ambient aerosols is that with water vapor. This equilibrium is important as it influences the size of the particles and in turn their aerodynamic properties (important for deposition to the surface, to airways, following inhalation, and to sampling instrumentation) and their light scattering properties. This section reviews recent work describing this equilibrium as it pertains to ambient aerosols.

Briefly the interaction of particles with water vapor may be described as follows. As relative humidity increases, crystalline soluble salts in aerosol particles undergo a phase transition to become aqueous solution aerosols. According to the phase rule, for particles consisting of a single component, this phase transition is abrupt, taking place at a relative humidity that corresponds to the vapor pressure of water above the saturated solution (the deliquescence point). With further increase in relative humidity the particle growth is such that the vapor pressure of the solution (concentration of which decreases as additional water is accredited) is maintained equal to that of the surrounding relative humidity; the particle thus tends to follow the equilibrium growth curve. As relative humidity decreases, the particle follows the equilibrium curve to the deliquescence point. However, rather than crystallizing at the deliquescence relative humidity, the particle remains a solution (supersaturated solution) to considerably lower relative humidities. Ultimately the particle abruptly loses its water vapor (efflorescence), returning typically to the initial, stable crystalline form. This behavior has been amply demonstrated in numerous laboratory studies (Tang and Munkelwitz, 1977; Tang, 1980). Recently Tang and Munkelwitz (1994) have presented data for water activity (equilibrium relative humidity) as a function of composition for several sulfate salts.

For particles consisting of more than one component, the solid to liquid transition will take place over a range of relative humidities, with an abrupt onset at the lowest deliquescence point of the several components, and with subsequent growth as crystalline

material in the particle dissolves according to the phase diagram for the particular multicomponent system. Under such circumstances a single particle may undergo several more or less abrupt phase transitions until the soluble material is fully dissolved. At decreasing relative humidity such particles tend to remain in solution to relative humidities well below the several deliquescence points; such behavior has been amply demonstrated. In the case of the sulfuric acid-ammonium sulfate-water system the phase diagram is fairly completely worked out. Mixed anion systems containing nitrate are more difficult due to the equilibrium between particulate NH_4NO_3 and gaseous NH_3 and HNO_3 (Tang et al., 1978, 1981; Spann and Richardson, 1985). Spann and Richardson also give the compositional dependence of the relative humidity of efflorescence. For particles of composition intermediate between NH_4HSO_4 and $(NH_4)_2SO_4$ this transition occurs in the range from 40% to below 10%, indicating that for certain compositions the solution cannot be dried in the atmosphere. At low relative humidities particles of this composition would likely be present in the atmosphere as supersaturated solution droplets (liquid particles) rather than as solid particles, thus they would exhibit hygroscopic rather than deliquescent behavior during relative humidity cycles.

Evidence of the interaction of ambient aerosol particles with water vapor has been obtained by several investigators. Koutrakis et al. (1989) found systematically increasing aerosol mean diameter with increasing relative humidity, which they attributed to water accretion on sulfates. Rood et al. (1989) examined the response of light scattering coefficient of ambient aerosols to increase in temperature and attributed the decrease in light scattering upon heating to loss of liquid water associated with the particles. However, heating can also cause the loss of NH_4NO_3 and semi-volatile organic material. More detailed information regarding the size dependence of hygroscopic properties has been obtained by examining the change in particle size of a monodisperse size cut selected with a mobility analyzer, subjecting that aerosol to an increase or decrease in relative humidity, and reanalyzing the size at the new humidity. Studies of this phenomenon in the Los Angeles area indicate this phenomenon, but also frequently indicate the presence of externally mixed aerosol, in which some of the aerosol exhibits the growth expected of soluble salts, where another, apparently hydrophobic, fraction does not exhibit such growth (McMurry and Stolzenburg, 1989). Such bimodal growth with relative humidity was exhibited by particles present at Hopi Point,

Arizona (Pitchford and McMurry (1994). In the latter study the relative humidity dependence of the size of the more hygroscopic fraction was found to be consistent with that expected for sulfate salts. Such external mixtures have also been commonly observed in European aerosols (Svenningsson et al., 1994). Saxena et al. (1995) have shown that the presence of organic compounds in particles may lead to more water condensation on particles (as shown by data collected in Arizona) or to less water condensation, probably because of the formation of an organic film that isolates inorganic salts from the ambient gas-phase (as shown by data collected in Los Angeles).

The time constant that characterizes the rate of exchange of water vapor between the gas phase and a solution droplet is of interest relative to the rate of response of particles to changes in relative humidity in the ambient environment, especially in the vicinity of surfaces, and relative to changes experienced by particles following inhalation or during sampling. It is generally assumed that the rate of this water exchange is rapid. The characteristic time for diffusional growth in response to a change in relative humidity was calculated by Pilinis et al. (1989) to be about 1×10^{-7} s. However Khlystov et al. (1993) noted that this estimate was erroneously low by several orders of magnitude. The latter investigators examined the characteristic time for establishment of phase equilibrium in response to a change in relative humidity for $(NH_4)_2SO_4$ aerosol particles (dry radius 0.5 μm). The characteristic time increases from ca 1 ms at 8% relative humidity to 1.6 s at 99% relative humidity. Above 99% relative humidity the characteristic time can become much longer because of the large change in droplet radius at such relative humidities. These calculations indicate that the water equilibrium can be expected to be rapidly achieved in the ambient environment. A possible but important exception is near 100% relative humidity, pertinent to dry deposition of particles to vegetation or to water, where the equilibrium size might not be reached in the time required for the particle to traverse the diffusive layer adjacent to the surface.

The lability of water associated with ambient aerosol has been evidenced in comparisons by Malm et al. (1994) of measured particulate light scattering coefficient obtained with an integrating nephelometer with values reconstructed from aerosol composition, taking into account the relative humidity dependence of light scattering coefficients of the aerosol components. The reconstructed values were found to

systematically exceed the measured value. However when in the reconstruction the relative humidity was taken as that in the nephelometer chamber (invariably lower than ambient because of heating in the chamber) the reconstruction was markedly improved.

3.2.2.5 Particle Growth in Fogs and Clouds

Several measurements of the aerosol mass distributions in urban areas have shown that two distinct modes can exist in the 0.1 to 1 μm diameter range (Hering and Friedlander, 1982; McMurry and Wilson, 1983; Wall et al., 1988; John et al., 1990). These are referred to as the condensation mode (approximate aerodynamic diameter 0.2 μm) and the droplet mode (aerodynamic diameter around 0.7 μm). Hering and Friedlander (1982) and John et al. (1990) postulated that the larger mode could result from aqueous-phase chemistry. Meng and Seinfeld (1994) proposed that growth of condensation mode particles by accretion of water vapor or by gas-phase or aerosol-phase sulfate production cannot explain the existence of the droplet mode. Activation of condensation mode particles, formation of cloud/fog drops followed by aqueous-phase chemistry, and aqueous droplet evaporation was shown by these authors to be a plausible mechanism for formation of the urban and regional aerosol droplet mode. The sulfate formed during fog/cloud processing of an air mass favors the aerosol particles that had access to most of the fog/cloud liquid water content, which are usually the particles with dry diameters around 1 μm (Pandis et al., 1990b). These two submicron mass-distribution modes have been also observed in non-urban continental locations (McMurry and Wilson, 1983; Hobbs et al., 1985; Radke et al., 1989), but the frequency of their co-existence remains unknown. Thus, cloud processing of an air parcel can clearly affect the scattering efficiency and in general the radiative properties of the corresponding aerosol (Hegg et al., 1992; Bower and Choularton, 1993).

The aerosol distribution is also modified during in-cloud processing by collision-coalescence of droplets and impaction scavenging of aerosols (Pruppacher and Klett, 1980). The aerosol scavenging by droplets is a relatively slow process, and collision coalescence among droplets of different sizes causes a redistribution of aerosol mass in such a manner that the main aerosol mass is associated with the main water mass (Flossmann et al., 1985). The processing of the remote aerosol distribution by clouds has been clearly demonstrated in a series of field studies (Frick and Hoppel, 1993). This multiple processing of remote aerosol by

nonprecipitating clouds results in an extra mode in the aerosol number distribution (Hoppel et al., 1986; Frick and Hoppel, 1993).

Clouds and fogs can influence the atmospheric aerosol number and mass concentration and chemical composition, the shape of the aerosol size distribution, the aerosol acidity and radiative properties. These effects can be important in all environments (urban, rural and remote) and all seasons. Our qualitative understanding of the aerosol-cloud interactions has improved significantly, but, with few exceptions, the quantification of these effects remains uncertain (Altshuller, 1987; Kelly et al., 1989; Pandis et al., 1992b).

3.2.3 Resuspension of Particulate Matter

The resuspension of deposited material as well as the suspension of material which has not been previously airborne can be an important source of particulate contamination (Gillette, 1980). This discussion will use "resuspension" to include both resuspension and suspension. Surface contamination may result from the atmospheric deposition of a number of materials; for some of these (e.g., plutonium), resuspension has been considered to be the most important exposure pathway. Likewise, resuspended soil particles have the greatest atmospheric mass over continents of any single particle type (Peterson and Junge, 1971). Despite this importance, the literature shows relatively few experimental or theoretical studies for the resuspension mechanism compared to other aerosol generation mechanisms. The following summarizes work on the physics of resuspension, physical/chemical properties of resuspension generated particles, and levels of production and transport of resuspended particles.

3.2.3.1 Resuspension Mechanics

Resuspension studies may be divided into applied research and detailed studies of mechanisms. Applied studies are usually motivated by atmospheric deposition of hazardous substances (i.e., radionuclides from the Chernobyl 1982 accident [Cambray, 1989]) and the need to predict the spreading of contamination and the lifetime of hazardous air concentrations. Resuspension experiments have been conducted over a wide range of surface types. Many experiments have been conducted in dry or arid regions, simply because many contamination events have occurred in such locations (i.e., the Nevada Test Site). Of the

experiments conducted over vegetation, most have been related to short grass. Alternately, applied studies may be motivated by mitigation efforts for soil erosion by wind or by need for measurement of high atmospheric particulate concentrations caused by resuspension, so-called "fugitive dust". Experiments concerning wind erosion have largely occurred in locations where wind erosion is prevalent, e.g., in the "Dust Bowl" area of the central United States.

3.2.3.2 Applied Studies

Resuspension can occur due to the action of wind or by mechanical stresses. Applied research considers resuspension factors, K (air concentration divided by surface concentration) (units of length^{-1}) and resuspension rates (flux of contaminant divided by surface concentration) (unit of time^{-1}). Mechanical stresses, such as disturbances by traffic or agricultural operations, might result in large amounts of resuspension over short intervals in specific localities. For example, Sehmel (1984) quotes K values of 4×10 m^{-1} (for beryllium particles by vigorous sweeping in an unventilated room) to 7×10^{-3} m^{-1} for plutonium particles in extensive traffic at the Nevada Test Site to 3×10^{-7} m^{-1} for gamma-radioactive-fallout by walking on the deposit in an Australian desert.

Wind generated resuspension is considered to be of major importance because it can be relatively continuous and can occur over large regions. Resuspension has been found to increase as a power of wind speed (with the resuspension rate being related to the second or third power of wind speed). Examples of resuspension factors from wind stresses quoted by Sehmel (1984) range from 3×10^{-4} m^{-1} for uranium at Maralinga trials to 9×10^{-11} m^{-1} for yttrium chloride on a cleared, sandy soil. Part of the range of Ks quoted above might be caused by the aging of deposits, although a lack of understanding of the mechanisms dominant in the resuspension process has precluded identifying any reasons for the wide range of results.

Nicholson's (1988) data verify previous work, giving an approximate 1/time decrease of the resuspension rate. Makhon'ko's (1986) data for resuspension from grass suggest a relationship between relative resuspension rate K´ versus phytomass *m* in grams per square meter, $K' = 2.9 \times 10^{-8}\ m^{-1.4}$ [sec^{-1}].

3.2.3.3 Aerodynamic Resuspension

Aerodynamic models include (1) balance of forces models and (2) statistical mechanisms. Balance of forces models account for forces holding the particles to the surfaces versus those forces acting to remove the particles from the surfaces. Experimental studies of particle motions show that particles being entrained into a turbulent fluid tend to move vertically into the stream with unsteady motions (Sutherland, 1967). Braaten et al. (1989) and Braaten and Paw U (1992) stressed the importance of bursts of a sweeping eddy having the characteristics of large shear stress near the wall where particles are sparsely deposited, breaking up the viscous sublayer and transporting fluid forces to the particles. This mechanism removes particles from a surface in short bursts followed by periods of little resuspension activity. Observations of Lycopodium spores placed on the flat floor of a wind tunnel were used to verify the model.

Reeks et al. (1988) proposed a different aerodynamic mechanism that would account for sudden random injections of particles into the air, the injections taking place more randomly in time than in the above force balance model. Their mechanism calls for the individual particles to accumulate energy from the turbulent stream (most efficiently at a resonant frequency for the particle). Accumulation of energy takes place because energy dissipation is limited by the local fluid and substrate. Once sufficient energy has accumulated to overcome the potential energy well holding it in place, the particle is resuspended. Slow motion movies of saltating sand surfaces showed such a vibrating motion of a particle before it becomes airborne (Willetts, 1992).

3.2.3.4 Mechanical Resuspension

The importance of mechanical disturbance is seen in the differences of resuspension factors given by Sehmel (1984) for mechanical activities over contaminated soil versus those for wind. Another example of the comparison of resuspension by mechanical disturbance with resuspension by the wind was given by Garland (1979) as a two-order-of-magnitude increase of the resuspension factor for the mechanical disturbance of a full 5-liter bottle dragged along the grass 20 times in 5 minutes in wind compared to the 10 m/s wind alone. Sehmel (1984) conducted experiments to determine the fraction of tracer particles resuspended by driving cars and trucks through the deposited tracer or near the deposited

tracer. The fraction increases with speed and size of vehicle. The fraction resuspended per vehicle pass increased as the first power of vehicle speed for the truck driven through the tracer, the fourth power of vehicle speed for a car driven through the tracer, and the third power of the vehicle speed for a car driven near the tracer.

The emission of PM_{10} particles in wind erosion is driven by the mechanical process of sandblasting, although Shinn et al. (1983) have pointed out the importance of direct aerodynamic emission for low emission rates below erosion threshold. Threshold velocities for particles smaller than 10 micrometer diameter are several times greater than that for 100 micrometer particles (Bagnold, 1941). Nonetheless, one observes submicrometer to 10-micrometer particles in wind erosion events for winds very much below the threshold velocity for the above mentioned particles. Gillette and Walker (1977) interpreted this to be caused by the mechanical suspension (sandblasting) of fine particles by more-easily-eroded sand particles. Shao et al. (1993) showed that sand-grain bombardment (saltation) is the overwhelmingly dominant mechanism in maintaining fine particle emissions from the surface. To derive an expression for the emission of dust, Shao et al. (1993) assumed that the number of dust particles dislodged from a surface per sand grain impact was proportional to the ratio for the kinetic energy loss of the impacting sand grain to the binding potential energy holding a dust particle to the surface. This assumption led to the prediction that the dust flux is proportional to the sand grain mass flux, which was in turn proportional to the friction velocity cubed. Dust emission is highly sporadic. After the wind stress threshold is surpassed, the vertical flux increases with the third power of friction velocity.

3.2.3.5 Physical and Chemical Properties of Resuspended Particles

The physical and chemical properties of resuspended particles depend partly on the properties of the particles that were deposited on the surface in the initial stage of resuspension. But, "the deposited particles probably lose their individual identity by becoming attached to host (soil) particles. When the pollutant particle is transported downwind, it is usually attached (aggregated) to this host particle" (Sehmel, 1973).

Furthermore, the host particle is most likely an aggregate itself. Studies of the cross section of particles, mineralogy, and scanning electron microscope analysis of dust samples show that

particles suspended from the soil are aggregated. For these reasons, this section describes physical properties of the aggregated (host plus pollutant) particles.

The size distribution of resuspended soil particles may be described as lognormal bimodal with one mode at 2 to 5 micrometers and another mode at 30 to 60 micrometers (Sviridenkov et al., 1993; Patterson and Gillette, 1977a,b; Gillette and Nagamoto, 1992; Gillette, 1974). Because the mass mode of the distribution for particles smaller than 10 micrometers is roughly at 2.5 micrometers, a rough approximation is that half the PM_{10} mass is smaller than 2.5 micrometers and half is larger. The ratio

$$\frac{v_{sed}}{u_*} < 0.1 \qquad (3\text{-}4)$$

defines the upper size of suspended dust, where v_{sed} is the sedimentation velocity of the upper size limit, and u_* is friction velocity. Data from Pinnick et al. (1985) show that very similar size distributions result from resuspension by traffic.

The mineralogical components of dust collected in Texas dust storms, given in order of abundance, are: for particles 1 to 10 micrometers: quartz, mica, kaolinite, mixed layer phyllosilicates and feldspars; for particles smaller than 1 micrometers: mica, kaolinite, quartz, and mixed layer phyllosilicates (Gillette et al., 1978). Studies of elemental composition show that composition of the resuspended material, compared to that of the total sediment, is enriched in elements associated with the smallest particles (i.e., titanium) and impoverished in elements associated with the coarsest materials (i.e., silicon).

3.2.3.6 Levels of Production and Transport of Resuspended Aerosols

Airborne dust measurements in the southern and central Great Plains states of the United States were made in the early 1970's. The total mass of dust produced by individual dust storms was 0.3 to 0.5×10^{12}g (Gillette et al., 1978). Individual dust storm production rates may be compared to the global production rate estimated by d'Alameida (1989) of 1,800 to 2,000 $\times$ 10^{12}g per year. The Great Plains study, part of a severe storm study, showed that the dust storms were typically associated with vigorous frontal activity, and that the dust travels great distances (many 100's of km) as tracked by jet aircraft. Estimates of

transport distance for dust of well over 1,000 km (from West Texas dust storms to deposition sites in northern Minnesota) were supported by isentropic trajectories, positions of rainclouds and elevated concentrations of calcium in collections of rainwater in the National Acid Deposition Program/National Trends Network. Even greater transport distances of resuspended dust are shown by oxygen isotopic 18 to 16 ratios (δ^{18}) in quartz (parts per thousand). By matching the δ^{18} value for deposited quartz and source areas for the quartz (wind erodible soils) the following long-range transport paths were found: Asian deserts to Hawaii; Sahara desert to the Caribbean, South America, and Florida; and U.S. sources to Greenland and northern Europe (Jackson et al., 1973).

A model developed for national acid rain and desertification/paleoclimate studies (Gillette and Passi, 1988) expressed the emission of dust for a given study area as an integral over friction velocity (expressing the forcing function), and the threshold friction velocity (expressing the resistance of the soil and environment to ablation). Results from the model for the contiguous United States (Figure 3-7) show a strong agreement of the model dust emissions with known emissions from dusty areas (Gillette and Hanson, 1989). Predicted alkaline emissions also agree in many respects with observed wet deposition patterns of alkaline elements (Gillette et al., 1992). A considerable fraction of wind emitted dust is from dust devils (Gillette and Sinclair, 1990).

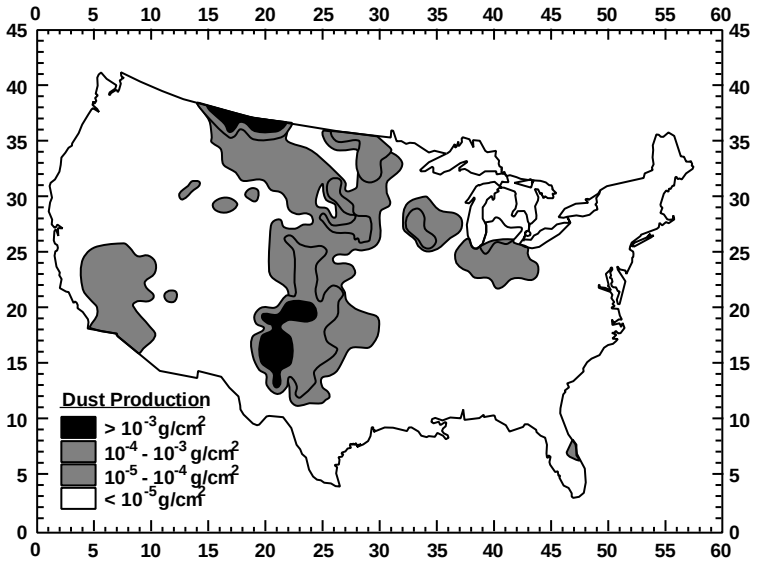

Figure 3-7. Model dust emissions for the United States.

Source: Gillette and Hanson (1989).

3.2.4 Particle Removal Mechanisms and Deposition

Particles in the air are in constant motion. They are subject to Brownian motion, which is the constant random movement along an irregular path caused by the bombardment by surrounding air molecules. This process is most important for small particles, and is related to the particle diffusion coefficient. Particles are also subject to the earth's gravitational force, as characterized by a sedimentation velocity. Gravitational settling is most important for larger particles. Both of these processes involve the motion of the particle relative to its surrounding air medium.

A particle subject to any constant external force will reach a terminal velocity called the drift velocity. The proportionality between the particle drift velocity (V_{drift}) and the external force (F_{ext}) is called the particle mobility, B, and is defined by:

$$B = \frac{V_{drift}}{F_{ext}} = \frac{C}{3\pi\mu D_p} \qquad (3\text{-}5)$$

where C is the Cunningham correction factor and μ is the particle velocity. The Cunningham correction factor must be introduced because when the particle diameter, D_p, approaches the same order as the mean free path of air, the resistance to particle motion becomes less than that predicted by continuum theory. The Cunningham correction factor increases as the particle size decreases. When the external force is that due to gravity (F_{ext} = mg), the drift velocity is the settling (sedimentation) velocity ($V_{drift} = V_{TS}$ = Bmg). If the external force is an electric field, then the drift velocity equals qEB where q is the electric charge on the particle and E is the electric field. Small particles are the most mobile. For particle diameters much smaller than the mean free path (D_p < 0.066 μm for air at standard conditions), B varies as the inverse square of the particle diameter. For large particles, B varies inversely with particle diameter. The particle diffusion coefficient is related to particle mobility by D = BKT.

Brownian diffusion is important for small particles, whereas gravitational settling is important for large ones. During a time period of 1 s a 0.1 µm particle will travel a total distance of about 40 µm due to Brownian motion, while it will fall about 1 µm due to gravity. In the same 1 s time period, a 1 µm particle will travel a total distance of about 8 µm due to Brownian motion and will fall 35 µm due to gravity. Note that the diffusion

constant is directly proportional to the particle mobility B, while the settling velocity depends on the product of particle mass and mobility, mB. Diffusion constants and settling velocities are plotted in Figure 3-8.

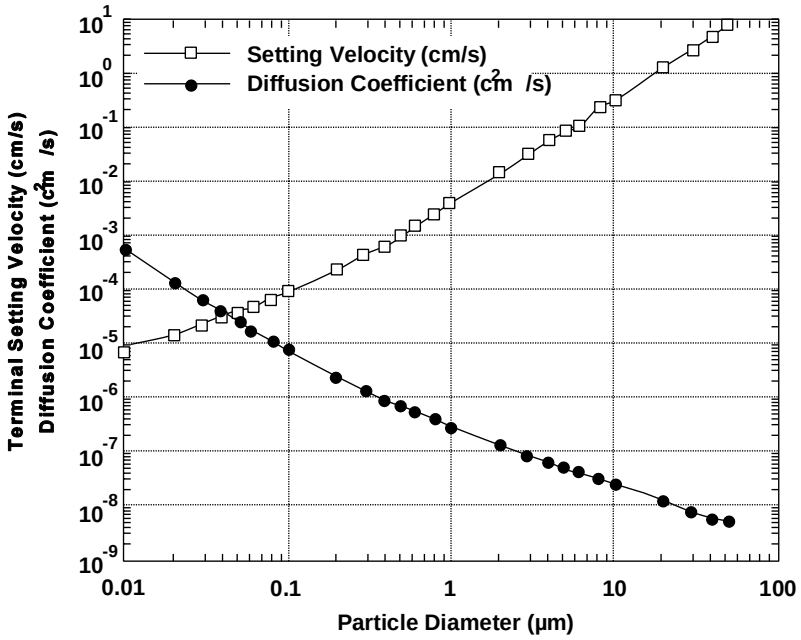

Figure 3-8. Diffusion constants and settling velocities for particles.

The deposition of particles in the atmosphere is not easily modeled, and is characterized by a deposition velocity, which is defined as the ratio of the flux of particles to the surface to the ambient concentration. Results from wind tunnel studies, shown in Figure 3-9, show characteristic minima. Small particles are collected by diffusion, larger particles are collected by impaction and sedimentation. Deposition models which account for these mechanisms are given by Sehmel (1980), Fernandez de la Mora and Friedlander (1982) and Fernandez de la Mora (1986). Atmospheric data from Lin et al. (1994), shown in Figure 3-10, show that inertial mechanisms, as well as sedimentation, are important for the deposition of large particles. As can be seen in Figure 3-9, these various removal mechanisms are least effective for particles in the 0.1 to 1.0 μm diameter size range. Therefore, accumulation mode particles, which occur mainly in this size range, have long

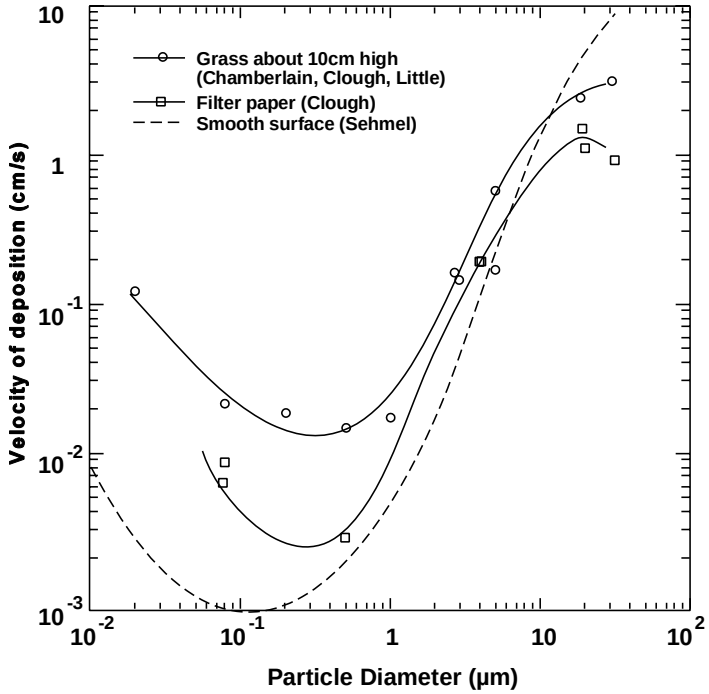

Figure 3-9. Particle deposition from wind tunnel studies.

Source: Chamberlain (1983).

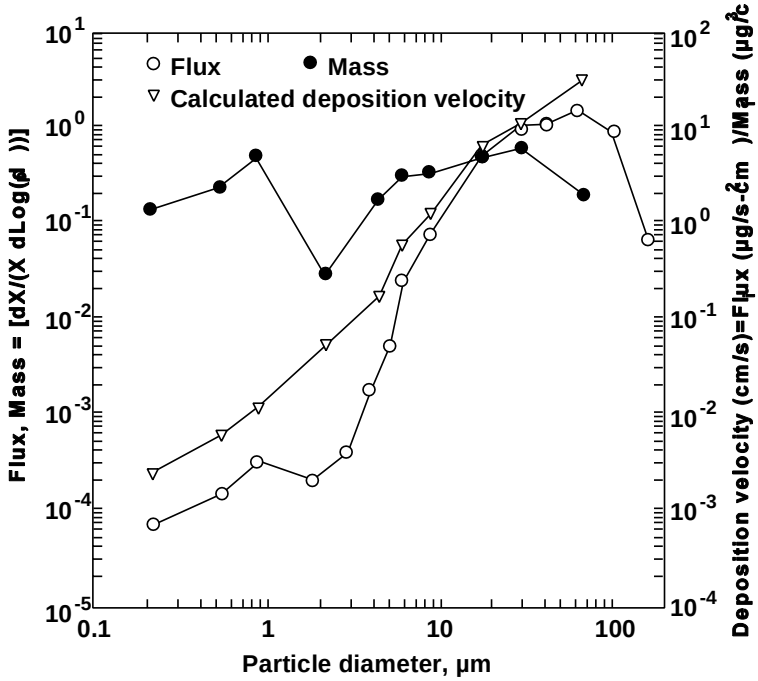

Figure 3-10. Sedimentation and inertia effects on large particle deposition.

Source: Lin et al. (1994).

lifetimes in the atmosphere. Such particles act as nuclei for the formation of cloud droplets and are removed when the cloud droplets grow large enough to fall as rain. Falling rain drops also remove larger particles by impaction and smaller particles by diffusion. More details on removal processes may be found in Sections 3.5 and 3.6.

3.3 CHEMICAL COMPOSITION AND PROCESSES

3.3.1 Acid Aerosols and Particulate Sulfates

Sulfuric acid and its neutralization products with ammonia constitute a major anthropogenic contribution to fine particle aerosol. This section reviews recent advances in understanding of the sources, removal processes, loadings and properties of tropospheric sulfate aerosols. Emphasis is given to properties and processes pertinent to these aerosols in regions influenced by anthropogenic emissions as distinguished from remote locations influenced primarily by natural sources.

3.3.1.1 Aerosol Acidity

Aerosol acidity can occur in suspended particulate matter (liquid or solid) or in the gas phase. The concept of aerosol acidity includes both the actual acid dissociation and the H^+ potentially available for reaction when the gas or particle contacts a liquid or solid surface (Waldman et al., 1995). With respect to pulmonary surfaces and fluids, many components in the air are acidic. The extent and location of acid deposition in the airways is greatly affected by whether exposure is to gaseous or particulate acids and also varies according to the size of particles.

The principal acids found in the atmosphere are related to mineral acids: particulate sulfuric acid (H_2SO_4) and bisulfate (HSO_4^-) and gaseous nitric (HNO_3), nitrous (HNO_2), and hydrochloric (HCl) acids. Organic acids (such as carboxylic and dicarboxylic acids) can also be found in the particulate and gaseous forms. Formic and acetic acids are the most abundant of organic acid compounds. As weak acids, these tend to exist in the nondissociated form and will often be volatile. In the atmosphere, the magnitude of particle acidity contributed from organic acids is generally found to be minor compared to particle strong acids (Lawrence and Koutrakis, 1994). However, organic and inorganic acids may be generated indoors (Zhang et al., 1994).

Particle strong acidity (PSA) has recently been reviewed by Waldman et al. (1995). The primary source of PSA is sulfuric acid, formed largely by oxidation of SO_2. When the acid is formed in the gas phase, it rapidly condenses to very small particles; these grow in the atmosphere by condensation and coagulation. When formed within cloud or fog droplets, the acidic sulfates are also found in the accumulation mode after the droplets evaporate. Measurements in southern Ontario for aerosols in several size ranges indicated that the vast majority of PSA was in the range of 0.2-2 μm (Koutrakis et al., 1989). The contribution to PSA from nuclei mode (<0.1 μm) particles is not substantial; acidic particles in this size range either grow or are neutralized rapidly. Particles larger than 2 μm contain little sulfate, but include wind-blown materials, in which there is often an abundance of alkaline materials.

The form of PSA is rarely pure sulfuric acid; H_2SO_4 can be partially neutralized to forms that are still acidic. A variety of crystalline forms intermediate in acidity between H_2SO_4 and $(NH_4)_2SO_4$ may be observed in the solid state. However, in the atmosphere, sulfate salts will usually be present in solutions containing H^+, NH_4^+, HSO_4^-, and $SO_4^=$. PSA is defined, in terms of molar or equivalent concentrations, as the sum of H^+ and HSO_4^-. Some writers have recommended that PSA be defined as the concentration of free H^+ ions in the particles as they exist in the atmosphere (Saxena et al., 1993). In this definition HSO_4^- would not be counted as contributing to the PSA. There are several disadvantages to this definition. The water associated with a particle increases as the relative humidity increases; as the solution becomes more dilute, more HSO_4^- dissociates and the PSA increases. Thus for this definition PSA varies with relative humidity and must be calculated from equilibrium theory. As a particle enters the lung the relative humidity increases to near 100% relative humidity and the PSA will also increase. If deposited in the lung all of the H^+ in HSO_4^- will be available for reaction. Therefore, it seems most useful for health effects purposes to define PSA as $[H^+] + [HSO_4^-]$ (Schlesinger, 1994; Saxena, 1994).

In practice PSA is measured by extracting collected particles and determining H^+ from a measurement of the pH of the solution. One technique uses a pH=4 solution of perchloric acid ($HCLO_4$), which prevents dissociation of weak acids but dilutes the solution sufficiently to allow dissociation of HSO_4^- (Koutrakis et al., 1988a,b; Suh et al., 1994a). PSA may also be measured by extracting the collected particles with water, titrating with base, and using

the Gran titration technique to determine strong acidity separate from weak acidity (Brosset et al., 1975).

Theory predicts a very fast neutralization reaction between PSA and atmospheric ammonia, which limited laboratory experiments with pure compounds appear to confirm (Huntzicker et al., 1980). However, measurements seem to indicate that neutralization is slower under field conditions and that some amount of PSA may persist even with ammonia present (Brauer et al., 1991; Liang and Waldman, 1992; Harrison and Kitto, 1992). Measurements of PSA and ammonia are normally averages over time periods of several to 24 h. Thus, it is possible that nonzero concentrations occur in different time intervals and only appear to be coincident. Recent research has evaluated the possibility that organic compounds retard the rate of neutralization (Daumer et al., 1992). Attenuation of regional PSA levels in central city locations has been observed to varying degrees. People and their activities generate ammonia, and in areas with higher population densities, ambient ammonia concentrations are generally higher. A study in Philadelphia showed daily decreases, in the city center relative to the suburbs, as high as 60%, although these were during a summer with pollution levels notably lower than the previous and subsequent summers (Suh et al., 1995). PSA levels are also attenuated indoors due to ammonia generated by people (Suh et al., 1992, 1994b).

The recent articles by Spengler et al. (1989) and Thompson et al. (1991) on the Harvard 24-cities study PSA results and Thurston et al. (1992) report data for daily (or alternate-day) sampling over the entire year at fixed sites. These have shown that the largest PSA exposures occur in the warmer months. The highest levels are specifically associated with summertime, regional stagnation periods. Frequently, PSA episodes are coincident with photochemical smog and high ozone levels, although the converse is not always the case. Simultaneous measurements on a regional scale have confirmed the spatial homogeneity in PSA levels over large areas. Good correlations for daily PSA concentrations among suburban sites 100 km apart were observed in New York (Thurston et al., 1992).

3.3.1.2 Sources of Sulfate

Knowledge of the sources of sulfates is important to understanding the processes responsible for the observed loading, composition, and size distribution of sulfates and to

developing effective methods to control sulfate concentration. Ambient sulfate may be either primary or secondary. Primary refers to material emitted into the atmosphere as particulate sulfate or as gas-phase SO_3 or H_2SO_4, species which readily nucleate and condense to form particles. Secondary refers to material that is formed by gas to particle conversion following the chemical reaction of SO_2, or other sulfur containing gases, to form SO_3, H_2SO_4, or $SO_4^=$ in solution. Most sulfate in the troposphere is secondary sulfate formed from SO_2.

Atmospheric oxidation of SO_2 takes place both by gas-phase reaction and by aqueous-phase reaction. The principal gas-phase mechanism is thought to be the OH-initiated reaction. The principal aqueous-phase reactions are thought to be oxidation by H_2O_2, O_2 (when catalyzed by trace metals), and O_3. Aqueous-phase reactions followed by cloud evaporation can result in formation of aerosol. Evaporation can be a major production route for atmospheric sulfate aerosols. The relative proportion of sulfate aerosol produced by the aqueous and gas-phase routes is not well established.

3.3.1.3 Gas-Phase Oxidation of Sulfur Dioxide

Gas phase oxidation of SO_2 is thought to occur largely, if not entirely, by a sequence of reactions initiated by the reaction of OH with SO_2.

$$SO_2 + OH + M \rightarrow HSO_3 + M \quad (3\text{-}6)$$

$$HSO_3 + O_2 \rightarrow SO_3 + HO_2 \quad (3\text{-}7)$$

$$SO_3 + H_2O \rightarrow H_2SO_4 \quad (3\text{-}8)$$

The gaseous H_2SO_4 subsequently adds to existing particles or may nucleate to form new particles.

Until recently the evidence for the occurrence of this reaction in the atmosphere has relied on modeled OH concentrations and on laboratory-determined reaction rate coefficient (Gleason et al., 1987) for the OH + SO_2 reaction. However, recent measurements of OH and H_2SO_4 in the atmosphere provide empirical evidence for this mechanism (Eisele and Bradshaw, 1993; Eisele and Tanner, 1993; Eisele et al., 1994). Simultaneous measurements

of OH and SO_2 allow the gas-phase reaction production rate of H_2SO_4 to be calculated at the time and location of the measurement. Likewise, measurements of particle size distribution allow the effective first-order rate coefficient for diffusive uptake of H_2SO_4 monomer by aerosol particles to be calculated, and measurement of the concentration of H_2SO_4 monomer allows the loss rate by this mechanism to be calculated. Comparison of the calculated production and loss rates of H_2SO_4 monomer show them to be equal, consistent with the observed steady state concentration of this species. This study lends substantial confidence to the applicability of the laboratory mechanism and rate to evaluation of the rate of sulfuric acid formation in the ambient atmosphere.

The reaction of SO_3 has recently been reexamined by Kolb et al. (1994), who find that the reaction is second order in water vapor and propose that the reaction takes place by interaction of SO_3 with water vapor dimer:

$$\mathbf{SO_3 + (H_2O)_2 \rightarrow H_2SO_4 + H_2O} \qquad (3\text{-}9)$$

The investigators note that it is probable that sufficient water dimer exists in the atmosphere to allow the reaction to efficiently form sulfuric acid vapor.

3.3.1.4 Aqueous-Phase Oxidation of Sulfur Dioxide

Aqueous-Phase Equilibria

The liquid water content of the atmosphere, w_L, is usually expressed either in g of water per m^3 of air or as a dimensionless volume fraction L (e.g., m^3 of liquid water per m^3 of air). Typical liquid water content values are 0.1 to 1 g m^{-3} ($L = 10^{-7} - 10^{-6}$) for clouds, 0.05 to 0.5 g m^{-3} ($L = 5 \times 10^{-7} - 5 \times 10^{-6}$) for fogs, and only 10^{-5} to 10^{-4}g m^{-3} ($L = 10^{-11} - 10^{-10}$) for aerosols. Cloud chemistry has been reviewed by Schwartz (1984a, 1986a). Aqueous-phase oxidation of SO_2 has recently been reviewed by Martin (1994).

For dilute solutions the equilibrium distribution of a reagent gas A between the gas and aqueous phases is given by Henry's law

$$[A] = H_A p_A \qquad (3\text{-}10)$$

where p_A is the partial pressure of A in the gas-phase, [A] is the equilibrium aqueous-phase concentration of A and H_A is the Henry's law coefficient for species A. The customary units of H_A are mole l^{-1} atm^{-1}. H_A can be viewed as the equilibrium constant of the reaction

$$A(g) \leftrightharpoons A(aq) \tag{3-11}$$

Table 3-2 gives the Henry's law coefficients of some atmospheric gases in liquid water at 298 K. The values given reflect only the physical solubility of the gas regardless of the subsequent fate of the dissolved species A. Some of the species included in Table 3-2 dissociate after dissolution or react with water. Henry's law constants do not account for these processes, and the modifications necessary will be discussed in the next paragraph. Henry's law coefficients generally decrease for increasing temperatures, reflecting the lower solubilities of gases at higher temperatures (Seinfeld, 1986).

Several gases, after dissolving in the aqueous-phase, ionize and establish an aqueous-phase chemical equilibrium system. For example for SO_2,

$$\mathbf{SO_2(g) \leftrightharpoons SO_2 \cdot H_2O} \tag{3-12}$$

$$\mathbf{SO_2 \cdot H_2O \leftrightharpoons HSO_3^- + H^+} \tag{3-13}$$

$$\mathbf{HSO_3^- \leftrightharpoons SO_4^{=} + H^+} \tag{3-14}$$

with

$$[_{\mathbf{SO_2}} = \frac{\mathbf{[SO_2 \cdot H_2O]}}{\mathbf{p_{SO_2}}},\ \mathbf{K_{s1}} = \frac{\mathbf{[HSO_3^-][H^+]}}{\mathbf{[SO_2 \cdot H_2O]}},\ \mathbf{K_{s2}} = \frac{\mathbf{[SO_4^{=}][H^-}}{\mathbf{[HSO_3^-]}} \tag{3-15}$$

K_{s1} and K_{s2} are the first and second dissociation constants for SO_2. It is convenient to

TABLE 3-2. HENRY'S LAW COEFFICIENTS OF SOME ATMOSPHERIC GASES DISSOLVING IN LIQUID WATER

Species	H (M/atm) (298 K)
O_2	1.3×10^{-3}
NO	1.9×10^{-3}
C_2H_4	4.8×10^{-3}
NO_2	1.0×10^{-2}
O_3	1.2×10^{-2}
N_2O	2.5×10^{-2}
CO_2	3.4×10^{-2}
H_2S	0.12
SO_2	1.23
CH_3ONO_2	2.6
OH	55.
HNO_2	49.
NH_3	57.
HO_2	2.0×10^{3}
HCOOH	5.6×10^{3}
HCHO	6.3×10^{3}
CH_3COOH	8.7×10^{3}
H_2O_2	1×10^{5}
HNO_3	2.1×10^{5}

Source: Schwartz (1986a).

consider the total dissolved sulfur in oxidation state IV as a single entity and refer to it as S(IV),

$$[S(IV)] = [SO_2 \cdot H_2O] + [HSO_3^-] + [SO_4^=] \quad (3\text{-}16)$$

The three sulfur species are in rapid equilibrium and therefore [S(IV)] changes only when SO_2 is transferred between the gas and aqueous phases. The total dissolved sulfur, S(IV), can be expressed as a function of only the pH and the partial pressure of SO_2 over the solution by:

$$[S(IV)] = H_{SO_2} p_{SO_2} \left[1 + \frac{K_{s1}}{[H^+]} + \frac{K_{s1}K_{s2}}{[H^+]^2} \right] \quad (3\text{-}17)$$

The above equation can be expressed in a form similar to Henry's law as

$$[S(IV)] = H^*_{S(IV)} p_{SO_2} \quad (3\text{-}18)$$

where $H^*_{S(IV)}$ is the effective (or modified) Henry's law coefficient given for S(IV) by

$$H^*_{S(IV)} = H_{SO_2} \left[1 + \frac{K_{s1}}{[H^+]} + \frac{K_{s1}K_{s2}}{[H^+]^2} \right] \quad (3\text{-}19)$$

The modified Henry's law coefficient relates the total dissolved S(IV) (not only $SO_2 \cdot H_2O$) with the SO_2 vapor pressure over the solution. The effective Henry's law coefficient always exceeds the Henry's law coefficient, indicating that the dissociation of a species enhances its solubility in the aqueous phase.

Several of the species that are in rapid equilibrium can be also considered as single entities:

$$[S(VI)] = [H_2SO_4(aq)] + [HSO_4^-] + [SO_4^{=}] \quad (3\text{-}20)$$

$$[N(V)] = [HNO_3(aq)] + [NO_3^-] \quad (3\text{-}21)$$

$$[NO_2^T] = [HNO_2(aq)] + [NO_2^-] \quad (3\text{-}22)$$

$$[HCHO^T] = [HCHO] + [H_2C(OH)_2] \quad (3\text{-}23)$$

Equations relating the total concentrations of these aqueous-phase species with the corresponding equilibrium concentrations of the gas-phase species can be derived similarly to those for S(IV).

Aqueous-Phase Reaction Mechanisms

The aqueous-phase conversion of dissolved SO_2 to sulfate is thought to be the most important chemical transformation in cloudwater. Dissolution of SO_2 in water results in the formation of three chemical species: hydrated SO_2 ($SO_2 \cdot H_2O$), the bisulfite ion (HSO_3^-) and the sulfite ion ($SO_3^=$). At the pH range of atmospheric interest (pH =2-7) most of the S(IV) is in the form of HSO_3^-, whereas at low pH (pH <2), all of the S(IV) occurs as $SO_2 \cdot H_2O$. At higher pH values (pH >7), ($SO_3^=$) is the preferred S(IV) state (Seinfeld, 1986). The individual dissociations are fast, occurring on timescales of milliseconds or less (Martin, 1984; Schwartz and Freiberg, 1981; Seinfeld, 1986). Therefore, during a reaction consuming one of the three species, $SO_2 \cdot H_2O$, HSO_3^-, or $SO_3^=$, the corresponding aqueous-phase equilibria are re-established instantaneously. The dissociation of dissolved SO_2 enhances its aqueous solubility. The total amount of dissolved S(IV) is quite pH dependent but always exceeds that predicted by Henry's law for SO_2 alone. The Henry's law coefficient for SO_2 alone, H_{SO_2}, is 1.23 M atm^{-1} at 298 K, while for the same temperature, the effective Henry's law coefficient for S(IV), $H^*_{S(IV)}$, is 16.4 M atm^{-1} for pH=3, 152 M atm^{-1} for pH=4 and 1,524 M atm^{-1} for pH=5. Equilibrium S(IV) concentrations for SO_2 gas-phase concentrations of 0.2-200 ppb, and over a pH range of 1 to 6 vary approximately from 0.001 to 1000 mM.

Several pathways for S(IV) transformation to S(VI) have been identified involving reactions of S(IV) with O_3, H_2O_2, O_2 (catalyzed by Mn^{2+} and Fe^{3+}), OH, SO_5^-, HSO_5^- SO_4^-, PAN, CH_3OOH, $CH_3C(O)OOH$, HO_2, NO_3, NO_2, N(III), HCHO and Cl_2^- (Pandis and Seinfeld, 1989a; Martin, 1994).

Although ozone reacts very slowly with SO_2 in the gas phase, the aqueous-phase reaction is rapid. The possible importance of O_3 as an aqueous-phase oxidant for S(IV) was first suggested by Penkett (1972) and the kinetics of

$$\mathbf{S(IV) + O_3 \rightarrow S(VI) + O_2} \qquad (3\text{-}24)$$

have been studied by several investigators (Erickson et al., 1977; Penkett et al., 1979; Maahs, 1983). Hoffmann and Calvert (1985), after a detailed investigation of existing

experimental kinetic and mechanistic data, suggested the following expression for the rate of the reaction of S(IV) with dissolved ozone:

$$= -\frac{d[S(IV)]}{dt} = (k_0[SO_2 \cdot H_2O] + k_1[HSO_3^-] + k_2[SO_3^{=}])[O$$ (3-25)

recommending the values $k_0 = 2.4 \times 10^4$ M^{-1} s^{-1}, $k_1 = 3.7 \times 10^5$ M^{-1} s^{-1} and, $k_2 = 1.5 \times 10^9$ M^{-1} s^{-1}. They also proposed that this reaction proceeds by nucleophilic attack on ozone by $SO_2 \cdot H_2O$, HSO_3^-, and $SO_3^{=}$. An increase in the aqueous-phase pH results in an increase of all three, [$SO_2 \cdot H_2O$], [HSO_3^-] and [$SO_3^{=}$], equilibrium concentrations and therefore in an increase of the overall reaction rate. For an ozone gas-phase mixing ratio of 30 ppb, the reaction rate varies from less than 0.001 mM h^{-1} (ppb SO_2)$^{-1}$ at pH=2 (or less than 0.01% SO_2(g) h^{-1} (g water /m^3 air)$^{-1}$) to 3,000 mM h^{-1} (ppb SO_2)$^{-1}$ at pH=6 (7,000% SO_2 (g) h^{-1} (g water /m^3 air)$^{-1}$). The gas-phase SO_2 oxidation rate is of the order of 1% h^{-1} and therefore the S(IV) heterogeneous oxidation by ozone is significant for pH values greater than 4. The strong positive dependence of the reaction rate on the pH renders this reaction self limiting. The production of sulfate by this reaction lowers the pH and effectively decreases the rate of further reaction. The availability of atmospheric ozone guarantees that this reaction will play an important role both as a sink of gas-phase SO_2 and as a cause of cloudwater acidification as long as the pH of the atmospheric aqueous phase exceeds 4.

Hydrogen peroxide, H_2O_2, is one of the most effective oxidants of S(IV) in clouds and fogs (Pandis and Seinfeld, 1989a; Jacob and Hoffmann, 1983; Chameides, 1984; Schwartz, 1986a; Seigneur and Saxena, 1988; Nair and Peters, 1989; Bott and Carmichael, 1993). H_2O_2 is very soluble in water and under typical ambient conditions its aqueous-phase concentration is approximately six orders of magnitude higher than that of ozone. This reaction has been studied in detail by several investigators (Hoffmann and Edwards, 1975; Penkett et al., 1979; Martin and Damschen, 1981; Cocks et al., 1982; Kunen et al., 1983; McArdle and Hoffmann, 1983) and the reproducibility of the measurements suggests a lack of susceptibility of this reaction to influence of trace constituents. The proposed rate expression is (Hoffmann and Calvert, 1985)

$$R_2 = -\frac{d[S(IV)]}{dt} = \frac{k[H^+][H_2O_2][HSO_3^-]}{1 + K[H^+]} \quad (3\text{-}26)$$

with k=7.45 × 10^7 M^{-1} s^{-1} and K=13 M^{-1} at 298 K. Noting that H_2O_2 is a very weak electrolyte; that $[H^+]$ $[HSO_3^-]$ = $H_{SO_2}K_{s1}p_{SO_2}$ (Equation 3-15); and that for pH> 2, 1 + K $[H^+]$~1, one concludes that the rate of this reaction is practically pH independent in the pH range of atmospheric interest. For a H_2O_2(g) mixing ratio of 1 ppb the rate is roughly 300 mM h^{-1} (ppb SO_2)$^{-1}$ (700% SO_2(g)h^{-1} (g water /m^3 air)$^{-1}$). The near pH independence can also be viewed as the result of the cancellation of the pH dependence of the S(IV) solubility and the reaction rate constant. The reaction is very fast and indeed both field measurements (Daum et al., 1984a) and theoretical studies (Pandis and Seinfeld, 1989b) have suggested that H_2O_2(g) and SO_2(g) rarely coexist in clouds and fogs. The species with the lowest concentration before the cloud or fog formation is the limiting reactant, and is rapidly depleted inside the cloud or fog layer.

The fastest, aqueous-phase, atmospheric reaction of SO_2 is believed to be with hydrogen peroxide, and with ozone at higher pH values. However, results of a study by Hofmann and Jacob (1984) show that in heavily polluted atmospheric water droplets, such as those found in urban fogs, metal-catalyzed oxidation by O_2 contributes significantly to formation of sulfate in the liquid phase, and in such situations may be more important than oxidation by hydrogen peroxide. Organic peroxides have been also proposed as potential aqueous-phase oxidants of dissolved sulfur (Graedel and Goldberg, 1983; Lind and Lazrus, 1983; Hoffmann and Calvert, 1985). However, simulations for typical continental clouds suggest that these reactions are of minor importance for the S(IV) oxidation and represent only small sinks for the gas-phase methylhydroperoxide (0.2% CH_3OOH h^{-1}) and peracetic acid (0.7% $CH_3C(O)OOH$ h^{-1}).

The S(IV) oxidation by O_2 is known to be catalyzed by Fe^{3+} and Mn^{2+}

$$S(IV) + 1/2\ O_2 \xrightarrow{Mn^{2+},\ Fe^{3+}} S(VI) \quad (3\text{-}27)$$

This reaction has been the subject of considerable interest (Hoffmann and Boyce, 1983; Martin, 1984, 1994; Martin et al., 1991; Hoffmann and Jacob, 1984; Hoffmann and Calvert, 1985; Clarke and Radojevic, 1987) and significantly different measured reaction rates, rate laws and pH dependencies have been reported (Hoffmann and Jacob, 1984). Martin and Hill (1987a,b) have demonstrated that this reaction is inhibited as ionic strength increases. They explained most of the literature discrepancies by differences in these factors during the various laboratory studies.

In the presence of oxygen, iron in the ferric state, Fe(III), catalyzes the oxidation of S(IV) in aqueous solutions. Fe(II) appears not to catalyze the reaction directly but must be first oxidized to Fe(III) before S(IV) oxidation can begin (Huss et al., 1982a,b). The recent review by Martin (1994) gives a comprehensive discussion of the oxidation of SO_2 by O_2 in the presence of iron.

For pH values from 0 to 3.6 the iron-catalyzed S(IV) oxidation rate is first order in iron, first order in S(IV) and is inversely proportional to $[H^+]$ (Martin and Hill, 1987a),

$$\mathbf{R} = -\frac{\mathbf{d[S(IV)]}}{\mathbf{dt}} = \mathbf{k_1}\frac{\mathbf{[Fe^{3+}][S(IV)]}}{\mathbf{[H^+]}} \tag{3-28}$$

This reaction is inhibited by ionic strength and sulfate and these effects are described by:

$$\mathbf{k_1} = \mathbf{k_1^*} \times \mathbf{10}^{\frac{-2\,I^{1/2}}{1 + I^{1/2}}} \tag{3-29}$$

and

$$\mathbf{k_1} = \mathbf{k_1^*}\frac{\mathbf{1}}{\mathbf{1 + 150[S(VI)]^{2/3}}} \tag{3-30}$$

where I is the ionic strength of the solution and [S(VI)] is in M. A rate constant $k_1^* = 6\ s^{-1}$ has been recommended by Martin and Hill (1987a). Sulfite appears to be almost as equally inhibiting as sulfate.

The rate expression for the same reaction changes completely above pH 3.6. This suggests that the mechanism of the reaction differs in the two pH regimes, and is probably a

free radical chain at high pH and a non radical mechanism at low pH (Martin et al., 1991). The low solubility of Fe(III) above pH 3.6 presents special experimental problems. At high pH the reaction rate depends on the amount of iron in solution, rather than on the total amount of iron present. At this range the reaction is second order in dissolved iron (zero order above the solution iron saturation point) and first order in S(IV). The reaction is still not very well understood and Martin et al. (1991) proposed the following phenomenological expressions (in M s^{-1})

$$\text{pH4.0: } -\frac{d[S(IV)]}{dt} = 1\times10^{9}[S(IV)][Fe^{3+}]^{2} \tag{3-31}$$

$$\text{pH5.0-6.0: } \frac{d[S(IV)]}{dt} = 1\times10^{-3}[S(IV)] \tag{3-32}$$

$$\text{pH7.0: } -\frac{d[S(IV)]}{dt} = 1\times10^{-4}[S(IV)] \tag{3-33}$$

for the following conditions:

$$[S(IV)] \simeq 10\mu M, [Fe^{3+}] > 0.1\mu M,\ I < 0.01M,\ [S(VI)] < 100M,\ \text{and}\ T = 298K.$$

Note that iron does not appear in the pH 5-7 rates because it is assumed that a trace of iron will be present under normal atmospheric conditions. This reaction is important in this high pH regime (Pandis and Seinfeld, 1989a,b; Pandis et al., 1992b).

Martin et al. (1991) also found that non-complexing organic molecules (e.g., acetate, trichloroacetate, ethyl alcohol, isopropyl alcohol, formate, allyl alcohol, etc.) are highly inhibiting at pH values of 5 and above, and are not inhibiting at pH values of 3 and below. They calculated that, for remote clouds, formate would be the main inhibiting organic, but by less than 10%. In contrast, near urban areas formate could reduce the rate of the catalyzed oxidation by a factor of 10-20 in the high pH regime.

The manganese catalyzed S(IV) oxidation was initially thought to be inversely proportional to the H^{+} concentration. Martin and Hill (1987b) suggested that ionic strength, not

hydrogen ion, accounts for the pH dependence of the rate. These authors were also able to explain some unusual behavior described in the literature on this reaction and to partially reconcile some of the literature rates. The manganese catalyzed reaction obeys zero-order kinetics in S(IV) in the concentration regime above 100 mM S(IV),

$$-\frac{d[S(IV)]}{dt} = k_o[Mn^{2+}]^2 \quad (3\text{-}34)$$

$$k_o = k_o^* \times 10^{\frac{-4.07\ I^{1/2}}{1 + I^{1/2}}} \quad (3\text{-}35)$$

with $k_o^* = 680\ M^{-1}\ s^{-1}$ (Martin and Hill, 1987b). For S(IV) concentrations below 1 mM the reaction is first order in S(IV),

$$-\frac{d[S(IV)]}{dt} = k_o[Mn^{2+}][S(IV)] \quad (3\text{-}36)$$

$$k_o = k_o^* \times 10^{\frac{-4.07\ I^{1/2}}{1 + I^{1/2}}} \quad (3\text{-}37)$$

with $k_o^* = 1{,}000\ M^{-1}\ s^{-1}$ (Martin and Hill, 1987b). It is still not clear which rate law is appropriate for use in atmospheric calculations, although Martin and Hill (1987b) suggested the provisional use of the first order, low S(IV) rate.

When both Fe^{3+} and Mn^{2+} are present in atmospheric droplets, the overall rate of the S(IV) reaction is enhanced over the sum of the two individual rates. Martin (1984) reported that the rates measured were 3 to 10 times higher than expected from the sum of the independent rates. Martin et al. (1991) obtained at pH 3.0 and for [S(IV)] < 10 mM the following rate law

$$\frac{[S(IV)]}{dt} = 750[Mn(II)][S(IV)] + 2600[Fe(III)][S(IV)] + 1.0\times10^{10}[Mn(II)][Fe(III)][S(I$$

(3-38)

and a similar expression for pH 5.0 in agreement with the work of Ibusuki and Takeuchi (1987).

Free radicals, such as OH and HO_2, either heterogeneously scavenged by the aqueous phase or produced in the aqueous phase, participate in a series of aqueous phase reactions (Graedel and Weschler, 1981; Chameides and Davis, 1982; Graedel and Goldberg, 1983; Schwartz, 1984b; Jacob, 1986; Pandis and Seinfeld, 1989a).

Pandis and Seinfeld (1989a) proposed that under typical remote continental conditions there are two main radical pathways resulting in the conversion of S(IV) to S(VI):

$$S(IV)(+OH) \rightarrow SO_5^- \ (+O_2^-) \rightarrow HSO_5^- \ (+HSO_3^-) \rightarrow S(VI) \qquad (3\text{-}39)$$

$$S(IV)(+OH) \rightarrow SO_5^- \rightarrow SO_4^- \ (+Cl^-, HSO_3^- \rightarrow S(VI) \qquad (3\text{-}40)$$

with the first of these two pathways typically being faster that the second.

Nitrogen dioxide has a low water solubility and therefore its low resulting aqueous-phase concentrations suggests that its oxidation of S(IV)

$$2NO_2 + HSO_3^- \xrightarrow{H_2O} 3H^+ + 2NO_2^- + SO_4^= \qquad (3\text{-}41)$$

should be of minor importance in most cases. This reaction has been studied by Lee and Schwartz (1983) at pH 5.0, 5.8 and 6.4 and was described as a reaction that is first order in NO_2 and first order in S(IV), with a pH-dependent rate constant. The evaluation of this rate expression (3-41) was considered tentative by Lee and Schwartz (1983), in view of evidence for the formation of a long-lived intermediate species. The apparent rate constant was found to increase with pH. This reaction is considered of secondary importance at the concentrations and pH values representative of clouds. However, Pandis and Seinfeld (1989b) reported that for fogs occurring in urban polluted areas with high NO_2 concentrations this reaction could be a major pathway for the S(IV) oxidation, if the atmosphere has enough neutralizing capacity, e.g. high NH_3 (g) concentrations.

Sulfite and bisulfite can form complexes with various dissolved aldehydes. One important example is the reaction of sulfite or bisulfite with formaldehyde to produce hydroxymethanesulfonate ion (HMS) (Boyce and Hoffmann, 1984; Munger et al., 1984, 1986; Olson and Hoffman, 1989; Facchini et al., 1992).

The HMS formed acts as a S(IV) reservoir protecting it from further oxidation, and its formation has been advanced to explain high S(IV) concentrations that have been observed in clouds, fogs, and dew (Pierson and Brachaczek, 1990). The rates of S(IV) complexation and oxidation are highly dependent on cloud pH and on the concentrations of HCHO and oxidants. Characteristic times for S(IV) depletion through complexation and oxidation can be compared for typical ranges of HCHO, H_2O_2, and pH. At pH values below about 4, the rate of complex formation is several orders of magnitude slower than the reaction of S(IV) with dissolved H_2O_2. Thus, in this range oxidation predominates over complexation. The characteristic times of the two reactions become approximately comparable at pH around 5 so that complexation with HCHO becomes competitive with oxidation by H_2O_2. When pH exceeds 6, the reactions of S(IV) with HCHO became more important than reaction with H_2O_2. HMS formation can inhibit S(IV) oxidation if the S(IV) complexation rate is comparable to, or greater than, the S(IV) oxidation rate and the rate of SO_2 mass transport into the drop controls the rate of S(IV) oxidation. The effectiveness of HMS as a S(IV) reservoir depends critically on its resistivity to OH attack.

Formation of Sulfates in Clouds

The atmospheric aqueous phase (clouds, fogs) can be viewed as a processor of the aerosol size/composition distribution (Pandis et al., 1990a,b). Precipitating clouds are well known to be the major removal mechanism of aerosol particles from the atmosphere. At the same time, the liquid droplets provide the reacting medium for aqueous-phase reactions (Graedel and Weschler, 1981; Chameides and Davis, 1982; Graedel and Goldberg, 1983; Jacob and Hoffmann, 1983; Munger et al., 1983; Chameides, 1984; Seigneur and Saxena, 1984; Hoffmann and Jacob, 1984; Fuzzi et al., 1984; Hong and Carmichael, 1986a; Hill et al., 1986; Jacob, 1986; Jacob et al., 1985, 1986a,b; Johnson et al., 1987; Fuzzi et al., 1988; Dlugi, 1989; Pandis and Seinfeld, 1989a,b; Munger et al., 1990; Forkel et al., 1990; Bott, 1991; Joos and Baltensperger, 1991; Barth, 1994; De Valk, 1994). Several gaseous species dissolve in cloudwater and react giving products that remain in the aerosol phase after the cloud dissipates; for example, the dissolution of SO_2, its ionization, and subsequent oxidation to sulfate. These species can attract additional gaseous species, such as ammonia and water into the aerosol phase and thereby increase further the aerosol mass. Therefore, aerosol processing by nonprecipitating clouds represents a

mechanism by which atmospheric particles can grow during their residence time in the atmosphere. A detailed review of the state of science in 1990 has been presented by United States National Acid Precipitation Assessment Program (U.S. NAPAP) (1991).

A cyclical relationship between the occurrence of smog and fog in polluted areas has been proposed by Munger et al. (1983) and was termed the smog-fog-smog cycle. In a polluted atmosphere with high aerosol concentration, the formation of late night and early morning fogs is augmented enhancing smog production, visibility reduction, and aerosol sulfate the next day (Cass, 1979; Cass and Shair, 1984; Pandis et al., 1990a,b). Processing of aerosol by clouds can result in similar cyclical relationships and enhanced contribution of the aerosol produced in clouds to ground-level particulate concentrations (Altshuller, 1987). This processing cycle accelerates the production of atmospheric acidity through aqueous-phase reactions (Schwartz, 1989).

Cloud Effects on Particle Number Concentration

There has been a series of observations of enhanced aerosol number concentrations in the vicinity of clouds (Saxena and Hendler, 1983; Hegg et al., 1990; Radke and Hobbs, 1991; Hegg et al., 1991). Saxena and Hendler (1983) suggested that the observed high aerosol number concentrations near clouds could be due to the shattering of rapidly evaporating droplets. Hegg et al. (1991) proposed that the high actinic radiation fluxes near cloud tops could lead to high OH concentrations and nucleation of new H_2SO_4/H_2O particles. The high relative humidity areas around clouds often have total particle number concentrations about twice those in the air at the same level but well removed from the cloud boundaries (Radke and Hobbs, 1991). Kerminen and Wexler (1994a,b) have demonstrated that there is high nucleation probability associated with these high relative humidity areas, especially near relatively clean clouds. All these speculated mechanisms for production of new particles produce negligible new aerosol mass, but may influence the shape of the aerosol distribution, especially in remote regions. Aqueous-phase reactions producing sulfate and nitrate increase the aerosol mass, but do not influence directly the aerosol number concentration, unless some cloud droplets shatter into many smaller droplets.

The removal of gas-phase SO_2, H_2SO_4, and NH_3, due to their transfer to the aqueous-phase, indirectly slows down the production of new particles in the vicinity of the cloud.

Cloud Effects on Aerosol Mass Concentration

Significant production of sulfate has been detected in clouds and fogs in different environments (Lazrus et al., 1983; Hegg and Hobbs, 1987, 1988; Pandis and Seinfeld, 1989b; Husain et al., 1991; Swozdziak and Swozdziak, 1990; Pandis et al., 1992b; De Valk, 1994; Liu et al., 1993). The detection of sulfate-producing reactions is often hindered by the variability of cloud liquid water content and the temporal instability and spatial variability in concentrations of reagents and product species (Kelly et al., 1989). The production of sulfate has also been detected and investigated in laboratory clouds (Hansen et al., 1991). Aqueous-phase oxidation of HSO_3^- by H_2O_2 is particularly fast, as illustrated by the mutual exclusivity of SO_2 and H_2O_2 observed in clouds (Daum et al., 1984a,b, 1987). Other reactions, including oxidation of dissolved SO_2 by ozone and oxidation by O_2 catalyzed by Fe^{3+} and Mn^{2+}, may also contribute, significantly in some cases, to sulfate production (Pandis et al., 1990b; Barth et al., 1992; Barth, 1994). During aqueous-phase sulfate production the reactants including SO_2, H_2O_2, O_3, and OH are transferred from the gas phase to the cloud droplets. This transport includes a series of steps (gas-phase diffusion, transport across the gas-liquid interface, dissociation and aqueous-phase diffusion) that ultimately couple the gas and aqueous phases and in some cases control the overall sulfate production rate (Schwartz, 1988).

The formation of sulfate in raining and non-raining clouds has been modeled (Seigneur et al, 1984; Seigneur and Saxena, 1988; Seigneur and Wegrecki, 1990). The results have been compared to experimental measurements of cloud chemistry. Contributions to sulfate formation from gas-phase reactions and from various aqueous phase mechanisms during daytime and nighttime can be compared.

Hydrogen peroxide is the most important oxidant for the conversion of SO_2 in cloud water at pH 4.5 or lower (Calvert et al., 1985) and dominates the aqueous sulfate formation pathways (McHenry and Dennis, 1994) in the northeastern United States. The measured H_2O_2 gas-phase mixing ratio over the northeastern and central United States has been reported to vary from 0.2 to 6.7 ppb (Sakugawa et al., 1990) with the highest values during

the summer and the lowest during the winter months. The H_2O_2 concentrations usually increase with decreasing latitude and increasing altitude (Sakugawa et al., 1990). The availability of hydrogen peroxide may be the limiting factor in sulfate formation in clouds. This limitation is more pronounced near SO_2 sources and during the winter months. The seasonal contribution of clouds to sulfate levels depends on both the availability of oxidants and on the cloud cover. In cases where the sulfate cloud production is oxidant limited, changes in aerosol sulfate levels will be less than proportional to SO_2 emission changes, with the relationship being more nonlinear in winter than in spring or summer (U.S. NAPAP, 1991).

Evaluations of the rate of the SO_2-H_2O_2 reaction in cloudwater indicate that the characteristic time for this reaction is a few minutes to an hour, depending on conditions (Schwartz, 1984a; Meagher et al., 1990). Since such a reaction time is shorter than the lifetime of stratiform clouds in the troposphere it is anticipated that the reaction of SO_2 and H_2O_2 will proceed to completion in liquid water stratiform clouds. Evidence of this occurring would be that only one or the other of these species would be present in such clouds, but not both at the same time. This expectation has been borne out in field measurements supporting the inference of rapid reaction given by the model estimates. Daum and colleagues (Daum et al., 1984a; Daum, 1988) have presented results of simultaneous aircraft measurements of H_2O_2 in collected cloudwater samples and SO_2 in air (filter pack measurements) in nonprecipitating stratiform clouds indicating that in almost all instances either one or the other species was at very low concentrations, and by inference that the reaction has proceeded essentially to completion in the clouds. A rather different set of results was reported by Husain et al. (1991) who conducted measurements of gas-phase SO_2 and H_2O_2 during cloud events at Whiteface Mountain, NY. Although a general negative correlation between the two species concentrations was exhibited, the data indicated substantial periods of apparent coexistence of these species.

There is the possibility of spatial inhomogeneities in the clouds that are not resolved in the sampling period (typically 30 min in the Daum studies; an hour or more for the Husain studies), in which one region was H_2O_2 rich and another SO_2 rich. In such instances a lack of coexistence of the two species would be masked by the extended duration of sampling. Such spatial inhomogeneities might also account for the few instances reported by Daum in

which SO_2 and H_2O_2 apparently coexisted in clouds. Additionally, local patches of subsaturated air in the clouds during the sampling period might also account for these observations, although Daum took efforts to exclude such instances from their data base. Yet another possible explanation of the Husain results is that the cloud was relatively newly formed, and the material had not had time to react. An obvious improvement in this approach is to measure the species, as well as cloud liquid water content, with greater time resolution. Burkhard et al. (1994) have reported aircraft measurements of gas-phase SO_2 and H_2O_2 during in-cloud flights; traces of liquid water content are also shown. These data support a strong anticorrelation of SO_2 and H_2O_2 in clouds on various time (location) scales, with numerous instances of peaks of SO_2 coincident with valleys of H_2O_2 and vice versa.

A quantitative estimate of the amount of cloudwater sulfate that is formed by in-cloud reaction can be gained by inferring the amount of cloudwater sulfate that derives from preexisting sulfate aerosol. Husain et al. (1991) has used selenium as a tracer to allow such inferences to be drawn. By measuring the sulfate to selenium ratio in clear air aerosol that is representative of the aerosol that is the pre-cloud aerosol of the clouds under investigation, and by assuming that the fractional incorporation of the sulfate and selenium into cloudwater is identical (and/or by measuring this ratio), it is possible to infer the amount of cloudwater sulfate derived from preexisting sulfate aerosol and, by difference, the amount formed by in-cloud reaction. A series of such studies carried out at Whiteface Mountain, NY, indicates that the assumption of identical scavenging of sulfate and selenium is valid (1.04 ± 0.29; 1.04 ± 0.19 in two separate cloud systems). Evidence of enhanced sulfate in cloudwater, attributed to sulfate formed by in-cloud reaction, was found in five of six cloud systems studied; amounts formed were consistent with ambient SO_2 concentrations. Examination of the pH dependence of the concentration of in-cloud produced sulfate inferred by this technique indicated that sulfate was produced by in-cloud reaction only at pH values below 4.0, consistent with oxidation by H_2O_2, but not with oxidation by O_3.

Recently Snider and Vali (1994) reported studies of oxidation of SO_2 in winter orographic clouds in which SO_2 was released and the extent of increased concentrations of sulfate in cloudwater (relative to the unperturbed cloud) were compared to decreased concentrations of H_2O_2 (sum of gaseous plus aqueous, inferred from aqueous concentrations). Despite considerable scatter, the data fall fairly close to the one-to-one line, indicative of the

expected stoichiometry of reaction, Figure 3-11. The investigators also modeled the reaction kinetics. The rate of reaction is sensitive to the liquid water content (LWC) of the cloud during the time between the point of cloud condensation to the point of sampling. Since this profile was not known the investigators assumed a linear profile for LWC versus time. The resulting model predictions agreed closely with the extent of reaction inferred from changes in H_2O_2 and sulfate concentrations, supporting the applicability of the model.

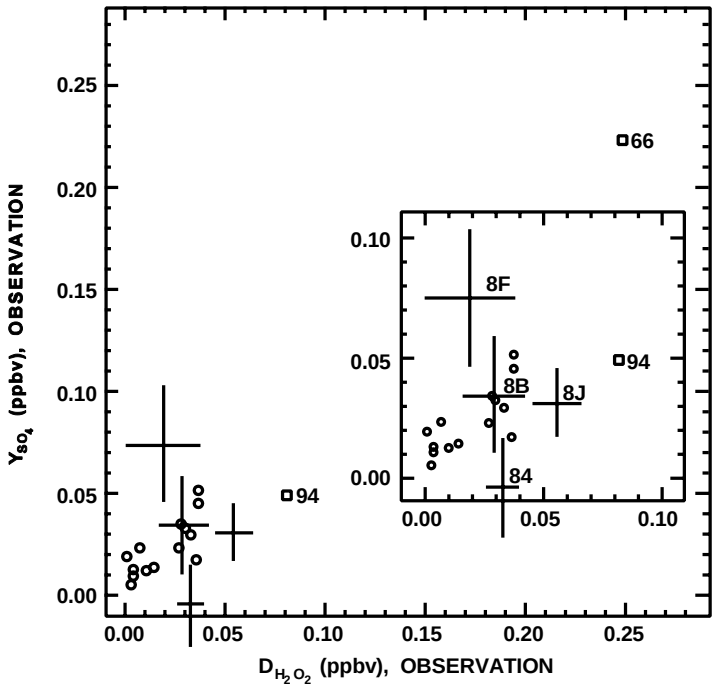

Figure 3-11. Comparison of observed hydrogen peroxide (H_2O_2) depletions ($D_{H_2O_2}$, abscissa) and observed sulfate yields (Y_{SO4}, ordinate). Errors associated with experiments 84, 8B, 8F, and 8J are indicated and data values from these experiments are labeled in the inset figure. Data values corresponding to experiments 94 and 66 are also labeled. The slope of the best fit line, forced through the origin, and calculated using only those data values indicated by circles is 1.21 (±0.13).

Source: Snider and Vali (1994).

In contrast to the H_2O_2 reaction, oxidation of SO_2 by O_3 exhibits a strong pH dependence. The reaction is quite rapid at high pH (~6) but is expected to greatly slow down as strong acid is

produced in the course of the reaction. However, if concentrations of NH_3 or other basic materials are sufficiently high to maintain a pH above 5, the reaction can continue to proceed at a high rate.

Walcek et al. (1990) calculated that, during the passage of a midlatitude storm system, over 65% of the sulfate in the troposphere over the northeastern United States was formed in cloud droplets via aqueous-phase chemical reactions. The same authors indicated that, during a 3-day springtime period, chemical reactions in clouds occupying 1 to 2% of the tropospheric volume were responsible for sulfate production comparable to the gas-phase reactions throughout the entire tropospheric volume under consideration. McHenry and Dennis (1994) estimated that annually more than 60% of the ambient sulfate in Central and Eastern United States is produced in clouds with the non-precipitating cloud production dominating over precipitating cloud production. Spatial variability of emissions and ambient H_2O_2 concentrations induces spatial variability in the contribution of in-cloud sulfate production, making it highest in the south. These conclusions are in quantitative agreement with similar calculations of Dennis et al. (1993) and Karamchandani and Venkatram (1992). Aqueous-phase oxidation in clouds is also the most important pathway for the conversion of SO_2 to sulfate on the global scale (Hegg, 1985; Langner and Rodhe, 1991).

Clouds could under some conditions also be a significant source of aerosol nitrate during the night. Choularton et al. (1992) and Colvile et al. (1994) observed production of around 0.5 $\mu g\ m^{-3}$ of nitrate during the processing of an air parcel by a hill cap cloud. They speculated that the sources of this nitrate were gaseous N_2O_5 and NO_3.

Chemical heterogeneities in the droplet population affect significantly the overall sulfate production rate and the produced sulfate size distribution (Seidl, 1989; Twohy et al., 1989; Lin and Chameides, 1991; Pandis et al., 1990a,b; Ayers and Larson, 1990; Hegg and Larson, 1990; Bower et al., 1991; Ogren and Charlson, 1992; Roelofs, 1992a,b; 1993; Carter and Borys, 1993; Bott and Carmichael, 1993; Collett et al., 1993b). Neglecting these chemical concentration differences could result in significant underestimations of the sulfate production rates in some cases (Hegg and Larson, 1990; Roelofs, 1993). Ice-related microphysical processes can also have a significant impact on cloud chemistry (Taylor, 1989; Wang and Chang, 1993; Collett et al., 1993a).

Fogs in polluted environments have the potential to increase aerosol sulfate concentrations by droplet phase reactions but at the same time to cause reductions in the aerosol concentrations of nitrate, chloride, ammonium and sodium, as well as in the total aerosol mass concentration, because of the more rapid deposition of larger fog droplets compared to smaller particles (Pandis et al., 1990a). Pandis et al. (1992b) calculated that more than half of the sulfate in a typical Los Angeles air pollution episode was produced inside a fog layer the previous night. This heterogeneously produced sulfate represented 5 to 8% of the measured PM_{10} mass.

Aqueous-Phase Oxidation of Sulfur Dioxide in Aerosols

Until recently it was thought that the low amount of liquid water associated with particles (volume fraction on the order of 1×10^{-10}, compared to clouds, for which the volume fraction is the order of 1×10^{-7}) precluded significant aqueous-phase conversion of SO_2 in such droplets. However, field studies (McMurry, et al., 1981; McMurry and Wilson, 1982, 1983) of aerosol growth as a function of size suggest the occurrence of aqueous-phase reactions. Model studies (Saxena and Seigneur, 1987) indicate that conversion of SO_2 to sulfate in aerosols at 90% relative humidity can contribute perhaps 10% to the total sulfate formation (90% due to the gas-phase reaction of SO_2 with OH). At night the conversion rate is lower, 10% of the daytime rate, and is almost all due to aqueous-phase reactions. At higher relative humidities and/or lower temperatures the aqueous-phase contribution would be expected to increase.

Sievering and colleagues (1991) have also called attention to the possibility of rapid oxidation of SO_2 by O_3 in aqueous sea-salt aerosols, which are buffered by the alkalinity of sea salt particles,. Indeed, it appears that such a rate may initially be quite rapid, 1 $\mu M\ s^{-1}$ corresponding to 8% h^{-1}, in the example given by Sievering et al. (1991) for liquid water content 50 $\mu g\ m^{-3}$ and SO_2 concentration 2 n mol m^{-3} (mixing ratio 0.05 ppb). Despite this rapid initial rate, it would appear that the extent of such oxidation may be quite limited. For the example given by Sievering et al. (1991), the sea-salt sodium concentration is given as 100 n mol m^{-3}. Based on the concentrations of (HCO_3^- + $CO_3^=$) and Na^+ in seawater (2.25 and 454 m mol kg^{-1}, respectively), the alkalinity of the sea salt aerosol is expected to be 0.5 n mol m^{-3}. Consequently, after only 0.25 n mol m^{-3} of SO_2 is taken up in solution

and oxidized (i.e., 12% of the initial SO_2), the initial alkalinity would be exhausted, and the reaction rapidly quenched.

Sievering et al. (1994) have presented field measurements over Lake Michigan of coarse-mode sulfate (diameter 5-20 μm), which they ascribe at least in part to oxidation of SO_2 in such particles derived from wind driven spray of lake water, in which the pH is maintained high by alkalinity present in the lake water. Calculations were carried out for liquid water volume fraction of 13×10^{-12} ($13\ \mu g\ m^{-3}$). The alkalinity was inferred from the measured cation minus anion difference (cations NH_4^+, Mg^{++}, Ca^{++}; anions $SO_4^=$, NO_3^-) in the coarse mode, which averaged 26 neq m^{-3}, corresponding to an aqueous alkalinity of 2×10^{-5} M. In the absence of mass transport limitation the rate of the aqueous-phase O_3-SO_2 reaction was calculated to be $7 \pm 3 \times 10^{-4}$ M s^{-1}; however, mass transport limitation reduced this rate by a factor of 20 to 40 at pH 7. The conversion rate referred to gas-phase SO_2 was calculated as 0.5 to 1.7% h^{-1}. The investigators concluded that this mechanism is a significant contributor to the SO_2 oxidation under these conditions. Again, however, concern may be raised with that conclusion, namely that the indicated oxidation rate, 2×10^{-5} M s^{-1} after taking mass transport limitation into account, would quickly produce an acidity equal to the initial alkalinity, thereby quenching the reaction.

3.3.2 Particulate Nitrates

3.3.2.1 Sources

By analogy to the sulfur system, sources of aerosol nitrates might be distinguished into primary, gas-phase, and aqueous-phase. However, as primary nitric acid emissions are considered to be small, the present discussion focuses on in situ production mechanisms in the atmosphere. Once nitric acid has been formed its reaction with ammonia in the gas phase may lead to the formation of particulate ammonium nitrate. Nitric acid may also react with salts of chloride or carbonate, releasing the corresponding acid, and forming a particulate salt or a solution.

3.3.2.2 Major Gas-Phase Reaction

The principal mechanism for gas-phase production of nitrates is reaction of OH with NO_2 to form HNO_3.

$$OH + NO_2 + M \rightarrow HNO_3 \quad (3\text{-}42)$$

Here, as with SO_2, the mechanism and rate of the gas-phase reaction is well established from laboratory studies (see Hicks et al., 1991), and the principal source of uncertainty in describing the reaction rate is the concentrations of the reagent species, mainly OH.

The reaction of OH with NO_2 is approximately 10 times as fast as the reaction of OH with SO_2 (Equation 3-6) (Finlayson-Pitts and Pitts, 1986). Therefore, NO_2 is preferentially converted to HNO_3 and the conversion of SO_2 to H_2SO_4 is delayed until much of the NO_2 has reacted (Gillani and Wilson, 1983).

3.3.2.3 Major Aqueous-Phase Reaction

A second key pathway for formation of nitric acid is the reaction sequence:

$$NO_2 + O_3 \rightarrow NO_3 + O_2 \quad (3\text{-}43)$$

$$NO_3 + NO_2 \rightleftharpoons N_2O_5 \quad (3\text{-}44)$$

$$N_2O_5 + H_2O(l) \rightarrow 2HNO_3(aq) \quad (3\text{-}45)$$

The reaction of N_2O_5 with water vapor is thought to be slow, but reaction with condensed water, in cloud or fog droplets, or in or on the surface of wet particles, is thought to be fast (Tuazon et al., 1983). Other reactions of NO_3 and/or N_2O_5, for example N_2O_5 with aromatics (Pitts et al., 1985a,b) must also be considered. Reaction of N_2O_5 with liquid water appears to be rapid and irreversible. Studies of the uptake of N_2O_5 on aqueous sulfuric droplets give mass accommodation coefficients of about 0.1 (Mozurkewich and Calvert, 1988; Van Doren et al., 1990; Fried et al., 1994) . Thus the overall rate and yield of this reaction can be evaluated from the pertinent gas-phase rate constants and the mass transfer rate constant for uptake of N_2O_5 by aqueous aerosol or cloud droplets (Finlayson-Pitts and Pitts, 1986).

3.3.2.4 Other Reaction Mechanisms

Reactions of NO_3 other than Equation 3-39 must be considered. In daytime NO_3 may undergo photolysis.

$$NO_3 \xrightarrow{h\nu} NO + O_2 \qquad (3\text{-}46)$$

However, during the night NO_3 concentration can build up sufficiently that formation of HNO_3 by hydrogen abstraction from alkanes and aldehydes may become significant (Finlayson-Pitts and Pitts, 1986).

The aqueous-phase reactions of NO and NO_2 to yield HNO_3 also need to be considered. Field measurements comparing the chemical composition of cloud droplets and rain with that of the surrounding air suggest the conversion of nitrogen oxides to nitric acid in the aqueous phase (Lazrus et al., 1983; Colvile et al., 1994). The aqueous-phase conversion of NO_2 to nitric acid,

$$2NO_2 + H_2O(l) \rightarrow 2H^+ + NO_2^- + NO_3^- \qquad (3\text{-}47)$$

has been proposed. However, laboratory studies indicate that this reaction in pure water is too slow to be an important source of HNO_3 in clouds (Schwartz, 1986b). Measurements in smog chambers and indoor environments, however, suggest that a heterogeneous analog of Equation 3-43 may be occurring.

Aqueous phase reactions of NO_2 with O_2, O_3, and H_2O_2 are also though to be insignificant under representative atmospheric conditions (Schwartz, 1986b). The chemical kinetics of the aqueous-phase oxidation of NO by O_2 has been reexamined by two groups (Lewis and Deen, 1994; Pires et al.,1994). Evaluation of the rate of this reaction in cloudwater confirms that the reaction rate is negligible under atmospheric conditions, as indicated earlier by Schwartz and White (1983).

3.3.2.5 Ammonium Nitrate Vaporization Equilibria

In the sulfate system the vapor pressure of H_2SO_4 is negligible, so that all sulfate may be considered present in the particles. Also, at least for acidic sulfates (that is, not fully neutralized) the vapor pressure of NH_3 is likewise negligible. Even for fully neutral $(NH_4)_2SO_4$ any hydrolysis of NH_4^+ to form NH_3 that might escape to the vapor phase is suppressed by the resultant acidity. In contrast, nitrates in aerosols are distinguished from sulfates because of the volatility of NO_3^- (as HNO_3) and of NH_4NO_3 (as $NH_3 + HNO_3$). The equilibrium

$$\mathbf{NH_4NO_3\ (s)\ or\ (aq)\ \rightleftharpoons\ NH_3(g) + HNO_3(g)} \qquad (3\text{-}48)$$

is such that at ambient conditions the partial pressures of NH_3 and/or HNO_3 are appreciable above crystalline NH_4NO_3 and likewise above solutions containing NH_4^+ and NO_3^- ions (of not necessarily equal concentrations). It is thus necessary to consider these equilibria not just for the crystalline material but also for solutions, in the latter case as a function of concentration or, equivalently, water activity. Such a treatment has been given in detail by Stelson and Seinfeld (1982a,b), and that study is the basis for much subsequent interpretation of field measurements.

As an example of such a study, Harrison and Msibi (1994) compare the measured concentration product of HNO_3 and NH_3 versus the equilibrium constant for the reaction. Agreement is found roughly within a factor of 2 or so based on assumption of equilibrium with pure NH_4NO_3 (crystal or solution). However, when the observations were stratified by relative humidity, no strong trend of measured concentration product with relative humidity was evidenced.

As noted above, the time scale of reaching this equilibrium is of interest, for example as it may influence dry deposition or accommodation to changing gaseous environments, as in human airways. Wexler and Seinfeld (1990) modeled the time dependence of achieving this equilibrium and concluded that equilibrium is generally reached within seconds to minutes for typical aerosol loadings. By evaluating the time scales for equilibrium of vapor-phase species with a population of aerosol particles, Wexler et al. (1992) found that ammonium salts in the gas and aerosol phases are not always in equilibrium, especially under

less polluted and cooler conditions. Thus, both transport and thermodynamic properties of the aerosol population govern the distribution of ammonium salts. At low temperatures and low aerosol loadings the time constant for achieving this equilibrium could be a day or more.

An important implication of the high vapor pressure of ammonium nitrate (as $NH_3 + HNO_3$) is that ammonia will distill from any ammonium nitrate if there is an acidic site present, for example acidic sulfate that is less than fully neutralized by ammonia. As a consequence ammonium nitrate aerosol cannot exist indefinitely in the presence of acidic sulfate aerosol (Gebhart et al., 1994).

A further consequence of this equilibrium is the influence it may exert on dry deposition. Sievering et al. (1994) reported steep gradients of NH_4NO_3 concentration with height above forest canopies, and inferred high rates of deposition of particulate nitrate, 2 to 9 cm s^{-1}, comparable to those of gaseous HNO_3. They attribute this to the large particle size of the nitrate, 2 to 2.5 μm mean diameter, citing calculation of Peters and Eiden (1992). An alternative explanation of the observations, which does not appear to be ruled out, is that the deposition is actually of HNO_3. The deposition of HNO_3 may perturb the equilibrium of NH_4NO_3 with $NH_3 + HNO_3$, leading to a decrease of NH_4NO_3 in the vicinity of the surface and giving the appearance of enhanced deposition of the particulate species.

3.3.2.6 Sulfate/Nitrate Interaction

In the eastern United States enough H_2SO_4 is usually formed to react with the available NH_3. Indeed, the sulfate is frequently acidic, the average composition in the summer being approximately NH_4HSO_4. Since appreciable concentrations of NH_3 and HNO_3 are present in equilibrium with NH_4NO_3, while the vapor pressure of NH_3 in equilibrium with $(NH_4)_2SO_4$ or NH_4HSO_4 is very low, NH_4NO_3 is not stable in the presence of NH_4HSO_4 and transformations produce $(NH_4)_2SO_4$ and HNO_3. However, if SO_2 emissions are reduced and less H_2SO_4 is formed, some NH_3 may be left over after all H_2SO_4 has been converted to $(NH_4)_2SO_4$. Particulate NH_4NO_3 will form if the concentrations of HNO_3 and excess NH_3 are sufficient to exceed the equilibrium constant of Equation 3-38, $K_p = [HNO_3][NH_3]$, which at 17°C, is 4 ppb^2 over the solid and 1 ppb^2 over the solution droplet at 85% relative humidity (Harrison and Msibi, 1994).

If the H_2SO_4 formed in the atmosphere is insufficient to react with all available NH_3, i.e. $1/2[H_2SO_4]<[NH_3]$, the concentration of sulfate plus nitrate may be controlled by the amount of NH_3 available (until the concentration of sulfate plus nitrate is less than the amount needed to react with NH_3, i.e., $1/2[H_2SO_4] + [HNO_3] < [NH_3]$. Thus, as SO_2 emissions are reduced, NH_4NO_3 may replace $(NH_4)_2SO_4$.

NH_4NO_3 would not be expected to have as long a lifetime in the atmosphere as $(NH_4)_2SO_4$. It is likely that HNO_3 will have a very high dry deposition rate. As HNO_3 is removed by dry deposition, NH_4NO_3 will evaporate to maintain the $[HNO_3][NH_3]$ concentration product. Modeling studies have not addressed this issue, perhaps because of lack of certainty in the necessary parameters: the NH_4NO_3 equilibrium constant, the NH_4NO_3 evaporation rate, the HNO_3 dry deposition rate, and the atmospheric concentrations of NH_3.

Sampling problems caused by the volatility of NH_4NO_3 are discussed in Chapter 4, Section 4.2.10.1. Reliable measurements of NH_4NO_3 require special techniques, e.g. denuders to remove gas-phase HNO_3 and nylon filters to absorb any HNO_3 vapors that evaporate from collected NH_4NO_3 (Benner et al., 1992; Koutrakis et al., 1992). Large concentrations of NH_4NO_3, observed in areas of California where NH_3 is high and SO_2 emissions are low (Hering et al., 1988; Benner et al., 1991), suggest that replacement of $(NH_4)_2SO_4$ by NH_4NO_3 as SO_2 emissions are reduced is a possibility.

3.3.2.7 Ammonium Chloride Vaporization Equilibrium

Although particulate chloride is not a major component of the atmospheric ambient aerosol, it is of interest because it is involved in some particulate formation processes. For example, sea salt contains NaCl that may react with HNO_3 to lead to $NaNO_3$ coarse particles and a release of HCl. HCl could react with NH_3 to form particulate ammonium chloride (NH_4Cl). However, the concentrations of NH_3 and HCl are typically too low and the volatility of NH_4Cl too high, to lead to NH_4Cl condensation. However, in stack plumes with high concentrations of HCl and NH_3 (NH_3 may be emitted from a stack with a selective catalytic reduction system), NH_4Cl particles could be formed. Therefore, it is important to include NH_4Cl in formulations of aerosol equilibria (see e.g., Wexler and Seinfeld, 1990, 1991; Seigneur and Wu, 1992).

3.3.3 Carbon-Containing Particulate Matter

The carbonaceous fraction of ambient particulate matter consists of both elemental (EC) and organic carbon (OC). Elemental carbon, also called black carbon or graphitic carbon, has a chemical structure similar to impure graphite and is emitted directly into the atmosphere predominantly during combustion. Organic carbon is either emitted directly by sources (primary OC) or can be formed *in situ* by condensation of low volatility products of the photooxidation of hydrocarbons (secondary OC). Soot is sometimes used to refer to the primary carbonaceous aerosol (sum of primary EC and OC) but soot has no firmly established definition. Small additional quantities of aerosol carbon may exist either as carbonates (e.g., $CaCO_3$) or CO_2 adsorbed onto particulate matter (Appel et al., 1989; Clarke and Karani, 1992).

3.3.3.1 Elemental Carbon

Elemental carbon is a strong absorber of visible radiation and is the major species responsible for light absorption by atmospheric particles (Novakov, 1984; Goldberg, 1985; Finlayson-Pitts and Pitts, 1986; Japar et al., 1986; Sloane et al., 1991; Hamilton and Mansfield, 1991). Elemental carbon found in atmospheric particles is a complex three dimensional array of carbon with small amounts of other elements such as oxygen, nitrogen, and hydrogen incorporated in its graphitic hexagonal structure (Chang et al., 1982).

Wood-burning fireplaces and diesels are major sources of EC (Mulhbaier and Williams, 1982; Dasch and Cadle, 1989; Brown et al., 1989; Dod et al., 1989; Hansen and Rosen, 1990; Burtscher, 1992). In areas where wood burning is significant, more particulate graphitic carbon is expected in winter than in summer. Tracer techniques have been developed for the calculation of the source contribution to the EC concentrations, including use of K as a woodsmoke tracer (Currie et al., 1994) and use of the carbon isotopic tracers ^{14}C and ^{12}C (Lewis et al., 1988; Klouda et al., 1988; Currie et al., 1989). Around 47% of the EC in Detroit, 93% in Los Angeles and 30 to 60% in a rural area in Pennsylvania has been attributed to motor vehicle sources (Wolff and Korsog, 1985; Pratsinis et al., 1988; Keeler et al., 1990). The corresponding contribution of diesel emissions to EC concentrations in Western Europe is estimated to be 70 to 90% (Hamilton and Mansfield, 1991). Elemental carbon was also a major constituent of the

Kuwait oil fires, with concentrations as high as 178 mg m^{-3} inside the plume (Cofer et al., 1992; Daum et al., 1993; and references therein). Global emissions of EC were estimated by Penner et al. (1993) to be 12.6 to 24 Tg C yr^{-1}, while the EC emission for the US was 0.4 to 1.1 Tg yr^{-1} and for the rest of North America 0.2 Tg yr^{-1}.

Elemental carbon also scatters light (Appel et al., 1985) although its light scattering efficiency is smaller than the efficiencies of the other aerosol principal components (Sloane et al., 1991). Because EC both absorbs and scatters light, its contribution to total light extinction exceeds its contribution to fine particle mass. For example, in Los Angeles, EC was found to represent 8.5 to 10% of the fine particulate mass, but to account for 14 to 21% of the total light extinction (Pratsinis et al., 1984). A significant fraction of the dark colored fine EC particles is able to penetrate the indoor atmosphere of buildings and may constitute a soiling hazard of objects like works of art (Ligocki et al., 1993).

The concentration of EC varies with location and season. Elemental carbon concentrations in rural and remote areas usually vary from 0.2 to 2.0 μg m^{-3} (Wolff, 1981; Clarke et al., 1984; Goldberg, 1985; Cadle and Dasch, 1988; Japar et al., 1986; Shah et al., 1986; Pinnick et al., 1993) and from 1.5 to 20 μg m^{-3} in urban areas (Wolff, 1981; Delumyea and Kalivretenos, 1987; Pratsinis et al., 1984, 1988; Grosjean, 1984a; Heintzenberg and Winkler, 1984; Goldberg, 1985; Shah et al., 1986; Rau, 1989). The concentration of EC over the remote oceans is approximately 5 to 20 ng m^{-3} (Clarke, 1989). Average EC concentration values are around 1.3 and 3.8 μg m^{-3} for U.S. rural and urban sites respectively (Shah et al., 1986). Average PM_{10} EC values exceeding 10 μg m^{-3} are common for some urban locations (Chow et al., 1994). The ratio of EC to total carbon has been observed to vary from 0.15 to 0.20 in rural areas, to 0.2 to 0.6 in urban areas (Wolff et al., 1982; Gray et al., 1984; Grosjean, 1984a; Pratsinis et al., 1984; Chow et al., 1993a). The annual mean of this ratio was approximately 0.4 for the Los Angeles basin in 1982 (Gray et al., 1986), while this ratio in the same area decreases to 0.2 during summer midday periods (Larson et al., 1989; Wolff et al., 1991). Aging of an air mass results in lowering of the EC fraction of the aerosol due to its mixing with non-combustion particles or by condensation of material from the gas phase (Burtscher et al., 1993).

The distribution of EC emitted by automobiles is unimodal with over 85% of the mass in particles smaller than 0.12 μm aerodynamic diameter (Venkataraman et al., 1994). The ambient distribution of EC is bimodal with peaks in the 0.05 to 0.12 μm (mode I) and 0.5 to 1.0 μm

(mode II) size ranges (Nunes and Pio, 1993; Venkataraman and Friedlander, 1994). The creation of mode II is mainly the result of accumulation of secondary aerosol products on primary aerosol particles.

The degree of mixing of EC particles with other aerosol components is controversial. Particles emitted from spark-ignition engines have been found to consist of a core of EC covered with a layer of PAHs and an outermost shell of volatile compounds (Steiner et al., 1992). Ambient carbonaceous aerosol in urban areas has been found to consist of aggregated spherules, with a range of carbon structures from amorphous (OC) to graphitic (EC) within aggregates (Katrinak et al., 1992). These aggregates are often (especially during summer months) coated with sulfates and nitrates (Katrinak et al., 1992, 1993). However, often sulfate and EC are externally mixed (Covert and Heintzenberg, 1984). Coating of EC with organic compounds may alter its hygroscopicity and its lifetime in the atmosphere (Andrews and Larson, 1993). Noone et al. (1992a) reported that the interstitial aerosol inside urban fogs is enriched in EC, something that would tend to increase its lifetime in the atmosphere with respect to other species like sulfate or OC (Nunes and Pio, 1993). However, the degree of incorporation of EC in droplets is highly variable (0 to 80%) and its behavior appears to vary from hygroscopic to hydrophobic (Hansen and Novakov, 1989). Our lack of understanding of the processes, where by EC changes from hydrophobic to hygroscopic, makes a quantitative estimate of the atmospheric lifetime of EC problematic.

The participation of EC and soot in atmospheric chemical reactions with SO_2, O_3 and NO_2 has been the subject of a series of studies (Baldwin, 1982; Dlugi and Güsten, 1983; Akhter et al., 1984, 1985; Jassim et al., 1986; Sergides et al., 1987; Gundel et al., 1989; Chughtai et al., 1991). The strong dependence of the often conflicting results of these studies on the nature of the samples inhibits the extrapolation of their conclusions to the atmosphere. Chughtai et al. (1991) reported that oxidation and hydrolysis of accessible reactive sites on the soot surface result in particle solubilization and accelerated particle removal from the atmosphere. DeSantis and Allegrini (1992) suggested that NO_2 reactions in the presence of SO_2 on carbon-containing particles could be a source of HNO_2 in the urban environment. The reaction of soot with ozone is faster than its reaction with NO_2, which in turn is faster than its reaction with SO_2 (Smith et al., 1989). The review by Hoffmann and Calvert (1985) concludes that the reaction of soot with

SO_2 is not a major atmospheric pathway for sulfate formation.

3.3.3.2 Organic Carbon

The organic component of ambient aerosol both in polluted and remote areas is a complex mixture of hundreds of organic compounds (Cass et al., 1982; Seinfeld, 1986; Rogge et al., 1993d; Hahn, 1980; Simoneit and Mazurek, 1982; Zafiriou et al., 1985; Graedel, 1986; Gray et al., 1986). Only 10 to 20% of the organic material has been characterized in terms of molecular structure. Compounds identified in the ambient aerosol include n-alkanes, n-alkanoic acids, n-alkanals, aliphatic dicarboxylic acids, diterpenoid acids and retene, aromatic polycarboxylic acids, polycyclic aromatic hydrocarbons, polycyclic aromatic ketones and quinones, steroids, N-containing compounds, regular steranes, pentacyclic triterpanes, iso- and anteiso-alkanes, etc. (Graedel, 1986; Mazurek et al., 1989; Hildemann et al., 1991, 1993, 1994; Rogge et al., 1993d). OC does not strongly absorb light, but its light scattering efficiency in urban hazes is similar to that of nitrate and sulfate (McMurray et al., 1995; Lowenthal et al., 1995).

Aerosol OC measurements are often subject to sampling artifacts due to adsorption of organic vapors on the filters used or evaporation of the collected mass. These sampling problems are discussed in Section 3.3.3.1. Wolff et al. (1991) found that this sampling error represented roughly 20% of the measured OC under urban polluted conditions. McMurry and Zhang (1989) observed in ambient and smog chamber measurements that a consistently large fraction of the OC (40 to 70%) was collected on the quartz filters following their impactors. The strong possibility of sampling artifacts in the laboratory and field measurements presented below, increases the uncertainty of our current knowledge about aerosol OC. Most of the investigators report the OC concentration as concentration of carbon. These values neglect the contribution to the aerosol mass of the other elements (namely oxygen, hydrogen and nitrogen) of the organic aerosol compounds. Measured OC values have been multiplied by 1.5 (Wolff et al.. 1991) or 1.4 (White and Macias, 1989) to estimate the total organic mass.

The concentration of OC is around 3.5 μg C m^{-3} in rural locations (Stevens et al., 1984) and 5 to 20 μg C m^{-3} in polluted atmospheres (Grosjean, 1984a; Wolff et al., 1991).

Wolff et al. (1991) and Chow et al. (1994) summarizing measurements during the summer and fall of 1987 in the Los Angeles basin, reported that OC represented on average 10 to 18% of the PM_{10} mass and 11 to 24% of the $PM_{2.5}$ mass during the summer and 15 to 25% of the PM_{10} and 16 to 25% of the $PM_{2.5}$ during the fall. Wolff et al. (1991) suggested that these values should be reduced by roughly 20% to correct for the sampling bias and then multiplied by 1.5 to account for the non-carbon mass of the organic aerosol compounds (an overall increase by roughly a factor of 1.3). In rural areas of the western U.S. particulate OC concentrations are comparable to sulfate (White and Macias, 1989). In other areas OC contributes roughly 10 to 15% of the $PM_{2.5}$ and PM_{10} mass (Stevens et al., 1984). Organic compounds accumulate mainly in the submicrometer aerosol size range (Finlayson-Pitts and Pitts, 1986; McMurry and Zhang, 1989) and their mass distribution is typically bimodal with the first peak around diameter of 0.2 μm and the second around 1 μm (Pickle et al., 1990; Mylonas et al., 1991).

The contribution of the primary and secondary components of aerosol OC have been difficult to quantify. The lack of a direct chemical analysis method for the identification of either of these OC components has led researchers to the employment of several indirect methods. These methods include the use of tracer compounds for either the primary or the secondary OC (Larson et al., 1989; Turpin and Huntzicker, 1991, 1995; Turpin et al., 1991), the use of models describing the emission and dispersion of primary OC (Gray, 1986; Gray et al., 1986; Larson et al., 1989; Hildemann, 1990) and the use of models describing the formation of secondary OC (Pilinis and Seinfeld, 1988; Pandis et al., 1992a; Pandis et al., 1993). The above studies concluded that the secondary OC contribution is maximized in the early afternoon of summer days, varying from 30 to 60% of the total OC depending on location. The yearly averaged contribution of secondary OC is smaller, 10 to 40%.

The interactions of the OC compounds with each other and the inorganic aerosol species are poorly understood. The compounds have the potential to form organic films around the inorganic and EC core of the aerosol (Gill et al., 1983). Goschnick et al. (1993) provided evidence for such formation by reporting that carbon compounds and organic hydrogen were enriched within the particles' outer layer, while inorganics like NH_4NO_3 were enriched inside the particles. The presence of such films can inhibit the transport of water and other inorganic components between the gas and aerosol phases (Otani and Wang, 1984;

Rubel and Gentry, 1984). However, atmospheric OC may be water-soluble and hygroscopic as well as water-insoluble (Saxena et al., 1995) and organic particles may serve as cloud-condensation-nuclei (Novakov and Penner, 1993).

Primary Organic Carbon

Primary carbonaceous particles (OC) are produced by combustion (pyrogenic), chemical (commercial products), geological (fossil fuels), and natural (biogenic) sources. The complexity of the molecular composition of OC is such that tracer compounds are still necessary to decouple the contributions of the various sources. Rogge et al. (1991) suggested that fine aerosol cholesterol could be used as a tracer for meat smoke. An alternative proposed meat smoke tracer set consists of myristic acid (n-tetradecanoic acid), palmitic acid (n-hexadecanoic acid), stearic acid (n-octadecanoic acid), oleic acid (cis-9-octadecenoic acid), nonanal and 2-decanone (Rogge et al., 1991). Benzothiazole has been used as a tracer for tire wear contributions to ambient aerosol (Kim et al., 1990; Rogge et al., 1993b). Steranes and pentacyclic triterpanes (hopanes) can be used as tracer compounds for the vehicular sources (Rogge et al., 1993a). The odd carbon number n-alkanes ranging from C_{27} to C_{33} can serve as a molecular tracer assemblage for biogenic primary OC (green, dead, and degraded plant wax material directly emitted or resuspended from soil and road dust) (Mazurek and Simoneit, 1984; Simoneit, 1989; Rogge et al., 1993c). The iso- and anteiso- alkanes can be used to trace the cigarette smoke contribution to the outdoor atmosphere (Rogge et al., 1994),

Primary biogenic organic matter consists predominantly of lipids, humic and fulvic acids, and often represents a major fraction of the carbonaceous aerosol mass (Duce et al., 1983; Gagosian et al., 1987; Mazurek et al., 1989, 1991; Simoneit, 1984, 1986, 1989). Mamane et al. (1990) reported that most coarse OC in the Great Lakes region is of biologic origin while most fine OC is anthropogenic.

Secondary Organic Carbon

Secondary organic aerosol material is formed in the atmosphere by the condensation on already existing particles of low vapor pressure products of the oxidation of organic gases.

As the hydrocarbons are oxidized in the gas-phase by species such as the hydroxyl radical (OH), ozone (O_3) and the nitrate radical (NO_3), their oxidation products accumulate in the gas phase. If the concentration of such a product is smaller than its saturation concentration, the species remains mainly in the gas phase. Small amounts of the species can be adsorbed on aerosol surfaces or dissolved in the aerosol phase at this stage (Yamasaki et al., 1982; Pankow, 1987; Ligocki and Pankow, 1989; Pankow and Bidleman, 1991; Pankow, 1994a,b; Pandis et al., 1992a). If the gas-phase concentration of a species exceeds its saturation concentration, the species condenses on the available aerosol surface so that at equilibrium its gas-phase concentration equals its saturation concentration. If this gas-phase concentration is reduced to less than the saturation value as a result of dilution, deposition or chemical reaction, the aerosol species evaporates in an effort to maintain thermodynamic equilibrium (Pilinis and Seinfeld, 1988). Many volatile organic compounds (VOC) do not form aerosol under atmospheric conditions due to the high vapor pressure of their products (Grosjean and Seinfeld, 1989). These VOC include all alkanes with up to six carbon atoms (from methane to hexane isomers), all alkenes with up to six carbon atoms (from ethylene to hexene isomers), benzene and many low-molecular-weight carbonyls, chlorinated compounds and oxygenated solvents.

Organic aerosols formed by gas-phase photochemical reactions of hydrocarbons, ozone and nitrogen oxides have been identified in both urban and rural atmospheres (Grosjean, 1977). Most of these species are di- or poly-functionally substituted alkane derivatives. These compounds include aliphatic organic nitrates (Grosjean and Friedlander, 1975), dicarboxylic acids (adipic and glutaric acids) (O'Brien et al., 1975), carboxylic acids derived from aromatic hydrocarbons (benzoic and phenylacetic acids), polysubstituted phenols and nitroaromatics from aromatic hydrocarbons (Kawamura et al., 1985; Satsumakayashi et al., 1989, 1990). Some species that have been identified in ambient aerosol and are believed to be secondary in nature are depicted in Table 3-3. Despite the above studies, the available information about the molecular composition of atmospheric secondary OC and about the composition of the OC produced during the oxidation of specific hydrocarbons remains incomplete. The reaction mechanisms leading to the observed products are to a great extent speculative at present (Finlayson-Pitts and Pitts, 1986).

TABLE 3-3. SOME SECONDARY ORGANIC COMPOUNDS IDENTIFIED IN AMBIENT PARTICLES IN URBAN AIR

Compound	n
$HOOC(CH_2)_nCOOH$	1-8
$HOOC(CH_2)_nCHO$	3-5
$HOOC(CH_2)_nCH_2OH$	3-5
$HOOC(CH_2)_nCH_2ONO$ or $CHO(CH_2)_nCH_2ONO_2$	3-5
$CHO(CH_2)_nCH_2OH$	3-5
$CHO(CH_2)_nCHO$	3-5
$HOOC(CH_2)_nCOONO$ or $CHO(CH_2)_nCOONO_2$	3-5
$CHO(CH_2)_nCOONO$	3-4
$HOOC(CH_2)_nCOONO$	3-4
$HOOC(CH_2)_nCOONO_2$	4-5
$HOOC(CH_2)_nCH_2ONO_2$	3-4
(C_6H_5)-$(CH_2)_nCOOH$	1-3
$HOOC$-(C_6H_4)-$(CH_2)_nCH_3$	1-2

Source: Schuetzle et al. (1975), Cronn et al. (1977).

Natural hydrocarbons like the monoterpenes ($C_{10}H_{16}$) and isoprene (C_5H_8) are emitted by various types of trees and plants. In the United States the biogenic hydrocarbon sources are estimated to produce 30 to 60 Mt of carbon per year (isoprene and monoterpenes combined) whereas anthropogenic hydrocarbon sources have been estimated to account for 27 Mt of carbon per year (Lamb et al., 1987; Zimmerman, 1979; Altshuller, 1983). Laboratory investigations have indicated that biogenic hydrocarbons are very reactive under typical atmospheric conditions (Arnts and Gay, 1979). The aerosol forming potential of biogenic hydrocarbons has been investigated in a series of smog chamber studies (Kamens et al., 1981, 1982; Hatakeyama et al., 1989; 1991; Pandis et al., 1991; Zhang et al., 1992). These studies demonstrate that isoprene photooxidation does not contribute to the production of secondary aerosol under ambient conditions. On the other hand, pinenes and other monoterpenes form secondary aerosol in their reactions with O_3 and OH and have the potential to contribute significantly to aerosol in areas

with high vegetation coverage. Monoterpenes were estimated to contribute around 15% of the secondary organic aerosol (SOA) in urban areas with low vegetation like Los Angeles, while they are expected to dominate the SOA in areas with high vegetation coverage like Atlanta (Pandis et al., 1991, 1992a).

The chemical composition of the majority of the aerosol products of the monoterpene photooxidation remains unknown or is speculative (Pandis et al., 1991; Palen et al., 1992). The few products that have been identified include nopinone, pinanediol, pinonic acid and 5-(1-hydroxy-1-methylethyl)-2-methyl-2-cyclohexen-1-one. Several investigators have studied the SOA formation from selected anthropogenic hydrocarbons. The literature data up to 1976 have been reviewed by Grosjean (1977). Other studies focused on toluene and other aromatic hydrocarbons (Leone et al., 1985; Stern et al., 1987; Gery et al., 1985, 1987; Izumi and Fukuyama, 1990), styrenes (Izumi and Fukuyama, 1990), cyclic olefins (Hatakeyama et al., 1985, 1987; Izumi et al., 1988), cresols and nitrocresols (Grosjean, 1985) and alkenes with more than six carbon atoms (Grosjean, 1984b; McMurry and Grosjean, 1985; Wang et al., 1992a,b). Measured and estimated aerosol yields from a variety of SOA precursors have been tabulated by Grosjean and Seinfeld (1989) and Pandis et al. (1992a).

The calculated contribution of the main individual secondary organic aerosol precursors to the secondary organic aerosol concentration in Los Angeles on August 28, 1987 is presented in Table 3-4 (Grosjean and Seinfeld, 1989; Pandis et al., 1992a). Toluene, the nonmethane hydrocarbon with the highest emission rate in the Los Angeles area (165 t d^{-1}) was predicted to contribute 28% of the secondary organic aerosols. Differences were attributed to sampling artifacts and calibration uncertainties during the interpretation of the ambient data.

Grosjean (1992) calculated the daily production rates of various chemical functionalities of the secondary organic aerosol formed *in situ* during a smog episode in Los Angeles using the precursor hydrocarbon emission inventory and the results of smog chamber studies. His estimates are presented in Table 3-5. These predictions were compared with the available measurements of ambient OC functional group relative abundances (Grosjean, 1992).

TABLE 3-4. PREDICTED PERCENT CONTRIBUTION TO SECONDARY ORGANIC AEROSOL CONCENTRATIONS AT LOS ANGELES

	Contribution	
Species	Grosjean and Seinfeld (1989)	Pandis et al. (1992a)
Aromatics	58	65
Biogenic Hydrocarbons	10	16
Alkanes	21	15
Olefins	11	4

TABLE 3-5. AMOUNT OF SECONDARY AEROSOL PRODUCED IN A TYPICAL LOS ANGELES SMOG EPISODE ACCORDING TO FUNCTIONAL GROUPS

	Aerosol produced (kg day^{-1})			
Precursor	Carbonyls	Aliphatic Acids	Nitrophenols	Aliphatic Nitrate
Alkenes	-	608	-	-
Cyclic olefins	62	131	-	9
Terpenes	295	623	-	41
Alkanes	243	-	-	121
Cycloalkanes	72	-	-	72
Aromatics	-	-	3118	-
TOTAL	672	1362	3118	243

Source: Grosjean (1992).

Pickle et al. (1990) and Mylonas et al. (1991) argued that the SOA mass size distribution in urban areas like Los Angeles is typically bimodal with maxima in the 0.1 and 1.0 μm size ranges. Our understanding of the mechanisms of creation of these two modes remains tentative (Pandis et al., 1993). The effect of relative humidity in the SOA partitioning between gas and aerosol phases is generally not understood. Thibodeaux et al. (1991) developed a theoretical model based on classical adsorption theory and predicted that as air relative humidity increases (remaining less than 60%) the equilibrium secondary organic carbon content on the aerosol particles decreases due to competition for adsorption sites with water molecules. This

theoretical result seems to be supported by the little available experimental information, but the necessary experimental data for the incorporation of these relative humidity effects on SOA partitioning into an aerosol model do not exist. Knowledge of the saturation concentrations of the organic condensable species remains incomplete. These concentrations are expected to vary significantly with temperature. The few available relevant measurements include the saturation vapor concentrations of monocarboxylic and dicarboxylic acids (Tao and McMurry, 1989) and the β-pinene aerosol products (Pandis et al., 1991). The saturation vapor concentrations of condensable products from the oxidation of some aromatic hydrocarbons (toluene, m-xylene, and 1,3,5-trimethylbenzene) were estimated to lie in the range 3 to 30 ppt (Seinfeld et al., 1987). McMurry and Grosjean (1985) estimated saturation vapor concentrations for condensable products from the oxidation of 1-heptene (0.14 to 1.28 ppb), o-cresol (0.06 to 1.6 ppb) and nitrocresol (1.7 to 2.2 ppb).

Polycyclic Aromatic Hydrocarbons

Polycyclic aromatic hydrocarbons (PAHs) are formed during the incomplete combustion of organic matter, for example, coal, oil, wood and gasoline fuel (National Research Council, 1983; Bjorseth and Olufsen, 1983). Stationary sources (residential heating, industrial processes, open burning, power generation) are estimated to account for roughly 80% of the annual total PAH emissions in the U.S. Mobile sources only account for 20% of the annual total PAH emissions in the U.S., however, they are the major contributors in urban areas (National Research Council, 1983; Freeman and Cattell, 1990). More than one hundred PAH compounds have been identified in urban air. The PAH observed in the atmosphere range from bicyclic species such as naphthalene, present mainly in the gas phase, to PAH containing seven or more fused rings, such as coronene, which are present exclusively in the aerosol phase (Finlayson-Pitts and Pitts, 1986). Intermediate PAH such as pyrene and anthracene are distributed in both the gas and aerosol phases (see also Section 3.3.3.4).

Measurements of the size distribution of PAH indicate that while they are found exclusively in the 0.01 to 0.5 μm diameter mode of fresh combustion emissions (Venkataraman et al., 1994) they exhibit a bi-modal distribution in ambient urban aerosol, with an additional mode in the 0.5 to 1.0 μm diameter range (Venkataraman and Friedlander, 1994). The growth

of nuclei-mode particles by condensation of secondary aerosol species like nitrate, sulfate and secondary organic aerosol has been proposed as an explanation of this distribution.

Polycyclic aromatic hydrocarbons adsorbed on the surfaces of combustion generated particles are released into an atmosphere containing gaseous co-pollutants including O_3, NO_2, SO_2, HNO_3, PAN, radicals and are exposed to sunlight. Under these conditions PAH undergo chemical transformations that might lead to significant degradation and formation of products more polar than the parent PAH (National Research Council, 1983). Several studies have focused on the reaction rates and products of reactions of PAH adsorbed on specific substrates and exposed in the dark or in the light to other pollutants. However, the extrapolation of these laboratory results to real atmospheric conditions remains difficult.

Benzo(a)pyrene (BaP) and other PAH on a variety of aerosol substrates react with gaseous NO_2 and HNO_3 to form mono- and dinitro-PAH (Finlayson-Pitts and Pitts, 1986). The presence of HNO_3 along with NO_2 is necessary for PAH nitrification. The reaction rate depends strongly on the nature of the aerosol substrate (Ramdahl et al., 1982, 1984), but the qualitative composition of the products does not. The aerosol water is also a favorable medium for heterogeneous PAH nitration reactions (Nielsen et al., 1983). Nielsen (1984) proposed a reactivity classification of PAH based on chemical and spectroscopic parameters (Table 3-6). The PAH nitration rate under typical urban conditions remains poorly understood. Bjorseth et al. (1979) observed a lack of significant PAH reactions during their transport from central to northern Europe and suggested that these reactions are slow in most environments. However, this may not be the case in heavily polluted areas with high NO_2 and HNO_3 concentrations and acidic particles (Finlayson-Pitts and Pitts, 1986). Reactions of fluoranthene and pyrene with NO_2 in the gas phase and condensation the 2-nitro-PAH derivatives on the aerosol surface have been proposed as an alternative reaction pathway for the production of the observed aerosol nitro-PAH (Pitts et al., 1985a).

Nitrogen oxide (N_2O_5) has been proposed as an additional nitrating agent for certain PAH during nighttime (Kamens et al., 1990). Pitts et al. (1985b) exposed six PAH to N_2O_5

TABLE 3-6. REACTIVITY SCALE FOR THE ELECTROPHILIC REACTIONS OF POLYCYCLIC AROMATIC HYDROCARBONS (REACTIVITY DECREASES IN THE ORDER I TO VI)

I	Benzo(a)tetracene, dibenzo(a,h)pyrene, pentacene, tetracene
II	Anthanthrene, anthracene, benzo(a)pyrene, cyclopenta(cd)pyrene, dibenzo(a,l)pyrene, dibenzo(a,i)pyrene, dibenzo(a,c)tetracene, perylene
III	Benz(a)anthracene, benzo(g)chrysene, benzo(ghi)perylene, dibenzo(a,e)pyrene, picene, pyrene
IV	Benzo(c)chrysene, benzo(c)phenanthrene, benzo(e)pyrene, chrysene, coronene, dibenzanthracene, dibenzo(e,l)pyrene
V	Acenaphthylene, benzofluoranthenes, fluranthene, indeno(1,2,3-cd)fluoranthene, indeno(1,2,3-cd)pyrene, naphtalene, phenanthrene, triphenylene
VI	Biphenyl

Source: Finlayson-Pitts and Pitts (1986).

and proposed the following reactivity order: pyrene > fluoranthene > BaP > benz(a)anthracene > perylene > chrysene. Nitro-PAH photodecompose into quinones and possibly phenolic derivatives. For example 6-NO_2-BaP on silica gel photolyses to the 1,6-, 3,6-, and 6,12- isomers of BaP quinones and a host of other oxy-PAH (Finlayson-Pitts and Pitts, 1986). These reactions are expected to depend strongly on the chemical composition and structure of the aerosol substrate and are not well understood for ambient particles.

Aerosol PAH react with O_3 to produce oxidized PAH. Pyrene, BaP and anthracenes react rapidly and the benzofluoranthenes slowly (Finlayson-Pitts and Pitts, 1986; Alebic-Juretic et al., 1990). Reaction rates of 15 to 30% hr^{-1} were observed for the most reactive PAH adsorbed on filters during exposure to 200 ppb of O_3 (Pitts et al., 1986). However, other researchers (Atkinson and Aschmann, 1987; Coutant et al., 1988; De Raat et al., 1990) have suggested that the PAH-O_3 reaction is of negligible importance for typical atmospheric conditions. Relatively little is known about the full ranges of products and the mechanisms of their formation. Polycyclic aromatic hydrocarbons exposed to sunlight have been found to photodegrade in a series of laboratory studies (Valerio et al., 1984; Behymer and Hites, 1988). The photodegradation rates depend strongly on the chemical composition and the pH of the aerosol substrate (Dlugi and Güsten, 1983; Valerio et al., 1984; Behymer and Hites, 1988). Polycyclic

aromatic hydrocarbons appear to be more stable when adsorbed on ambient aerosol than when present in pure form or in solution or on artificial surfaces (Baek et al., 1991). The occurrence of PAH-SO_x reactions remains uncertain (Baek et al., 1991).

3.3.3.3 Semi-Volatile Organic Compounds

General

Species that may exist in the atmosphere either in the gas phase or the condensed phase, and that may change back and forth between phases as a function of temperature, concentration, or other atmospheric variables, are known as semi-volatile substances. They present special sampling and measurement problems, discussed in Chapter 4, Sections 4.2.10.2 and 4.3.4.3.

Semi-volatile organic compounds (SOCs) may be defined as organic compounds whose saturation vapor pressures (p_L^o) are in the range of 10^{-2} to 10^{-9} torr, intermediate between solids and gases. Understanding the factors controlling the relative amounts of SOCs and semi-volatile inorganic materials in the gaseous (G) and aerosol particulate (P) phases is important for sampling and health reasons.

Several processes may lead to partitioning of atmospheric species between the gasphase and the condensed phase (Saxena and Hildemann, 1996). These include normal equilibrium vapor pressure, adsorption, absorption, and chemical reaction.

Equilibrium Vapor Pressure

A specific organic compound may be characterized by a temperature-dependent saturation vapor concentration that represents, under equilibrium conditions, the maximum capacity of the air for this species. If the gas-phase concentration of the compound exceeds this saturation concentration, the species can homogeneously nucleate or condense on available aerosol surfaces such that at equilibrium its gas-phase concentration equals the saturation concentration. If the gas-phase concentration of the species is less than this saturation concentration, it will not condense into the liquid phase of the pure compound. If the concentration of a species in the gas phase is reduced to less than the saturation concentration as a result of dilution, deposition, or chemical reaction, the condensed-phase component will evaporate to maintain thermodynamic equilibrium.

Adsorption (Condensation on Solid Surfaces)

A gas-phase species can be adsorbed on available aerosol particles even if its concentration is less than its saturation concentration (Pankow, 1987). The phase distribution is estimated by a temperature-dependent equilibrium constant and the relationship is called an adsorption isotherm (Adamson, 1976; Hänel, 1976). Several investigators have applied adsorption theory to study the partitioning of relatively nonpolar compounds such as PAHs and pesticides to atmospheric aerosol and fog systems (e.g., Jung, 1977; Yamasaki et al., 1982; Pankow, 1987; Storey and Pankow, 1992; Valsaraj et al., 1993). Such an adsorption process has been found to be significant for polycyclic aromatic hydrocarbons (Ligocki and Pankow, 1989) but the extent of this process for other secondary organic aerosol species is uncertain (Pankow, 1994).

Absorption (Condensation on Existing Droplets)

If aqueous aerosol particles, cloud or fog droplets are already present (e.g., sea-salt particles in marine environments; inorganic particles containing sulfate and nitrate in continental air masses), then a water-soluble organic compound would distribute between the vapor and liquid phases according to its air-water equilibrium constant and the relative volumes of the two phases. No threshold gas-phase concentration is needed: absorption, i.e., condensation onto, or solution into, existing droplets, would take place at all partial pressures.

Similar considerations would hold for absorption on or into liquid organic particles (or components of particles). Some information is available on the partitioning of organic and inorganic gases with respect to water (Henry's Law, Table 3-2). However, the properties for other specific adsorbate and adsorbent pairs are not widely known and the process of absorption into complex mixtures is not well understood. In comparison to absorption, adsorption remains poorly understood. Absorptive phase partitioning of primary organic emissions (Turpin et al., 1991) and secondary organic species formed by reactions in the atmosphere (Pandis et al., 1992a) has been studied. Organic gases may also dissolve into aerosol particles containing plant wax (Pankow, 1994a,b).

Chemical Reaction

If a gas-phase species reacts with another gas-phase species to form a compound with a lower saturation vapor pressure, condensed-phase material may form by nucleation or

condensation. A gas may also react with an existing condensed-phase particle to add to it or to replace another species. Such processes are known for inorganic species, e.g., $NH_3(g) + HNO_3(g) \rightleftharpoons NH_4NO_3(s)$. However, similar reactions are possible with organic species.

Theory

A useful parameterization of G/P partitioning is (Yamasaki et al., 1982; Pankow, 1991)

$$K_p = \frac{F / TSP}{A} \tag{3-49}$$

where: K_p ($m^3\ \mu g^{-1}$) = partitioning constant; TSP ($\mu g\ m^{-3}$) = concentration of total suspended particulate matter; and F ($ng\ m^{-3}$) and A ($ng\ m^{-3}$) = the P-associated and G concentrations of the compound of interest, respectively. The symbols F and A originate in the common usage of a filter followed by an adsorbent to collect the P and G portions, respectively. With urban particulate matter, a given SOC at a given temperature T tends to exhibit similar K_p values from sampling event to sampling event. The fraction ϕ of the total compound that is on/in the P phase is given by

$$\phi = \frac{F}{A + F} = \frac{K_p\, TSP}{K_p\, TSP + 1} \tag{3-50}$$

Though not yet used in practice, it may also prove useful to define $K_{p,10} = (F_{10} / PM10) / A$ where $PM10$ ($\mu g\ m^{-3}$) = concentration of particles with aerodynamic diameters smaller than 10 μm, and F_{10} ($ng\ m^{-3}$) = $PM10$-associated concentration of the compound of interest.

Theory (Pankow, 1994a) predicts that the values of K_p for a given compound class will be given by a relation of the form $K_p = [C_1 + C_2] / p_L^o$, where C_1/p_L^o and C_2/p_L^o represent the adsorptive and absorptive contributions to K_p, respectively. Log K_p values measured under given conditions (*e.g., T*) for a compound class such as the polycyclic aromatic hydrocarbons (PAHs) will thus tend to be linearly correlated with the corresponding log p_L^o values according to $\log K_p = m_r \log p_L^o + b_r$. For PAHs sorbing to urban particulate matter in Osaka, Japan, $m_r \approx -1.028$ and $b_r \approx -8.11$ (Pankow and Bidleman, 1992). (Table 3-7 gives p_L^o values for several PAHs at 20 °C.) This correlation allows K_p to be predicted for a compound that is within the compound class of interest, but was not examined in a given study. K_p for a given compound depends on T

(Kelvin) according to $\log K_p = m_p/T + b_p$ where m_p depends on the enthalpy of desorption; values of the intercept b_p will be similar within a given compound class (Table 3-8). Increasing the relative humidity from 40 to 90% appears to cause K_p values to decrease by a factor of about two for PAHs sorbing to urban particulate matter (Pankow et al., 1993).

For constant K_p, then ϕ will increase as *TSP* increases. For constant *TSP* and *T*, as volatility increases (*i.e.*, as p_L^o increases), then K_p and ϕ will decrease. When $\phi \approx 0$, one can sample just the G phase when determining the atmospheric concentration of an SOC; when $\phi \approx 1$, one can sample just the P phase; when ϕ is between 0 and 1, one must sample both phases.

Sampling Methods and Associated Sampling Artifacts

Atmospheric SOCs have been determined using a *filter* followed by an *adsorbent*. These collect the P and G portions, respectively. Filter types include glass fiber filters (GFFs), quartz fiber filters (QFFs), and teflon membrane filters (TMFs). Adsorbent types includes polyurethane foam (PUF), Tenax, and XAD resins. Safe sampling volumes for G-phase SOCs on Tenax and PUF can be predicted based on studies of retention volumes on these adsorbents (Pankow, 1988 and 1989). *Volatilization losses from particles* (*i.e.*, "blow-off") can occur from a filter/adsorbent when *T* increases during sampling, when the general level of air contamination decreases during sampling, and/or when a large pressure drop develops across the filter (Zhang and McMurry, 1991). In the first case, K_p for a given compound and the already-filtered particles will decrease, leading to desorption from the sampled P-phase. In the second case, even with *T* constant, if *A* in the air being sampled decreases, then desorption losses from the collected particles can occur.

TABLE 3-7. VALUES OF LOG P_L^o FOR VARIOUS PAHS AT 20 °C

Compound	log p_L^o (torr)
Fluorene	-2.72
Phenanthrene	-3.50
Anthracene	-3.53
Fluoranthene	-4.54
Pyrene	-4.73
Benzo[a]fluorene	-5.24
Benzo[b]fluorene	-5.22
Benz[a]anthracene	-6.02
Chrysene	-6.06
Triphenylene	-6.06
Benzo[b]fluoranthene	-7.12
Benzo[k]fluoranthene	-7.13
Benzo[a]pyrene	-7.33
Benzo[e]pyrene	-7.37

Source: Pankow (1994a).

TABLE 3-8. m_p VALUES FOR PAHS SORBING TO UPM IN OSAKA, JAPAN. (Obtained by Fitting to a Common *Y*-intercept B_p of −18.48)

Compound	m_p
Phenanthrene and Anthracene	4,124
Methylphenanthrene and Methylanthracene	4,240
Fluoranthene	4,412
Pyrene	4,451
Benzo[a]fluorene and Benzo[b]fluorene	4,549
Benz[a]anthracene, Chrysene, and Triphenylene	4,836
Benzo[b]fluoranthene and Benzo[k]fluoranthene	5,180
Benzo[a]pyrene and Benzo[e]pyrene	5,301

Source: Pankow (1991).

Volatilization is of particular concern with long sampling times since large overnight *T* cycles and/or large changes in the level of contamination are then more likely. Material volatilized from the filter will be collected on the adsorbent following the filter. *Adsorption gains to particles* from the gas phase due to decreases in *T* and/or increases in *A* during sampling is a second possible artifact type with filter/adsorbent samplers. *Adsorption to the filter* from the G phase is a third artifact type. In this last case, a portion of the value of *A* for an SOC of interest sorbs directly to the filter and so incorrectly contributes to the measured value of *F* for the compound. It is difficult to generalize regarding the magnitudes of the first two artifact types. One can attempt to correct for the third artifact type through the use of a backup-filter (Hart and Pankow, 1994). For sampling of urban particulate matter in Portland, Oregon, Hart and Pankow (1994) estimated that failure to correct for gas adsorption to the filter caused *F* values for PAHs to be overestimated by a factor of ~1.4. Correction of the G-adsorption effect through the use of a backup filter is subject to two possible confounding effects: 1) the atmospheres to which the front and back filters are exposed may differ, making for different G-adsorption to the two filters; 2) organic compounds sorbed to a backup filter could have in part volatilized from the front filter. Table 3-9 summarizes how the three artifact types act to cause measured values of *F*, *A*, and ϕ to deviate from the true, volume-averaged values.

TABLE 3-9. EFFECTS OF THREE TYPES OF ARTIFACTS ON VOLUME-AVERAGED VALUES OF ϕ MEASURED USING A FILTER/ADSORBENT SAMPLER

	Artifact Effect	
Artifact	On *A*	On *F* and ϕ
Volatilization from collected particles	Too large	Too small
Adsorption to collected particles	Too small	Too large
Gas adsorption to filter itself	Too small	Too large

A sampler employing a *diffusion denuder* may avoid some of the artifact problems of filter/adsorbent samplers. Air drawn into a diffusion denuder can be stripped of G-phase SOCs by a sorbent that coats the walls of the denuder: G-phase SOCs diffuse from the core of the air

flow toward the walls. Sorbent coatings that have been used include silicones, gas chromatographic stationary phases (Krieger and Hites, 1992 and 1994), finely divided XAD resin (Gundel et al., 1995; Kamens et al., 1995), and carbon impregnated filter paper (Eatough et al., 1995). The majority of the P-phase SOCs do not deposit on the walls of the denuder because aerosol particles have much smaller diffusion coefficients than do gaseous molecules. The particles exiting the denuder are collected on a filter. Because the air stream flowing onto the filter has been largely stripped of G-phase SOCs, some desorption of the filtered P-phase SOCs can occur, and so an adsorbent is often placed after the filter to collect any such desorbed SOCs. *F* for a given compound is taken as the sum of the amounts on the filter and the subsequent adsorbent. Analysis of the denuder sorbent provides *A*. When the denuder sorbent cannot be analyzed (as with silicone rubber), *A* can be determined by difference using a second, total ($A + F$) determination for SOCs (Lane et al., 1988; Coutant et al., 1988 and 1992; and Eatough et al., 1989 and 1993). Although sampling artifacts are not often discussed for denuder-based samplers, artifacts cannot be assumed to be absent. *In the denuder section*, less than 100% efficiency for G-phase collection will tend to make measured *A* values too small and *F* and ϕ values too large; greater than 0% efficiency for P-phase collection will tend to make measured *A* values too large and *F* and ϕ values too small. Turpin et al. (1993) have presented a new denuder design which does not use a sorbent-coated wall. Rather, a laminar flow separator is used to separate a portion of the G phase from a mixed G+P flow; collection of the G-phase compounds on a sorbent like PUF allows determination of the G-phase concentrations. P-phase concentrations are determined by difference. Other sampling and analysis issues and a more detailed discussion of the diffusion denuder technique are presented in Chapter 4 of this document.

3.3.4 Metals and Other Trace Elements

The major components of fine particles are sulfate, nitrate, organic and elemental carbon, ammonium ions and a variety of trace elements (Godish, 1985; Finlayson-Pitts and Pitts, 1986). Trace elements that are found predominantly in the fine particle size range are Pb, Zn, Cd, As, Sb, Ag, In, La, Mo, I, and Sm. Elements which are found in both fine and coarse modes are Na, K, Fe, V, Cr, Co, Ni, Mn, Cu, Se, Ba, Cl, Ga, Cs, Eu, W, and Au. Elements found primarily within large particle size range are Ca, Al, Ti, Mg, Sc, La, Lu, Hf, and Th (Klee, 1984;

Bernstein and Rahn, 1979). The concentrations and the relative proportions of these species in the various particle size ranges depend on a number of factors such as the nature of the emissions, the photochemical activity and the meteorology (Finlayson-Pitts and Pitts, 1986). The concentration ranges of various elements associated with particulate matter in the atmosphere are shown in Table 3-10. For most elements the range in concentrations is greater than three orders of magnitude. This reflects the different sources and the different pollution control strategies that exist in each area. This information was compiled by Schroeder et al. (1987), and includes a large number of studies from the United States, and abroad, which indicates the need to complete site specific evaluations for high end concentrations (references can be found in the original paper by Schroeder et al., 1987).

In general, remote areas recorded measurable concentrations of some elements associated with crustal origin, as well as some elements indicative of anthropogenic sources. This supports hypotheses which suggest that long range transport occurs in these remote areas (Schroeder et al., 1987). The urban data (Table 3-10) reflect elemental concentrations in different parts of the world. Elements such as lead, iron, and copper are measured in greatest abundance in particulate matter from all locations, while elements such as cobalt, mercury and antimony are found in the smallest quantities (Schroeder et al., 1987).

Potential sources of trace metals found in fine airborne particles are primarily anthropogenic and include combustion of coal and oil, wood burning, waste incineration, and metal smelting operations. Biomass burning which includes residential wood combustion and forest fires, is another source for the release of trace elements in the atmosphere. In a profile of biomass burning, zinc was the characteristic trace element present in the fine particles in concentration ($0.0866 \pm 0.0355\%$) of primary mass emitted. Other trace elements present were Cl ($1.9083 \pm 0.6396\%$), K ($3.9926 \pm 1.2397\%$) and S ($0.5211 \pm 0.1761\%$) (Chow et al., 1992).

The chemical composition of particulate matter analyzed in New Jersey as part of the Airborne Toxic Element and Organic Substances project (ATEOS), identified the trace elements Pb, Fe, Zn, V and As (Daisey, 1987; Morandi et al., 1991). The main source for

TABLE 3-10. CONCENTRATION RANGES OF VARIOUS ELEMENTS ASSOCIATED WITH PARTICULATE MATTER IN THE ATMOSPHERE (ng/m^3)

Elements	Remote	Rural	Urban (USA)
As	0.007 - 1.9	1.0 - 28	2 - 2,320
Cd	0.003 - 1.1	0.4 - 1,000	0.2 - 7,000
Ni	0.01 - 60.0	0.6 - 78	1 - 328
Pb	0.007 - 64	2 - 1,700	30 - 96,270
V	0.001 - 14	2.7 - 97	0.4 - 1,460
Zn	0.03 - 460	11 - 403	15 - 8,328
Co	0.001 - 0.9	0.08 - 10.1	0.2 - 83
Cr	0.005 - 11.2	1.1 - 44	2.2 - 124
Cu	0.029 - 12	3 - 280	3 - 5,140
Fe	0.62 - 4,160	55 - 14,530	130 - 13,800
Hg	0.005 - 1.3	0.05 - 160	0.58 -458
Mn	0.01 - 16.7	3.7 - 99	4 - 488
Se	0.0056 - 0.19	0.01 - 3.0	0.2 - 30
Sb	0.0008 - 1.19	0.6 - 7.0	0.5 - 171

Source: Schroeder et al. (1987).

atmospheric lead concentration is the combustion of leaded gasoline in motor vehicles. However with increased use of unleaded gasoline, levels of atmospheric lead have been reduced, and other sources of lead tend now to be more significant components of the residual lead. Morandi (1985) has reported evidence of contributions to airborne lead from resuspended soil, oil burning and small scale smelting, which taken together accounted for more than half of the airborne lead at a New Jersey site. Vanadium levels were derived from oil burning for space heating and power production, while Zn is attributed to a zinc smelter in the area (Daisey, 1987).

Road dust aerosols are analyzed for trace elements in a variety of studies (Barnard et al., 1987, 1988; Warren and Birch, 1987). Recent source apportionment studies, in California's South Coast Air Basin, provide additional information on trace element concentrations in roadside dusts as well as in motor vehicle exhaust for particle sizes < 2.5 μm (Watson et al.,

1994b). In addition to elemental carbon, Al, Si, K, Ca, Ti and Fe were present in paved road dust in abundances which exceeded 1%. Elevated concentrations of Pb and Br were detected, which illustrated the deposition from the tailpipe exhaust from vehicles that burned leaded fuels (Watson et al., 1994b; Chow et al., 1992, 1993b). Significant amounts of $SO_4^=$, Br^-, Cl^-, and Pb were detected in the motor vehicle exhaust profile, though Pb levels were much lower than those reported in earlier tests (Watson et al., 1994d; Pierson and Brachaczek, 1983).

Ambient measurements of the mass and chemical composition of PM_{10} and $PM_{2.5}$, and associated source profiles have been taken through the years. Data base summaries identify locations, sampling times and chemical species of data available since 1988, complementing previous existing databases (Watson and Chow, 1992; Lioy et al., 1980). Size specific measurements show that over 90% of the mass from geological material is in the coarse particle size fraction, while the combustion related source categories contained ~90% of their mass concentrations in the $PM_{2.5}$ size fraction (Chow et al., 1992, 1993b). In a municipal incinerator profile, elements in the fine particle fraction include Cu, Zn, As, Cd, Sb, Pb and Ba, while trace elements in the coarse particle fraction include Ca, Cr, Mn, and Ni (Olmez et al., 1988). In an oil-fired power plant, trace elements such as V, Ni, Co, Ba and Cu are present in both fine and coarse particles (Olmez et al., 1988).

Although a knowledge of the elemental and ionic composition of ambient particles is necessary in order to understand their sources and chemistry, the chemical forms in which important species exist are not known. For example, sulfate, nitrate and ammonium ions, which are the main constituents of fine particles, may exist in forms other than simple ammonium salts (Finlayson-Pitts and Pitts, 1986). Table 3-11 lists some compounds identified in aerosols by a roadway at Argonne National Laboratory, and Table 3-12 lists compounds observed in aerosols in a forested area, at State College, Pennsylvania (Tani et al., 1983). However, there are uncertainties associated with the compounds shown in Tables 3-11 and 3-12. Tani et al. pointed out that both physical and chemical changes may occur during or following impaction of aerosol particles on a collector, which would lead to the formation of compounds not initially present in the ambient aerosols (Tani et al., 1983).

TABLE 3-11. COMPOUNDS OBSERVED IN AEROSOLS BY A ROADWAY AT ARGONNE NATIONAL LABORATORY

SiO_2	$K_2Sn(SO_4)_2$
$CaCO_3$	$(NH_4)_2Co(SO_4)_2 \cdot 6H_2O$
$CaMg(CO_3)_2$	$(NH_4)_3H(SO_4)_2$ (letovicite)
$CaSO_4.2H_2O$	$3(NH_4NO_3).(NH_4)_2SO_4$
$(NH_4)_2Pb(SO_4)_2$	$2(NH_4NO_3).(NH_4)_2SO_4$
$(NH_4)_2Ca(SO_4)_2.H_2O$	$NH_4MgCl_3.6H_2O$
$(NH_4)HSO_4$	NaCl
$(NH_4)_2SO_4$	$(NH_4)_2Ni(SO_4)_2 \cdot 6H_2O$

Source: Tani et al. (1983).

TABLE 3-12. COMPOUNDS OBSERVED IN AEROSOLS IN A FORESTED AREA, STATE COLLEGE, PA

$(NH_4)_2SO_4$
$(NH_4)_3H(SO_4)_2$ (letovicite)
NH_4HSO_4
$2(NH_4NO_3).(NH_4)_2SO_4$
$(NH_4)_2Pb(SO_4)_2$

Source: Tani et al. (1983).

Metals such as Al, Ca, Fe, Mg and Pb known to be present in atmospheric aerosols, also exist in uncertain chemical forms (Finlayson-Pitts and Pitts, 1986). This is partially due to the use of analytical techniques that normally provide information on total metal content (Schroeder et al., 1987). It is generally assumed that many of the elements, especially from combustion sources, are present in the form of oxides (Olmez et al., 1988), while trace elements in incinerator emissions may be in the form of chlorides (Schroeder et al., 1987). Data from Los Angeles indicate that arsenic may be present in two chemical forms in atmospheric aerosols, as arsenite and arsenate. Both forms were identified in both the fine and coarse particle fractions (Rabano et al., 1989). Fe_2O_3, Fe_3O_4, Al_2O_3, and $AlPO_4$ have been identified in roadside particulate matter (Biggins and Harrison, 1980). Ca and Mg may exist in the form of oxides (i.e., CaO, MgO), although in the presence of water, Stelson and Seinfeld (1981) suggest that, on equilibrium considerations, CaO and MgO should react to form their hydroxides, $Ca(OH)_2$ and

$Mg(OH)_2$, respectively. Similarly the oxides Na_2O and K_2O should form NaOH and KOH when water is present. Lead has been observed in roadside particulate matter in a wide variety of forms, such as $PbSO_4$, Pb_3O_4, $PbSO_4.(NH_4)_2SO_4$, $PbO.PbSO_4$, $2PbCO_3.Pb(OH)_2$, $2PbBrCl.NH_4Cl$, PbBrCl, $(PbO)_2PbBrCl$, $3Pb_3(PO_4)_2.PbBrCl$, and elemental lead (Biggins and Harrison, 1980; Post and Buseck, 1985). Cr is present in the atmosphere in both the hexavalent and the trivalent forms. However, in the atmosphere the hexavalent form tends to be reduced to the less toxic trivalent form (Seigneur and Constantinou, 1995). Information is also available on the atmospheric compounds of Ni (Schmidt and Andren, 1980) and Se (Ross, 1984).

Heterogeneous oxidation of sulphur dioxide in air can be catalyzed by species such as iron, manganese (Barrie and Georgii, 1976) and cadmium, while vanadium is suspected to catalyze the formation of sulfuric acid during oil combustion. Oxides of iron, manganese and lead are reported to absorb SO_2 (Schroeder et al., 1987).

It has been suggested that the elements arsenic, cadmium, manganese, nickel, lead, antimony, selenium, vanadium and zinc volatilize at high temperatures during fossil fuel combustion and condense uniformly on surfaces of entrained fly ash particles as the temperature falls beyond the combustion zone (Linton et al., 1976). Accumulation of trace metals in the fine fraction of airborne dust sampled in iron foundries showed Pb and Zn localized on the surface of the fine particles (Michaud et al., 1993). From the viewpoint of toxicity, such emissions are more important than natural sources where trace elements are usually bound within the matrix of natural aerosols and thus less mobile and bioavailable (Schroeder et al., 1987).

Trace metal compounds found in road dust can accumulate from anthropogenic or natural sources. Subsequently these can become re-entrained in the atmosphere. In such samples lead and zinc were found to be strongly associated with carbonate and iron-manganese oxide phases, with small amounts being associated with an organic phase. Half of cadmium was associated with carbonate and iron-manganese oxide phases, while copper was mainly associated with the organic phase. These associations influence the relative mobility and bioavailability of trace metals in the environment (Harrison et al., 1981).

Resuspension of particles from contaminated surfaces may also contribute to an increase in the toxic trace elements in airborne particles (Kitsa et al., 1992; Kitsa and Lioy, 1992; Pastuszka and Kwapulinski, 1988; Falerios et al., 1992). Kitsa et al. (1992) measured elemental concentrations in particles resuspended from a waste site in New Jersey. Close to the

resuspension source, coarse particles were dominant, but farther downwind from the site, fine particles were prevailing. The fine particles were enriched in chromium and lead, indicating the potential for elevated human exposure through inhalation. Chromium may exist in different valence states, but the most stable and abundant are the trivalent and hexavalent states. Hexavalent chromium is classified as a known respiratory carcinogen in humans.

Oxidation of the species present in aerosols results from interaction with various atmospheric oxidants, such as molecular oxygen, ozone or hydrogen peroxide. The presence of oxides of As, Cd, Co, Cr, Cu, Hg, Mn, Ni, Pb, Sb, Se, V and Zn has been measured in emissions of cement plants, blast furnace and sintering operations, secondary iron foundries, non-ferrous smelting of arsenic-bearing ores, zinc and lead smelters and many other sources (Schroeder et al., 1987).

Sulphation, and possibly nitration, of metallic oxides can be surmised to be an important transformation as particles age. A statistical assessment of multielemental measurements in a study in the rural and urban atmospheres of Arizona showed strong correlations of lead, copper, cadmium and zinc with sulfates in the rural atmosphere and moderate correlation of lead and copper with sulfates and nitrates in urban atmosphere (Moyers et al., 1977). Nickel has also great affinity for sulfur which may lead to the emission of nickel sulfate containing particles from combustion sources. In the absence of sulfur, nickel oxides or complex metal oxides containing nickel may form (U.S. Environmental Protection Agency, 1986a).

Lead was formerly emitted in the air from automobiles as lead halides and as double salts with ammonium halides (e.g. $PbBrCl.2NH_4Cl$). From mines and smelters, the dominant species are $PbSO_4$, $PbO.PbSO_4$, and PbS. In the atmosphere lead is present as sulfate with minor amounts of halides. Lead sulfide is the main constituent of samples associated with ore handling and fugitive dust from open mounds of ore concentrate. The major constituents from sintering and blast furnace operations appeared to be $PbSO_4$ and $PbO.PbSO_4$ respectively (U.S. Environmental Protection Agency, 1986b).

3.4 FIELD STUDIES OF TRANSPORT AND TRANSFORMATIONS

Appropriate and reliable field measurements play a central role in shaping our understanding of atmospheric processes, in providing key model inputs, and in the evaluation of models. Real-world observations are all the more important in the case of atmospheric aerosols, which, on the one hand, are the end product of many complex processes and, on the other hand, are key precursors of important microphysical cloud processes. Field studies include short-term, three dimensional, high-resolution intensive research campaigns, as well as longer-term surface and upper-air monitoring programs (in routine mode, or in more comprehensive and higher-resolution research mode). Research studies are generally mechanistic (targeted at understanding of process rates and mechanisms), and/or diagnostic (aimed at development and testing of individual process modules or subgrid-scale parameterizations for use in complex models). Routine monitoring studies are aimed more at operational evaluation of overall model performance, or at generation of model input data including those (e.g., meteorological) which, through dynamic assimilation into the computations, can improve the realism of the simulations. Since atmospheric fine particles are substantially of secondary origin, measurements of their gaseous precursors and other reactants are also important. In North America, most of the anthropogenic emissions of fine particles and their precursors are from large point sources (power plants and smelters) and from urban-industrial complexes including vehicle emissions. Consequently, special attention is given in this section to measurements in the plumes of such emissions.

In the 1970s, many field studies were plume studies or urban-scale studies, and most models were Lagrangian and limited to linearized treatment of chemistry and other non-linear processes. Some of these field studies, along with regional visibility information and back-trajectories from local pollution episodes, pointed to the existence of long range transport and to the regional nature of air pollution and haze (Hall et al., 1973; Gillani and Husar, 1976; Wolff et al., 1977). In response, some of the major field studies in the 1980s had a regional scope with focus on acidic depositions, oxidants, or aerosols and visibility. That decade also saw major strides in measurement technology and in the development of increasingly sophisticated Eulerian air quality models with explicit treatment of non-linear processes. In these models, however, the treatment of plumes, particularly point-source plumes, was grossly distorted by varying degrees depending on the spatial resolution of the grid. New interest also began to emerge in global

climate change, global data, and global modeling. In the decade of the 1990s, the principal interests in modeling and measurements appear to be in two areas: global-scale issues, with particular focus on clouds and aerosols; and, regional and sub-regional issues, with special interests in comprehensive linked study of oxidants, aerosols and acidic depositions, and in multi-scale interactions (e.g., nested gridding and the treatment of subgrid-scale processes related to plumes, clouds, and air-surface interactions).

Topics related to field measurements are also covered in other parts of this document: methodologies for sampling and analysis of PM and acidic deposition in Chapter 4; ambient air measurements of PM concentrations and properties in Chapter 6; and field studies of visibility and PM in Chapter 8. The focus in this section is on North American field studies of the past 15 years or so, particularly as they relate to the following objectives: better understanding of atmospheric transport and transformation processes which *modify* the concentration, size and composition of PM; evaluation of source- or receptor- oriented models of PM air quality; and generation of model inputs.

3.4.1 Field Studies of Transport Processes

Except for the gravitational settling of coarse particles (included in dry deposition), the transport of PM is similar to that of gases. Following their emissions, gases and fine aerosols rise due to buoyancy effects, are advected downwind by the prevailing mean flow field, and are dispersed horizontally and vertically by ambient turbulence, wind-shear effects, and cloud processes. These dispersive mechanisms result from the interaction of large air masses, or from the disturbance of the larger-scale flow in a given air mass by insolation-driven surface fluxes of heat and moisture, and by surface drag effects. The influence of these surface effects is largely confined to the atmospheric boundary layer (ABL), the height of which varies diurnally and seasonally, peaking typically at between 1 and 3 km on summer afternoons over the continental U.S.A. Pollutant emissions may be within the ABL or above it (depending on emission height, momentum, and buoyancy), and their dispersion is markedly different in the two cases, being much more rapid and vigorous in the daytime convective boundary layer (CBL) than in the stable layers aloft or in the stable nocturnal boundary layer. Quantitative study of these transport and dispersion processes requires, ideally, simultaneous measurements of a large number of variables related to insolation and clouds, surface characteristics and surface fluxes of heat and

moisture, and dynamic 3-D fields of flow, temperature, humidity and concentrations of trace pollutants in the ambient atmosphere. Transport and dispersion processes also have a critical influence on plume chemistry and dry deposition, which are often diffusion-limited. Meteorological measurements must therefore be an integral part of any plume study, even when the focus is on chemistry or deposition. The shift to Eulerian grid modeling in the 1980s did not, in general, include adequate measures, particularly at the regional scale, to preserve the essence of the sub-grid-scale features of plumes, which were instantaneously dispersed over the entire emission grid cell (a volume of $\approx 10^{12}$ m^3 in RADM with 80 km horizontal resolution), thereby also grossly distorting plume chemistry, aerosol formation, and pollutant budgets. There is growing awareness now of the need for more realistic treatment of plumes in grid models. Two other sub-grid-scale issues which are receiving increasing attention pertain to pollutant redistribution by clouds (e.g., Hong and Carmichael, 1986b) and surface fluxes of heat and momentum related to inhomogeneous land use within a grid cell (e.g., Avissar and Pielke, 1989).

A large body of literature exists on studies (including field studies) of ABL structure and dynamics, and on the characteristics of the wind, temperature and moisture fields in the ABL and, to a lesser extent, in the free troposphere aloft. Those studies are outside the present scope. Some of the recent major advances in the knowledge about the ABL are reviewed by Briggs and Binkowski (1985). This discussion is limited to field studies of the transport and dispersion of PM and their precursors (e.g., SO_x and NO_x). Prior to 1975, most such field studies were limited to the behavior of point-source plumes in the γ-mesoscale range ($\lesssim$20 km), i.e., on plume rise and short-range dispersion. Such behavior is well understood qualitatively; quantitatively, it is well enough represented in models at the time scales characteristic of most commonly-used plume dispersion models ($\approx$1 h), but not at the much shorter time scales of relevance to plume chemistry and plume visibility. In this near-source range, instantaneous plume behavior is very different from the larger scale average behavior. In an intercomparison of four plume visibility models, it was concluded that much of the variation in visibility observed in the Navajo power plant plume in northern Arizona was probably due to fluctuations in source emissions and plume dispersion at scales below those resolvable by the models (White et al., 1985). Since the atmospheric residence of fine PM in the lower troposphere is on the order of days, our interest here is more on the transport and dispersion of plumes over the β- and α- mesoscale ranges ($\approx$20

to 200 and 200 to 2,000 km). Quantitative determination of transport over the mesoscale requires special field studies with controlled tracer releases. Such studies are relatively recent and very few, and they represent only a few isolated meteorological scenarios.

3.4.1.1 Field Measurements Related to Transport Modeling

Routine meteorological field measurements include surface weather observations of a broad variety of meteorological variables made every three hours at several thousand sites across the country by the National Weather Service, as well as upper-air soundings (radiosondes) of wind, temperature and relative humidity twice a day (noon and midnight) at a much more limited number of sites which, on average, are about 400 km apart. These data constitute the principal raw meteorological information used in regional transport models, which are either Lagrangian trajectory models or dynamic three dimensional (3D) Eulerian grid models. Most trajectory models are two-dimensional, with atmospheric flow patterns being analyzed on isobaric or terrain-following surfaces, or in bulk transport layers confined to the mixed boundary layer. These simplifying assumptions concerning vertical motions lead to large transport errors on the regional scale (Kuo et al., 1985). The vertical velocity can be calculated at grid points in a regional model domain from the continuity equation, but the temporal and spatial resolutions of the radiosonde data are so coarse in most areas that the result would be a gross approximation only. 3D flows may be best simulated by moist adiabatic trajectories, but since analysis methods cannot always resolve the stratified nature of the required moisture fields, the most reasonable practical simulations of 3D transport are probably dry adiabatic (isentropic) trajectories. Danielsen (1961) presented a case study showing a separation of ≈1,300 km after only 12 h of transport as simulated by isobaric and isentropic trajectories. It was probably an extreme case. The gridded wind field in regional Eulerian air quality models is typically generated by the application of dynamic 3D mesoscale meteorological models such as PSU/NCAR-MM5 (Grell et al., 1994) and CSU-RAMS (Pielke et al., 1992), which incorporate the routine NWS observations through a dynamic Four Dimensional Data Assimilation (FDDA) technique. The NWS surface weather database also includes a measure of prevailing visibility as determined by human observers. A number of field studies have established the reliability of such subjective visibility observations (e.g., Horvath and Noll, 1969; Hoffmann and Kuehnemann, 1979). They have proved to be a very useful indicator of regional haze and its long-range transport (Gillani

and Husar, 1976), and have been used to study the long-term trends of the spatial-temporal variability of regional haze and air quality in the eastern U.S. over many decades (Husar et al., 1981; Sloane, 1982).

Special field studies of transport and dispersion are based on observations of the transport of pressurized (constant density) balloons (called tetroons if their shape is tetrahedral), and of the evolution of plumes resulting from pollutant emissions or controlled releases of artificial tracers. Balloons have been used in mesoscale studies in three ways: as isolated Lagrangian markers of pollutant emissions (e.g., Clarke et al., 1983); in sequential releases to provide one-particle diffusion estimates (e.g., Thomas and Vogt, 1990); and in cluster releases to study relative diffusion (e.g., Er-El and Peskin, 1981). Tetroons generally carry a transponder which permits continuous tracking with a radar, thus providing the complete detailed 3D trajectory. The range of the tetroon experiment is normally limited by the tracking range of the radar (<100 km). This range can be extended to the full range of tetroon transport by including a tag which the finder can return with information, at least, about the terminal location. In some studies (e.g., Clarke et al., 1983), tetroons have been tracked continuously over much longer ranges by sequential tracking from the network of FAA radars used in support of aviation. Studies based on tracers and air pollutants also provide information about plume dispersion. Most early tracer studies were limited to a range of about 100 km due to the nature of the tracers then available and limitations of technology. Development of new tracers (e.g., the PFTs or perfluorocarbon tracers) and new sampling and analysis techniques have not only extended the range in more recent experiments by more than an order of magnitude, but the new data are also more reliable.

Pack et al. (1978) presented a detailed review of many early studies in which observations of the transport of pollutant plumes, tracers, or balloons were compared with results of diagnostic trajectory calculations. The models commonly used then were based on the kinematic approach (using objectively-analyzed wind fields based on measured winds) and a single transport layer. The observed winds were used as input in different ways: for example, surface winds or adjusted surface winds representing average winds in the whole transport layer; or, upper air winds averaged over the transport layer. The adjustment of surface winds included enhancement of the speed by as much as a factor of two, and a veer of the wind direction by as much as 40°, to account for the real-world wind speed shear and directional veer with height. The advantage of using surface winds was due to their much higher spatial and temporal

resolution, compared to the much coarser resolution of the upper-air radiosonde winds. The early results of comparisons of calculated and observed trajectories evidenced a broad range of discrepancy (10 to 54% of the trajectory length after only 100 km, and 55 to 60% after 650 km), and also the presence of large systematic errors, not always in the same direction, depending on the presence of complex flows due to fronts, complex terrain, etc. The best simulations were often obtained by the use of adjusted surface winds, and such adjustments varied between studies. The errors were found to be lowest for transport in the daytime CBL, and substantially larger for transport in stably-stratified layers.

Moran (1992) has tabulated (his Table 2-4) basic information about a number of formal β- and α- mesoscale tracer experiments since 1973, in which the release was at surface level and the measured transport range was at least 25 km (and up to 3,000 km). Table 3-13 summarizes, in chronological order, some of the major field studies of the past 20 years with measurements and modeling of transport extending into the α-mesoscale. It includes the major tracer studies as well as air quality and tetroon studies. The transport models in these studies were driven either by routine meteorological observations or by additional measurements made as part of the field studies. The following important observations are based on the studies listed in Table 3-13:

- The routine data of the radiosonde network (with resolution of ≈400 km, 12 h) are too coarse both spatially (Kahl and Samson, 1986, 1988) and temporally (Rolph and Draxler, 1990; Kuo et al., 1985) for accurate simulation of long range transport.

- The error in calculated trajectories is greatest under conditions of high speeds which generally accompany complex mesoscale systems (Rolph and Draxler, 1990).

- Initial errors in trajectory simulations (both in direction and vertical spread) play a critical role in overall model uncertainty (Draxler et al., 1991).

- Single-layer Lagrangian trajectory models do not spread the "plume" adequately, while Eulerian models spread it too much. Multi-layer Lagrangian models perform the best in terms of dispersion of point-source emissions (Clark and Cohn, 1990).

TABLE 3-13. RECENT FIELD STUDIES OF α-MESOSCALE TRANSPORT AND TRAJECTORY MODEL

Study	Period	Tracer(s)	Release Sites(s)	Tracking/Sampling	Maximum Range (Airshed)	Model Comparison(s)	Ref(s)	Comments
INEL Study Idaho Nat'l Eng. Lab	Feb-May 74	Kr-85	INEL (Idaho) fuel reprocessing plant (76 m stack)	Samplers at 11 Midwestern NWS sites; 10-h day and night samples.	~1,500 km	NOAA-ARL trajectory model with 300 m vertical resolution	Draxler (1982)	Small signal above b/g; 300 m layered approach to permit spread by wind dir'l shear necessary.
MISTT Midwest Interstate Sulfur Transport and Transformation Study	Summer 75 Summer 76	Plume sulfur	Labadie Power Plant near St. Louis, MO	In-situ aircraft measurements.	~300 km	Simple particle trajectory model	Gillani et al. (1978) Gillani (1986)	Quasi-Lagrangian pibal measurements of winds along plume transport.
VISTTA Visibility Impairment due to Sulfur Transport and Transformation in the Atmosphere	Jun, Jul, Dec-79	Anthropogenic aerosol, ozone	Los Angeles Basin	Detailed air quality and aerosol measurements at a Grand Canyon site.	~750 km	CAPITA Monte Carlo particle transport model	Macias et al. (1981)	Evidence also of long-range impact of Copper smelter plumes.
TPS Tennessee Plume Study	Aug-78	Tetroons (1 cu. m) with transponder	TVA Cumberland Steam Plant, TN	Radar to ~75 km; terminal point based on return tag.	~1,000 km (KY,IN,OH,ONT)	• NOAA-ATAD • NCAR isentropic • CAPITA Monte Carlo model	Clarke et al. (1983)	Part of a large plume transport/ chemistry study, including aircraft measts.
	15-Aug-78	"	"	"	~300 km (KY)	3D reg'l dyn. model	Warner (1981)	
NEROS Northeast Regional Oxidant Study	Summer 79 Summer 80	Tetroons (6 cu. m) Tetroons (1 and 6 cu. m)	MD, OH, PA, TN Columbus, OH	Continued FAA radars Radar and return tag.	~500 km to NE ~1,500 km to NE	NOAA, NCAR, CAPITA, as above	Clarke et al. (1983)	Part of a large urban and reg'l oxidant study.
Mt. Isa Smelters Plume Study	Jul-79	Excess plume S and Aitken Nuclei Count (ANC)	Mt. Isa, Australia (Sulphide smelters, ~0.6 km apart)	Aircraft measts. of Total S, ANC, COSPEC-SO2.	~1,000 km (Semi-arid region in N. Australia)	Simple layered wind trajectory model;	Carras and Williams (1981)	Exceptionally clean plume b/g.
Great Plains Mesoscale Tracer Expt.	Jul-80	Two PFTs (PMCH and PDCH) and two heavy methanes (ME-20, ME-21)	Norman, OK (1 m AGL)	Surface samplers: 17 on arc at 100 km 38 on arc at 600 km and aircraft sampling.	600 km to N NE	Different 3D regional models	Ferber et al. (1981) Moran (1992)	Important role of wind shear effects of nocturnal jet.
CAPTEX Cross-Appalachian Tracer Expt.	Sep/Oct 83	PFT (PMCH)	Dayton, OH Sudbury, ONT	Surface array of >80 samplers at arcs from 300-1,100 km and aircraft sampling.	~1,100 km (NE U.S.)	Different 3D regional models; also MESOPUFF II	Ferber et al. (1986) Moran (1992) Godowitch (1989)	Terrain-effects found important. Enhanced upper air met measts.
ANATEX Across North America Tracer Expt.	Jan-Mar 87	3 PFTs (PMCP, PMCH, PDCH)	Glasgow, MT St. Cloud, MN	Surface network (77); Towers (5); and aircraft sampling.	~3,000 km (Eastern U.S.)	3 single-layer LAGR, 6 multi-layer LAGR, 2 multi-layer Eulerian	Draxler et al. (1991) Rolph and Draxler (1990) Clark and Cohn (1990)	Enhanced upper air met measts.
MISERS GOLD	1-Jun-89	Indium oxide (vapor deposits on particles)	White Sands Missile Range, NM	In-situ aircraft: filter samples analyzed for tracer and particles.	~1,400 km NM to MO	Gifford's random-force diffusion theory	Kahl et al. (1991) Mason and Gifford (1992)	Dust plume from a military test explosion.

- Vertical information about tracer trajectories, based on continuously-tracked tetroons and aircraft measurements, contains much useful information not captured by surface sampling alone (Clarke et al., 1983). There is, for example, evidence of cloud venting of ABL pollutants into the free troposphere, where their residence time is longer and the flow field may be quite different.

- Terrain-induced effects played an important role in CAPTEX, and effects related to the nocturnal jet were important in the Great Plains Experiment (Moran, 1992). Nocturnal wind directional shear plays a major role in effectively dispersing plumes which have been dispersed vertically during the preceding daytime CBL.

- Directional wind shear plays an important role in plume dispersion even in the CBL during β-mesoscale transport (Gillani, 1986).

The issue of substantial overdispersion by Eulerian models is important because the state-of-the-art as well as the future direction in mesoscale modeling (meteorological/air quality/aerosol) appear to favor the Eulerian approach. A significant source of the problem must be related to the gross initial overdispersion of plumes in regional Eulerian models, particularly of elevated point-source plumes (carriers of most of the U.S. anthropogenic emissions of sulfur). The instantaneous false dilution of fresh emissions of NO_x into the NO_x-limited surrounding environment (e.g., in the eastern U.S.) greatly distorts plume chemistry and aerosol formation. Proper sub-grid-scale treatment of plumes remains an important outstanding issue in regional modeling. Other sub-grid-scale effects in need of more attention pertain to complex mesoscale flows (e.g., storms, fronts, cloud venting, complex terrain effects, etc.). They too are an important source of model errors. A few special field studies have been carried out to investigate such flows: for example, VENTEX (Ching and Alkezweeny, 1986) and PRESTORM (Dickerson et al., 1987) for cloud venting, and ASCOT (Allwine, 1993) and the NGS Visibility Study (Richards et al., 1991) for flows over complex terrain. Thermal effects and drainage flows also evidently play an important role in influencing particulate air quality, as in the occurrence of the Denver "brown cloud" phenomenon (Sloane and Groblicki, 1981).

There is considerable field evidence also for synoptic scale transport (~2,000 km) of airborne particles (see, for example, Gordon, 1991). The impact of such transport is important on the global scale. That subject is beyond the present scope.

3.4.1.2 Field Measurements Related to Dispersion Modeling

Gaussian semi-empirical models have been the basis of most applied diffusion modeling since their development around 1960. These models were based on Taylor's diffusion theory of stationary homogeneous turbulence (Taylor, 1922), and were built on a few field experiments that were quite limited in scope and technology. The results have been extrapolated far beyond the intended range of downwind distance and ambient conditions. Some of the extrapolations were guided by statistical theory, but most were freehand extrapolations (Briggs and Binkowski, 1985). Many research-grade field studies of atmospheric dispersion have since been performed, but most have been limited to the γ-mesoscale range. These have been reviewed by Draxler (1984), Irwin (1983), Briggs and Binkowski (1985) and others. β- and α-mesoscale studies, based on observations of the dispersion of pollutant and tracer plumes have been reviewed by Moran (1992).

Pollutant plumes remain vertically narrow in stable flows (e.g., elevated power plant plumes released at night), but rapidly fill up the CBL after fumigation in the daytime (see, for example, Gillani et al., 1984). Information about spreads of plumes in the elevated stable layers is particularly limited. The most common basis for estimation of such spreads (expressed as σ_y and σ_z, the RMS variances of lateral and vertical plume spreads) over distances under 100 km or so is the well-known Pasquill-Gifford (P-G) curves for different stability classes (Gifford, 1961), which make use of the routine meteorological measurements to determine applicable stability class. The P-G curves were developed mostly from data collected within the mixing layer. Another set of parameterizations of elevated plume spreads was developed by TVA (Carpenter et al., 1971) based on twenty years of experience in plume observations and aerial monitoring. These require the temperature profile to establish atmospheric stability. More recently, Smith (1981) analyzed aircraft measurements in elevated power plant plumes in different parts of the U.S., mostly in stable layers with small directional wind shear effects, and determined that the P-G curves overestimated plume spread in stable layers quite substantially both vertically and horizontally. Bergstrom et al. (1981) analyzed a smaller set of data in stable layers in which there was significant directional shearing of the plume, and found the P-G curves to underestimate horizontal plume spread. The TVA approach tended to underestimate the horizontal spread, but possibly overestimate the vertical spread. Evidently, there continues to be uncertainty about

plume spreads even at distances under 100 km. Of particular interest is horizontal plume dispersion, both because it is generally far greater over the mesoscale, and because it is highly variable. Close to the source, plume spread is largely by progressively larger turbulent eddies, but after the plume dimension substantially exceeds the scale of these eddies (typically less than 1 km), dispersion is increasingly by directional wind shear with height (Carras and Williams, 1981; Pasquill and Smith, 1983; McNider et al., 1988), and possibly also by other mechanisms involving the diurnal cycle of PBL stability changes and inertial oscillations (Pasquill, 1974; McNider et al., 1988). Directional wind shear is relatively small for the vertically thin nocturnal plume, moderate for the plume in the CBL, but maximum for the daytime plume which, after maximum vertical spread in the CBL, enters the nocturnal regime which is often characterized by strong directional shear effects (Gillani et al., 1984). Such a nocturnally sheared and stratified plume subsequently becomes vertically well-mixed following fumigation into the next day's mixing layer. The average crosswind spread rates of plumes from a large tall stack power plant emitted within the CBL on summer days in the Midwest were observed to be in the range 0.25 to 1.0 km per km of downwind transport until the plume attained a width of about 30 km (Gillani and Pleim, 1995). Direct observations of the three-dimensional nocturnal shearing of well-mixed daytime plumes are extremely sparse.

A common approach in Lagrangian studies of dispersion over long distances has been to use semi-empirical "mesoscale" dispersion coefficients by analogy with parameterizations of microscale turbulent spread. An important consequence of Taylor's statistical theory was that, in stationary homogeneous turbulence, σ_y grew linearly with time at first for $t \approx T_L$ (the Lagrangian time scale, ≈1 to 2 min in the CBL), and then asymptotically as $t^{1/2}$ within a few kilometers. Observations of a few α-mesoscale field studies have been interpreted to suggest that the regime of linear time dependence may apply also at long distances (see, for example, Pack et al., 1978), with the characteristic time scale (T_L) here being related to the diurnal and/or inertial scale (≈24 h). Others have proposed parameterizations of mesoscale σ_y which use powers of t ranging from 0.85 to 1.5 (see, for example, Carras and Williams, 1988). Thus, there is no consensus about simplistic modeling of mesoscale diffusion over scales exceeding 24 h. Given the wide range of conditions that plumes can experience during long range transport in different air masses, over a variety of terrain types, and over

multiple diurnal cycles during different seasons, such a controversy is not surprising. For transport in the first 24 h, the time and height of emission are critical influencing variables. Thus, for example, crosswind spreads after 24 h of transport of two plumes released from the same tall-stack power plant at 0800 and 2000 on a given day are likely to be very different. During the next diurnal cycle, however, these spreads, as a fraction of downwind distance travelled, are likely to converge. Alternate approaches of representing mesoscale plume dispersion include simulation of relative dispersion of hypothetical co-emitted conservative particles (McNider et al., 1988; Uliasz, 1993). In conjunction with instantaneous wind data (e.g., pibal soundings), such models have proved to be satisfactory over β-mesoscale distances (e.g., Gillani, 1986), but more work is needed to establish their application over long distances based on hourly-average gridded wind data such as are produced by the meteorological preprocessors of regional Eulerian models. Overall, based on field evidence, particulate air quality is significantly influenced by regional transport and dispersion, but quantitative simulation of these processes is still subject to considerable error.

3.4.2 Field Studies of Transformations

This section has three subsections. The first two subsections are focussed on the two most important transformation processes related to PM, viz., gas-to-particle conversion (chemical transformation) and the growth of hygroscopic aerosols by condensation of water on them (physical transformation). The latter process is important in clouds, fogs and other humid environments, and has important implications for atmospheric radiation, chemistry and pollutant scavenging. The third subsection is devoted entirely to what was possibly the most comprehensive field study of the past decade related to PM, the Southern California Air Quality Study (SCAQS).

3.4.2.1 Gas-to-Particle Conversion

A number of field studies of gas-to-particle conversion have been conducted in the plumes of large point-sources of SO_x and NO_x (e.g., coal- and oil-fired power plants and metal smelters). Fewer studies have focused on urban-industrial plumes. A number of studies pertain to the regional background. These studies have focused principally on quantifying the rates of aerosol formation and, to a lesser extent, on investigating the

mechanisms. Mechanistic studies are more difficult, particularly when multiple mechanisms are co-active, as is commonly the case.

Point-Source Plume Studies

In the NAPAP emissions inventory for base year 1985 (Placet et al., 1991), about 70% of the U.S. anthropogenic emissions of SO_2, and about 25% of the corresponding emissions of NO_x, were attributed to large point-sources with stack heights exceeding 120 m (probably less than 150 individual sources). The contribution of such sources is even higher in the eastern U.S., particularly in the Ohio and Tennessee River Valleys. Clearly, these large emissions are very important in the context of regional aerosols. Fortunately, many of these sources are located in rural areas, and their plume chemistry can be studied in isolation from the complications of interactions with other plumes. Much of the remaining anthropogenic emissions of SO_x and NO_x are contributed by urban-industrial area sources.

Point-source and urban plume studies of SO_2-to-sulfate transformations published before 1980 have been reviewed by Newman (1981) and in the earlier 1982 PM/SO_x Air Criteria Document (U.S. Environmental Protection Agency, 1982). Only a brief overview of those studies is provided here; the main focus here is on plume studies published after 1980. Since the plume mass is airborne, the most meaningful plume studies are based on measurements made from instrumented aircraft. Early studies (pre-1975) often reported SO_2 oxidation rates as high as 50% h^{-1}. They are now generally considered to be flawed due to limitations in the measurement technology then available. This technology has made major strides since. For example, the development of the filter pack (Forrest and Newman, 1973) has proved to be a useful method of simultaneous collection of high-volume samples of SO_2 and particulate sulfur. Such samples, however, only provide average concentrations over entire plume cross-sections or, at best, over long crosswind plume traverses. The development of continuous monitors for both SO_2 and particulate sulfur (Huntzicker et al., 1978; Cobourn et al., 1978) made it possible to study sulfate formation with crosswind plume detail. Such detail during a single plume traverse contains a nearly instantaneous snapshot of the full spectrum of chemistry between the high-NO_x regime in plume core to the low-NO_x regime at plume edge (Gillani and Wilson, 1980). With cross-sectionally averaged measurements, such a spectrum can only be discerned in

measurements ranging from near-source to far downwind. The technology of continuous measurements of nitrogen species with high sensitivity has also evolved greatly since 1980.

The period between 1974 and 1981 was very active in terms of plume studies focused particularly on estimating the rate of oxidation of SO_2. Studies by Brookhaven National Laboratory (Newman et al., 1975a,b; Forrest and Newman, 1977a,b) and TVA (Meagher et al., 1978) in coal- and oil-fired power plant plumes as well as a nickel smelter plume generally yielded low oxidation of SO_2 (seldom exceeding 5% over 50 km and several hours of plume transport, with an uncertainty of about a factor of two). These investigators found the oxidation rate to be highest close to the source, where it appeared to be correlated with plume particulate loading, and interpreted the oxidation to be due to a heterogeneous second-order mechanism which became quenched as the plume diluted (Schwartz and Newman, 1978). These results were in sharp contrast to those of Husar et al. (1976) for a coal-fired power plant plume, also over about 50 km of plume transport, which showed the oxidation rate to be slow during an early induction period, increasing thereafter to as much as 5% h^{-1}. No mechanistic interpretation was proposed by these authors.

This controversy was resolved by the subsequent findings of Gillani et al. (1978) resulting from two case studies which were remarkable for their coverage of downwind range exceeding 300 km and 10 to 12 h of transport of a coal-fired power plant plume during daylight as well as dark. The authors found the oxidation rate of SO_2 to be strongly correlated with sunlight, and also with the extent of plume dilution, and background ozone concentration (considered to be a surrogate for background reactivity). Maximum measured particulate sulfur as a fraction of total plume sulfur ranged as high as 18%. The daytime conversion rate in the plume was slow at first, but increased as the plume diluted, reaching maximum values on the two days of 1.8 and 3.0% h^{-1} in the afternoon. Such rates are consistent with theoretical rates based on the SO_2-OH reaction (Calvert et al., 1978; Höv and Isaksen, 1981). The entire plume transport on both occasions was in fairly dry environment (relative humidity < 70%). Presumably, the mixing of plume NO_x and background VOC led to photochemistry which generated the necessary oxidants for gas-phase oxidation of SO_2. The measurements of VOC in the background were both sparse and of limited reliability. The study also found the formation of substantial excess of ozone in aged plumes. The interpretation based on plume-background interaction satisfactorily explained the results of

the BNL and TVA studies in which the measurements of low oxidation of SO_2 were all in coherent stable elevated plumes during early morning and evening hours (low sunlight and little plume dilution), as well as of Husar et al. (1976) whose measurements were in the more polluted and convective summer daytime CBL.

As of the end of the 1970s, a number of factors had been implicated as being relevant to plume sulfur chemistry. Gillani and Wilson (1980) conducted a systematic investigation of the dependence of ozone and aerosol formation in power plant plumes on a variety of possible influencing factors, based on the plume data of five case studies. They found that temperature variations in the range 28 to 33 °C, and R.H. variations in the range 50 to 80% did not have an appreciable influence; the importance of sunlight, plume dilution and background composition was reconfirmed. Eatough et al. (1981, 1982) have observed a positive temperature dependence of a linear SO_2 oxidation rate in power plant and smelter plumes in western U.S. in the temperature range 0 to 30 °C.

Gillani and Wilson (1980) also presented direct evidence and interpretation of the role of plume-background interactions in plume photochemistry within the context of a common pattern of diffusion-limited plume chemical evolution through three stages in a moderately polluted environment. In the "early" stage, the plume is narrow and dominated by a high-NO_x regime in which ozone and other oxidants are sharply depleted by reaction with plume NO and SO_2; the VOC-NO_x chemistry, SO_2 oxidation, and aerosol formation are inhibited in the plume in this stage. As the plume spreads and dilutes with a background characterized by relatively high VOC/NO_x ratio, the VOC/NO_x ratio increases also in plume edges. This "intermediate" stage of plume chemistry is characterized by rapid formation of ozone and aerosols in plume edges, leading to an observed excess there of ozone over the background (ozone "wings") while the plume core still has an ozone deficit. Sharp "wings" of Aitken nuclei concentration have also been observed in plume edges at times, indicating directly the nucleation of new aerosol (Wilson, 1978; Gillani et al., 1981). With continuing dilution, the plume ultimately develops a condition of low-NO_x, high VOC/NO_x ratio and, in the summer, an ozone "bulge" throughout. In this "mature" stage, the rate of oxidation of SO_2 to sulfates (and presumably also of NO_x to secondary products) reaches its peak.

Gillani et al. (1981) provided a quantitative interpretation of the above observations by developing an empirical parameterization of the gas-phase conversion rate of SO_2 to sulfate in

terms of measured variables representing sunlight, mixing and background reactivity. The parameterization was verified based on the "dry" data of three different power plant plumes over ten days of measurements in two different summer periods. Crosswind-resolved reactive plume models capable of facilitating plume-background interactions and including detailed simulation of chemical kinetics have been developed and applied by Höv and Isaksen (1981), Stewart and Liu (1981), Seigneur (1982), Gillani (1986) and Hudischewskyj and Seigneur (1989). The reactive plume models of Seigneur and collaborators also include simulation of aerosol dynamics. These models can depict the observed behavior of ozone in the three plume stages. Their applications have shown that the evolution of OH in the plume (a measure of oxidation potential) mimics the above description of ozone evolution (Höv and Isaksen, 1981), and that plume oxidant and aerosol formation are very sensitive to background VOC and their ingestion into the plume (Gillani, 1986). However, these models continue to remain unevaluated adequately owing to a continuing lack of data characterizing the composition of plume background (especially VOC) and the crosswind detail of important intermediate and secondary species (e.g., OH, HO_2, HNO_3, etc.). Reactive plume models that describe the formation of oxidants and secondary particulate matter, as well as the evolution of the aerosol size distribution, have been developed and evaluated with available data (Eltgroth and Hobbs, 1979; Seigneur, 1982; Hudischewskyj and Seigneur, 1989). The most comprehensive model performance and evaluation available to date is that conducted by Hudischewskyj and Seigneur (1989). For example, they conclusively demonstrated that SO_2 oxidation occurs at a faster rate in smelter plumes than in power plant plumes, because in power plant plumes NO_2 competes effectively with SO_2 for OH radicals.

A number of plume studies have verified the sunlight dependence of the SO_2 oxidation process, observing higher seasonal conversion rates during summer, and higher diurnal rates during midday (Husar et al., 1978; Lusis et al., 1978; Roberts and Williams, 1979; Meagher et al., 1981; Hegg and Hobbs, 1980; Gillani et al., 1981; Forrest et al., 1981; Williams et al., 1981; Wilson, 1981; Wilson and McMurry, 1981; Liebsch and de Pena, 1982). In these studies, the peak daytime conversion rate was typically between 1 and 5% h^{-1} in the summer (higher under humid conditions), and much lower in winter. Wilson (1981) reviewed the data of twelve power plant and smelter plumes in the U.S., Canada and Australia, covering measurements during day and night, and summer and winter. The main conclusion was that diurnally, midday

conversion rates were relatively high and quite variable (1 to 10% h^{-1}), while the nighttime conversion rates were generally low (under 0.5% h^{-1}). Also, the rates were found to be lower in winter than in summer. Geographically, the measured plume conversion rates in the arid and relatively clean southwestern U.S. environment were found to be particularly low (0.5% h^{-1}) at all times, including summer midday. Williams et al. (1981) also found the rates to be low in a smelter plume in the arid, clean environment of north central Australia ($\approx$0.15% h^{-1} averaged over 24 h of transport).

Gillani et al. (1981) were able to formulate the parameterization of the gas-phase conversion rate by isolating case studies performed entirely in dry conditions when liquid-phase contributions were negligible. They also observed that for all cases when the plume had any history of wet exposure (clouds, fogs or high humidity), the oxidation of SO_2 invariably proceeded at a rate faster than that predicted by the gas-phase parameterization. Whereas the typical range of the peak summer daytime conversion rate was 1 to 5% h^{-1} in Project MISTT (Missouri, Illinois), it was closer to 1 to 10% h^{-1} in the more humid conditions of the Tennessee Plume Study (Tennessee, Kentucky). In the wetter daytime situations, evidently, liquid-phase chemistry was superposed over the underlying gas-phase chemistry. Gillani and Wilson (1983) focused their study on the plume data of such "wet" situations. They attributed to liquid-phase chemistry the part of the total measured conversion rate which was in excess of the rate estimated by the gas-phase parameterization. The liquid phase was found to be due to clouds, fogs and light rain, or due to wetted aerosols under conditions of high ambient humidity (relative humidity > 75%). The liquid-phase contribution to the conversion rate was found to be in excess of 40% of the total in two-thirds of the cases analyzed, being as high as 8% h^{-1} averaged over the whole plume over 6 h of transport in the most extreme case (clouds and light rain). Similar increases in conversion rates in power plant plumes interacting with high humidity have also been observed by others (e.g., Dittenhoefer and de Pena, 1978; Eatough et al., 1984; Richards et al., 1985).

Determination of the liquid-phase conversion rate involves quantification not only of the kinetics, but also of the discrete and variable extent of plume-cloud interaction. Gillani et al. (1983) formulated a parameterization of the conversion rate for plume-cloud interaction in which the physical extent of such interaction was represented probabilistically, and the higher liquid-phase conversion rate was applied only for the in-cloud portion of the plume. The

application of the parameterization to a case study corresponding to summer daytime plume transport within the CBL, in patchy contact with fair-weather cumulus above, permitted estimation of the average in-cloud conversion rate averaged over 7 h (1000 to 1700) to be 12% h^{-1}. Considering that the corresponding average liquid water content in the clouds was certainly less than 1 g m^{-3} (1 ppm), much higher actual oxidation rates within individual droplets are indicated. Gas-phase photochemistry at a much slower rate was concurrently quite active in the more extensive drier parts of the plume below, producing ozone and other oxidants which contributed to gas-phase as well as liquid-phase sulfur chemistry. It was not possible to relate the in-cloud kinetic rate to the critical variables controlling it, such as cloud liquid water content, H_2O_2 concentration, or droplet pH, because such measurements were not made. The role of concurrent gas-phase photochemistry is indeed essential to provide the oxidizing agents of liquid-phase chemistry. Clark et al. (1984) found the contribution of liquid-phase chemistry in a power plant plume to be negligible during long-range transport over water in a shallow stratocumulus-filled boundary layer, with limited plume dilution, low insolation, and little photochemistry.

A quite different approach based on aerosol growth laws applied to aerosol size distribution data was taken by McMurry et al. (1981) and McMurry and Wilson (1982) to study relative contributions of the principal mechanisms of gas-to-particle conversion. Theory predicts different growth laws for different chemical mechanisms of aerosol formation. The authors examined the functional dependence of calculated particle diameter growth rate on particle diameter. By matching field data with theoretical growth laws, it was possible to differentiate between mechanisms. Application of this approach indicated gas-phase chemistry and condensation of the product to be the predominant mechanism of aerosol formation in several power plant plumes in eastern and western U.S., with increasing contribution of heterogeneous mechanisms with increasing humidity (McMurry et al., 1981); in a case study of the urban plume of St. Louis, 75% and 25% of the aerosol formation were attributed to homogeneous and heterogeneous mechanisms, respectively, while most of the aerosol formation in the ambient air in the Great Smoky Mountains where relative humidities were high (up to 95%) was attributed to the droplet-phase mechanism (McMurry and Wilson, 1982).

In an overview of empirical parameterizations of sulfur transformations in power plant plumes, Gillani (1985) estimated that on a 24-h average basis, sulfate formation rates in a large

power plant plume in the U.S. Midwest in July 1976 were likely to be 0.8 ± 0.3% h^{-1} by gas-phase reactions (midday peak ≈ 2.6% h^{-1}) and at least half as much by liquid-phase reactions. Winter rates were estimated to be an order of magnitude lower than the summer rates for the gas-phase mechanism, but comparable for the liquid-phase mechanism. Since 1981, no new field studies of chemistry in large point-source plumes have been conducted in the eastern U.S. A comprehensive plume study with state-of-the-art aircraft measurements of primary and secondary sulfur and nitrogen species, as well as VOC and ozone, is planned to occur in the summer of 1995 as part of the Southern Oxidant Study (SOS) Nashville Field Measurement Program.

Smelter plume chemistry is different from that of power plant plumes in some significant ways. Based on aircraft measurements made in 1981 in two Arizona smelter plumes, Richards et al. (1982a,b,c) reported markedly higher SO_2 oxidation rates in these plumes compared to those observed in power plant plumes in similar arid and relatively clean environments. The authors also demonstrated that the oxidation mechanism was predominantly gas-phase, in spite of the relatively high primary aerosol (including iron and manganese) and water loading of those smelter plumes. They attributed the higher SO_2 oxidation rates in smelter plumes to the fact that these plumes contain little or no NO_x emissions, in sharp contrast to the high NO_x emissions in fresh power plant plumes. As a result of the absence of NO_x, there is no initial depletion of OH in the plume (and the associated inhibition of SO_2 oxidation), nor is there any competition to SO_2 oxidation by OH from NO_2. It is useful to note also that a major downward change has occurred since 1981 in the contribution of smelters nationally to atmospheric PM. The number of operational smelters has dropped from 18 to 7; in those still operational, SO_2 emissions have been reduced by more than an order of magnitude as a result of improvements in control technology; finally, the primary emissions of aerosols and water have also been sharply reduced. Unfortunately, no new detailed field studies of smelter plumes have been conducted since those reported in 1982.

Information about field measurements of nitrate formation in point-source combustion plumes is much more meager. Summertime plume measurements suggest that nitrate formation is principally in the form of nitric acid vapor (Hegg and Hobbs, 1979; Richards et al., 1981), and that oxidation of NO_x to HNO_3 may proceed about three times faster than the rate of oxidation of SO_2 (Richards et al., 1981; Forrest et al., 1979, 1981). Richards et al. (1981) observed that along the transport of the Navajo Generating Station in Arizona, there was adequate ammonia to neutralize the sulfate formed in the plume, but not enough to form ammonium nitrate. Forrest et al. (1981) found $NH_4^+/SO_4^=$ to increase with downwind distance and was mostly less than 2 (not enough to fully neutralize the sulfate), but sometimes more than 2, indicating a possibility of the formation of some ammonium nitrate. Eatough et al. (1981) observed that in the western desert region, the neutralization of sulfuric acid in plumes was due not only to ammonia, but also to other basic material (e.g., metal oxides and $CaCO_3$).

Urban Plume Studies

Field information about secondary formations in urban plumes is scantier than for power plant plumes for sulfur compounds, but possibly slightly more for nitrogen compounds. White et al. (1976, 1983) reported slow formation of ozone and aerosols at first in the St. Louis urban plume, but faster rates farther downwind. Average sulfate formation rates between successive downwind measurement locations on summer days were estimated at 2 to 4% h^{-1}. Isaksen et al. (1978) applied a reactive plume model to a subset of the St. Louis data, and estimated peak rates for the formation of sulfuric and nitric acid of 5 and 20% h^{-1}, respectively. Based on the same data set, Whitby (1980) estimated that about 1,000 tons of secondary fine aerosol may be produced in the plume in one summer irradiation day. Alkezweeny and Powell (1977) estimated peak sulfate formation rates in the St. Louis plume at 10 to 14% h^{-1}. Miller and Alkezweeny (1980) reported sulfate formation rates in the Milwaukee urban plume on two summer days in very different air masses to range from 1% h^{-1} (clean background) to 11% h^{-1} (polluted background). The most extensive studies of NO_x chemistry in urban plumes have been reported by Spicer and co-workers. They have reported results for the Los Angeles, Phoenix, Boston and Philadelphia urban plumes. In the Los Angeles studies, the transformation rate of NO_2-to-

products was estimated at 5 to 15% h^{-1} (Spicer, 1977a,b) and 5 to 10% h^{-1} (Spicer et al., 1979). The sum of transformation plus removal rates was estimated for the Phoenix and Boston plumes at <5% h^{-1} and 14 to 24% h^{-1}, respectively. The low rate for Phoenix was attributed partly to thermal decomposition of PAN after its formation in the plume. In a study of the Detroit plume, Kelly (1987) estimated the NO_x transformation rate at 10% h^{-1}, with 67 to 84% of the products being in the form of HNO_3. Measured concentrations of nitric acid, however, were much lower because of its higher removal rate. All of the above urban plume studies, and most of the power plant plume studies, have been daytime studies. Field measurements of nighttime chemistry of nitrogen oxides in plumes are almost non-existent.

Background Field Studies

Attention is now focused on studies of aerosol formation in background air. The plume studies have shown that the *rates* of oxidation of SO_2 and NO_x in the background represent approximately the upper limit of the conversion rates in the plume. In non-humid, moderately polluted conditions, the rates typically range between 1 and 5% h^{-1} for midday SO_2 oxidation in summer in the eastern U.S. (depending on the composition of volatile organic compounds (VOC) and the variability of VOC/NO_x, and up to 1% h^{-1} in the cleaner parts of the Western U.S. Winter rates are about an order of magnitude lower. By contrast, observed NO_x to nitrate conversion rates are about three times faster in summer than in winter (Parrish et al., 1986). Aerosol nitrate formation depends strongly on availability of NH_3 and on temperature. Background aerosol is generally more aged and its acidity more neutralized than plume aerosol.

The situation is more complex in humid conditions. Field measurements of the compositions of cloudwater, rainwater and the precursor clear-air aerosol have shown that strong acidity is substantially greater in cloud and rain water than in the clear-air aerosol (Daum et al., 1984b; Lazrus et al., 1983; Weathers et al., 1988). This is indicative of the contribution of aqueous-phase chemistry to cloudwater acidity in excess of that due to scavenged aerosol. Based on climatological data of clouds and SO_2 distribution, and assuming aqueous-phase oxidation of SO_2 by ozone, Hegg (1985) estimated contribution of the aqueous mechanism to global tropospheric sulfate production to be at least 10 to 15 times

greater than that due to the gas-phase mechanisms. Applications of more comprehensive global models have given estimated aqueous-phase contributions of 40 to 95% of the total sulfate production (Langner and Rodhe, 1991 and references therein). Regional models for North America suggest 50 to 80% of the sulfate deposited in precipitation to be formed in clouds (Fung et al., 1991; McHenry and Dennis, 1991).

A number of ambient studies have attempted to study aqueous chemistry based on in situ measurements in clouds. Determination of the rates and mechanisms of aqueous-phase chemistry is particularly ambiguous for several reasons. First, it is difficult to distinguish between the contributions of in situ chemistry and aerosol scavenging to the observed concentration of the solute in the droplet phase. Also, aqueous chemistry rate depends not only on the change in concentration, but also on the change in time. It is difficult enough to determine the difference in concentration of even one reactant or product species, but determining the corresponding *time* difference is even more difficult (Schwartz, 1987; Gervat et al., 1988; Kelly et al., 1989). In stratiform clouds, in particular, it is not always possible to determine what constitutes pre-cloud air corresponding to specific cloud water samples (Gillani et al., 1995). Finally, it is difficult, based on field data, to attribute the inferred chemistry to specific mechanisms (oxidation by H_2O_2 or O_3, etc.). The conclusions regarding rates and mechanisms of aqueous chemistry based on measurements in clouds are therefore quite uncertain, and have been a source of considerable controversy (e.g., Hegg and Hobbs, 1982, 1983a,b versus Schwartz and Newman, 1983). One important finding in support of in-cloud oxidation of SO_2 by H_2O_2 , however, is the almost universal mutual exclusion of these two species in non-precipitating stratiform clouds (Daum et al., 1984a; Daum, 1988). In such clouds, there is generally enough time available for the species to react fully until the one with the lower concentration in the precursor air is depleted. The implication is that the aqueous-phase oxidation of SO_2 by H_2O_2 takes precedence over other competing reactions.

Most field studies have been limited to estimating the amount or fraction of sulfate formed by the aqueous pathway, rather than the rate of formation. Liu et al. (1993) have summarized the results of a number of cloud studies between 1979 and 1991. In these studies, a number of different approaches have been used to resolve the contributions of aerosol scavenging and in situ chemistry to the observed cloudwater sulfate. The study of

Liu et al. (1993), which was part of the first intensive (summer 1988) of the Eulerian Model Evaluation Field Study (EMEFS), used three different approaches for estimating the scavenged fraction of observed sulfate, and attributed 27 to 55% of cloudwater sulfate to in situ production. The inferred results for the aqueous-phase production of sulfate in the collective studies vary widely. In winter studies, such production is low (e.g., Strapp et al., 1988), while in summer studies, it is generally higher (e.g., Mohnen and Kadlecek, 1989). Many studies implicate H_2O_2 as the principal oxidant (e.g., Van Valin et al., 1990), while others implicate ozone (e.g., Hegg and Hobbs, 1986).

There is a variety of evidence for and against the formation of HNO_3 in the cloud environment (e.g., Lazrus et al., 1983; Daum et al., 1984b; Hegg and Hobbs, 1986; Leaitch et al., 1986a). The heterogeneous mechanism involving N_2O_5 has received attention mostly as the "nighttime" mechanism (Lazrus et al., 1983; Richards, 1983) owing to the short life of the NO_3 radical (precursor of N_2O_5) in sunlight. To account for the comparable measured amounts of sulfate and nitrate deposited in winter storms in Ontario, Barrie (1985) suggested the possibility of the N_2O_5 mechanism for wintertime formation of nitrate in clouds. Leaitch et al. (1988) found substantial enhancement of NO_3^- in and near clouds on 8 of 12 days of winter measurements in central Ontario under freezing conditions and low insolation. On these occasions, variations in $NO_3^-/SO_4^=$ were associated with $H^+/SO_4^=$ in the cloud water, implicating HNO_3. Also, the observed levels of NO_3^- could not be simulated in a model without invoking the N_2O_5 mechanism. Based on a detailed examination of the nighttime behavior of the NO_3 radical, Noxon (1983) concluded that there was a significant loss of NO_3 compared to N_2O_5 by an unknown scavenger (wet particles?). In measurements at a rural site in central Ontario in August 1988 as part of EMEFS, Li et al. (1993) observed a gradual increase in the concentration of aerosol nitrate (NO_3^-) from 1800 to midnight, and then a gradual decrease. In a diagnostic model study, they concluded that the observations could be explained by heterogeneous reactions of NO_3 and N_2O_5 on wet particles. They attributed more than 80% of the NO_3^- formation to NO_3 and about 10% to N_2O_5, and less than 5% to HNO_3.

3.4.2.2 Field Studies of Water Uptake by Atmospheric Aerosols

Water is an important ingredient of atmospheric aerosols. The water content of atmospheric aerosols and the behavior of atmospheric aerosols with respect to changes in ambient humidity are of great importance in the global water cycle, the global energy budget, and also in atmospheric chemistry and optics. Understanding the relationship between atmospheric aerosols and water has proven to be a difficult problem. Most of the water associated with atmospheric aerosol is "unbound" (Pilinis et al., 1989) i.e., it can increase or decrease with ambient humidity in a non-linear manner. This non-linear relationship depends on particle size and composition, indeed on size-dependent composition. More recent studies have included monitoring of particle size distributions (either directly, or indirectly through light scattering and use of Mie theory) and size-dependent chemical composition under controlled relative humidity (e.g., Covert and Heintzenberg, 1984; Rood et al., 1985). Such studies have presented increasing evidence in favor of external mixtures in particles. Covert and Heintzenberg (1984) found that size spectra of sulfur-bearing species were sensitive to relative humidity while those of EC were not, and concluded that sulfur and EC are, to some extent, externally mixed. Harrison (1985) segregated the particles into CCN (cloud condensation nuclei) and non-CCN fractions and measured their chemical compositions. Both fractions contained sulfate, nitrate and soot, but sulfate was 15% of the CCN mass and only 5.8% of the non-CCN mass. Again, this was taken as evidence of external mixture to some extent. The differential mobility analyzer has been a useful tool permitting study of particle properties for monodispersed size classes. Using this instrument, Covert et al. (1990) and Hering and McMurry (1991) showed that monodispersed particles scatter varying amounts of light in a single particle optical counter, indicating different refractive indices, and hence, different chemical composition. Using a tandem differential mobility analyzer, McMurry and Stolzenberg (1989) showed that hygroscopic and hydrophobic particles of the same size co-exist frequently in Los Angeles, again an indication of external mixing.

In visibility studies, the water content of aerosols is of crucial importance. The estimation of visibility impairment involves use of models in conjunction with ambient data of both aerosols and relative humidity. Frequently, both sets of data are not available concurrently for all stations in a monitoring network such as IMPROVE (Interagency Monitoring of PROtected Visual Environments). In such cases, gaps in information must be

filled by the use of empirical relationships between average visibility impairment caused by soluble aerosols and average relative humidity derived from the available concurrent data. Such an application based on data at the 36 national IMPROVE sites is described by Sisler and Malm (1994).

Another important area which critically involves water uptake by soluble aerosols relates to aerosol-cloud interactions. Such interactions are a critical link in cloud formation and the global water cycle, in cloud optics and the global energy budget, in pollutant redistribution by clouds, in pollutant wet removal from the atmosphere, and in atmospheric chemistry. Of particular importance is the process of aerosol incorporation in clouds. Interstitial aerosols in clouds may become incorporated into cloud droplets by "activation" (droplet nucleation), Brownian diffusion, inertial impaction, coalescence, and phoretic effects. Of these microphysical cloud processes, aerosol activation is by far the most important. A soluble particle (the CCN) is activated when water vapor supersaturation around it (S) exceeds a critical value (S_c) which depends principally on particle dry size (D_0) and composition (commonly expressed in terms of the water-soluble solute fraction, ε). The works of Köhler (1936), Junge and McLaren (1971) and Hänel (1976) provide the underlying theory for condensation of water on aerosols based on assumptions of internally mixed aerosols. Based on properties of representative continental and marine CCN, Junge and McLaren predicted that S_c would be sensitive to CCN size, but to CCN composition only for $\varepsilon < 0.1$. Fitzgerald (1973) confirmed the insensitivity to ε in the range 0.15 to 0.35 based on simultaneous measurements of CCN size, ϵ and CCN activation spectra (functional dependence of activated fraction of aerosol on S) for S between 0.35 and 0.75%.

More recently, based on extensive year-long measurements of CCN spectra for continental aerosols (representative of eastern U.S. background), separated into narrow size bands within the accumulation mode, Alofs et al. (1989) derived a simple semi-empirical expression relating S_c to D_0 and ε applicable down to S = 0.014%. They also showed, based on their own data and a literature review, that for continental aerosols in industrialized regions, $\varepsilon \approx 0.5$ is a reasonable approximation, indicating that the activation of such aerosols is unlikely to be sensitive to particle composition. Based on their expression for S_c and using $\varepsilon = 0.5$, a supersaturation of about 0.1% (characteristic for stratiform clouds) would be adequate to activate most of the accumulation mode particles exposed to a cloud.

Cumuliform clouds with higher S would activate many Aitken mode particles also. In cumulus clouds, peak supersaturation is typically attained near cloud base, which is where maximum activation is likely to occur. The cloud module of the Regional Acid Deposition Model (RADM) is based primarily on a cumulus parameterization, and makes the assumption of 100% cloud scavenging efficiency for sulfates formed from the oxidation of SO_2 (Chang et al., 1991).

The principal interest in quantitative field studies of aerosol-cloud interactions is the scavenging of acidic aerosol mass by clouds. The focus of measurements in these studies (from aircraft or at fixed mountain sites) was on gross spatial averages (over 10s of km) of species mass concentrations (mostly of sulfate and nitrate) based on batch samples collected in cloud water, and in cloud and clear air (Scott and Laulainen, 1979; Sievering et al., 1984; Daum et al., 1984b, 1987; Hegg et al., 1984; Hegg and Hobbs, 1986; Leaitch et al., 1986b; Pueschel et al., 1986). In some studies, continuous measurements of aerosol size spectra were used to derive spatially-averaged aerosol volume concentrations (Leaitch et al., 1983; Hegg et al., 1984; Heintzenberg et al., 1989) based on which, aerosol volume scavenging efficiency was inferred. In one study, continuous measurements of light scattering coefficient were used as a surrogate for aerosol mass concentration (ten Brink et al., 1987). In these studies, inferences of the efficiency of aerosol scavenging were generally based on comparisons of species mass or volume concentrations (or their surrogates) in cloud water and/or cloud interstitial air with those in putative pre-cloud air. Such inferences can be confounded by incorrect identification of pre-cloud air, non-Lagrangian sampling, extended sampling periods and resultant averaging of spatial inhomogeneities (including clear air pockets within clouds), and inadequately resolved contributions of aqueous-phase chemistry. Not surprisingly, the results of the above studies varied quite widely. Most commonly, however, mass scavenging efficiency was found to be high (>0.8).

The above studies based on spatially-averaged particle *mass* concentrations could not address the issue of main concern with respect to radiative transfer, namely, the partitioning of cloud particles between droplets and interstitial aerosol in terms of their local *number* concentrations. Field studies focused on aerosol scavenging based on particle number concentrations are relatively scarce. In the study of Leaitch et al. (1986b) for stratiform and cumuliform clouds, the authors took special care to ensure Lagrangian adiabatic

interpretation by comparing the instantaneous cloud droplet number concentration at a single location within the adiabatic updraft core near cloud base with the below-cloud aerosol number concentration. They found that activation efficiencies so defined were generally high when pre-cloud AMP concentrations were less than about 750 cm^{-3}, but dropped off non-linearly at higher particle loading. Raga and Jonas (1993) made a similar observation when comparing droplet concentrations near cloud top with the sub-cloud aerosol concentrations on the assumption that the latter represented the pre-cloud condition.

Gillani et al. (1995) demonstrated that such an assumption was not generally valid in stratiform clouds which are layered and may include sharp inversions decoupling the layers from each other and from the sub-cloud layer. For such clouds, the adiabatic assumption made in 1-D cloud models is not generally valid. To circumvent this difficulty with respect to identification of pre-cloud air, Gillani et al. defined fractional activation (F) in terms of local variables only, as the ratio of cloud droplet concentration (activated particles) to total particle concentration (droplet concentration + concentration of unactivated accumulation-mode particles, 0.17 to 2.07 μm diameter). In their study (aircraft measurements in and near stratiform clouds near Syracuse, NY in the Fall of 1984), continuous *in situ* measurements were available for particle number concentrations in 15 size classes each for the droplets and for dried (by heating the probe inlet air) interstitial aerosols. Thus, they were able to determine F at a high spatial resolution throughout the clouds studied (continental stratiform). It was determined that accumulation-mode particles larger than 0.37 μm were efficiently activated in the cloud under all measurement conditions, but that particles in the range 0.17 to 0.37 μm were often activated only partially. Partial activation generally correlated with high local total particle concentration (>600 cm^{-3}) and with low temperature lapse rate (surrogate for cooling rate with ascent, $dT/dt = w.\ dT/dz$, where w= the mean long-wave updraft speed), the two conditions most responsible for limiting supersaturation. It is important to note that w is a most difficult quantity to measure, and is not generally available in field measurements. Under the most polluted conditions in a stable stratus, fractional activation of the accumulation-mode particles was as low as 0.1 in the core of the cloud. Statistically, based on ten days of measurements in the Syracuse study, it exceeded 0.9 in 36% of the data in cloud interior, but was below 0.6 in 28% of such data. It was generally

quite low in cloud edges. Evidently, the assumption made in RADM of total activation is questionable for stratiform clouds.

Simple parameterizations of fractional activation in clouds have been developed based on 1-D adiabatic Lagrangian models (e.g., Twomey, 1959; Ghan et al., 1994), and generally highlight the significance of particle loading and updraft speed (model calculated). The 1-D adiabatic approach is useful near cloud base and in updraft cores, but it breaks down near cloud edges and in the upper portions of clouds where entrainment and mixing effects are substantial. It is also questionable in the presence of additional complexities such as cloud layering (Gillani et al., 1995) and lifting and sinking motions (Baker and Latham, 1979; Pruppacher and Klett, 1980). These complex effects result in three-dimensional spatial inhomogeneities and multi-modal droplet size spectra which are uncharacteristic of the simple adiabatic model.

Noone et al. (1992b) studied activation in ground fogs. They were able to infer size-segregated volume and number scavenging efficiencies of aerosols (using a counterflow virtual impactor) in the fog under conditions of very high particle loading and extremely low supersaturations. For such highly-polluted fog conditions, they found high activation efficiencies (>0.8) only for particles larger than 0.8 μm.

In most cloud and fog studies which include considerations of particle composition, use is made of the concept of water-soluble mass fraction (ε). This implicitly assumes internally mixed particles. As was shown by Zhang et al. (1993), there may really be two ε's, one (ε_m) for the "more" hygroscopic particles, and one (ε_l) for the "less" hygroscopic aerosols. In the diagnostic modeling study of Pitchford and McMurry (1994), the two-ε concept was implemented. For clouds and fogs, this implies that S_c may be different for different particles in the same size range.

The interaction between aerosols and clouds modifies not only the clouds, but also the aerosols. The condensation-evaporation cycling of aerosols through non-precipitating clouds generally results in growth of the nuclei due to microphysical and chemical processes during their in-cloud residence (Hoppel, 1988; Hoppel et al., 1990).

3.4.2.3 Pertinent Results of the Southern California Air Quality Study

A separate section is devoted here to the Southern California Air Quality Study (SCAQS) because it was perhaps the most comprehensive and sophisticated field study related to PM conducted in the past decade. It was a major measurement and modeling program conducted during 1985 to 1990 under the sponsorship of a number of local/state/federal government agencies and industrial organizations to study the air quality, including PM_{10}, of the Southern California Air Basin (SoCAB). It was a remarkably comprehensive study in terms of participating scientists and organizations, pollutants studied, and measurements made. Evaluation of measurement methods was one of its stated major objectives. Accordingly, the main field studies of summer and fall 1987 were preceded in the summers of 1985 and 1986, respectively, by the Nitrogen Species Methods Comparison Study (overview and results published in a number of papers in Atmos. Environ. 22: 1517- , 1988) and the Carbonaceous Species Methods Comparison Study (overview and results published in a number of papers in the special issue of Aerosol Sci. Technol. 12(1), 1990). An overview of the study is contained in Lawson (1990), which also includes a summary of preliminary results of the 1987 field study presented at the 82nd Annual Meeting of the Air & Waste Management Association. A SCAQS data analysis meeting was held in Los Angeles in July 1992, the proceedings of which are available from AWMA as well as the California Air Resources Board (CARB). CARB has also compiled a listing of the principal publications resulting from SCAQS, and has produced a brief unpublished document entitled "SCAQS Summary of Goals and Conclusions". What follows is a brief overview of some of the principal findings of the SCAQS particulate and related measurements and analyses as they pertain to the subject of transformations. It is based on the CARB document summarizing goals and conclusions. No attempt is made here to identify the specific research studies which have generated these conclusions.

The SCAQS 1987 intensive field measurements were made during summer (11 days) and fall (6 days), when a wide range of air quality measurements were made at up to 36 surface sites. These were augmented by measurements from up to three instrumented aircraft, surface and upper air meteorological measurements at a number of sites, and other special measurements including photography. Some of the principal findings were as follows:

Source Characterization

Primary geological material was the major contributor to PM_{10} during summer at the eastern sites in SoCAB. Its contribution was generally lower in fall. There was a positive gradient from the coast inland, where it constituted about 30% of PM_{10}. Primary motor vehicle exhaust was generally the second largest contributor during the summer, with the largest fractional contribution (24% of PM_{10}) in downtown Los Angeles. Industrial facilities, vegetative burning and biogenic emissions were not major contributors.

Concentration, Size, and Composition

Concentrations of PM_{10} (24-h average) were highest in fall (> 200 $\mu g/m^3$); highest concentrations in summer were around 120 $\mu g/m^3$. The most abundant PM_{10} species at all sites were nitrate, sulfate, ammonium, OC, EC, calcium, sodium, chloride and iron. $PM_{2.5}$ constituted 1/2 to 2/3 of PM_{10} at all sites, being a higher fraction in fall than in summer. Average mass fractions of $PM_{2.5}$ were 15-30% OC, 4-9% EC (peaking during the morning traffic period), 12-36% nitrates (large site-to-site variation and midday peak preceding the ozone peak by about two hours), and 3-30% sulfate (large seasonal variation). About 20% of the total $PM_{2.5}$ were estimated to be due to non-fossil fuel combustion (modern C). Aerosols occurred in the local atmosphere in three size modes with relative maxima around 0.2, 0.7 and ~5 μm diameter. The predominant modes for sulfate and ammonium were around 0.7 μm, and for nitrate around 0.7 and 4-5 μm.

Ammonium Nitrate and Ammonium Sulfate

Ammonium nitrate concentrations were lowest at Hawthorne (1% of PM_{10}) closer to the coast, and highest at Riverside (24% of PM_{10}) downwind of a large source of ammonia near Rubidoux. For ammonium sulfate, the reverse was true, with the highest concentration at Hawthorne (31%) and the lowest at Riverside (8%). Together, the two species constituted about 1/2 to 2/3 of $PM_{2.5}$. In summer, ammonium nitrate was 5-10 times larger at Riverside than at other sites, its formation apparently being ammonia-limited at the other sites. In fall, it was the second highest contributor to PM_{10} at all sites, and it could not be determined if its formation was NH_3-limited or HNO_3-limited. Ammonium sulfate was rather uniformly

distributed over all sites during both seasons, with concentrations in fall being about half of those in summer.

Secondary Organic Carbon

Secondary OC was contributed significantly to peak 2-h PM_{10} during several episodes, being as high as 70% of total OC and 14 $\mu gC/m^3$, and its diurnal peak lagged the ozone peak by up to 2 h. Interestingly, its highest concentrations occurred on Saturdays.

Hygroscopic Nature of the Aerosol

As has been pointed out before, based on TDMA and MOUDI measurements, there were indications that the particles were to some extent externally mixed, with "more" hygroscopic and "less" hygroscopic components in monodisperse size classes, with a pattern of relationship to sulfate-to-carbon ratio.

A number of other findings with implications for aerosol formation and growth also resulted from SCAQS. Some of the principal ones are highlighted below:

- Measured concentration ratios VOC/NO_x in the morning traffic period were found to be 2 to 2.5 times higher than the corresponding values based on emission inventories. SCAQS tunnel studies indicated that this discrepancy may be due to an underestimation in the emission inventories of VOC and CO for motor vehicles by a factor of about 2. This finding had major potential implications not only for Los Angeles and California, but for the whole nation, because similar mobile-source emission models are used throughout the nation. This uncertainty is relevant to ozone formation as well as aerosol formation. Urban airshed model simulations were found to be in better agreement with ozone measurements when the VOC emission estimates were doubled.

- Nitrous acid, directly emitted as well as presumably formed by nighttime reactions involving NO_x, water and aerosols, may be the single largest source of OH radicals in the morning.

- Biogenic VOC were found to be relatively negligible in the SoCAB.

- Urban airshed model applications to SCAQS episodes were found to underpredict NO_x oxidation products. Also, the models did not satisfactorily simulate observed layers of ozone and other secondary pollutants near the top of the daytime mixed layer. The sources of these errors may be related to model formulation (terrain-following coordinate system), meteorological inputs, and transport simulation.

3.5 DRY DEPOSITION

3.5.1 Theoretical Aspects of Dry Deposition

Dry deposition is commonly parameterized by the deposition velocity, V_d (m s^{-1}) which is defined as the coefficient relating the pollutant deposition flux F (g $m^{-2}s^{-1}$) and the pollutant concentration c (g/m^3) at a certain reference height above the surface, i.e.,

$$\mathbf{F} = \mathbf{V_d c} \tag{3-51}$$

The deposition velocity can be expressed as the inverse of a sum of "resistances" in three layers adjacent to the surface (Sehmel, 1980; Hicks, 1984):

1. The aerodynamic layer (i.e., the layer in which atmospheric turbulent fluxes are constant [typically extending to about 20 m above the ground]). In this layer, pollutant transfer, whether gas or particle, is controlled by atmospheric turbulence.

2. The surface (or quasi-laminar) layer, a thin layer (~1 mm) just above the surface in which transport occurs by molecular diffusion. In this layer, gases transfer to the surface by molecular diffusion and particles undergo Brownian diffusion and inertial impaction.

3. The earth/canopy/vegetation surface, at which the pollutant gas molecule or particle is removed from the air by attachment to the surface.

For gases, the deposition velocity is a function of these three types of resistance as follows:

$$\mathbf{V_d} = (\mathbf{r_a} + \mathbf{r_s} + \mathbf{r_c})^{-1} \tag{3-52}$$

where r_a is the atmospheric resistance through the aerodynamic layer, r_s is the surface layer resistance, and r_c is the canopy/vegetation resistance. All resistances are in units of s m^{-1}.

The aerodynamic resistance r_a can be expressed (Wesely and Hicks, 1977) by:

$$r_a = \frac{1}{ku_*}\left[\ln(z_s/z_o) - \varnothing_h\right] \quad (3\text{-}53)$$

where z_s is the reference height (m) (~10 m), z_o is the roughness length (m), k is the von Kármán constant (0.4), u_* is the friction velocity (m s^{-1}), and $Ø_h$ is the stability correction factor. Roughness lengths vary from about 10^{-5} m for very smooth surfaces (ice, mud flats) to 0.1 m for fully grown root crops, to 1 m for a forested area, to 5-10 m for an urban core (Seinfeld, 1986).

The surface layer resistance can be parameterized as a function of the Schmidt number Sc = v/D, where v is the kinematic viscosity of air (m^2/s) and D is the molecular diffusivity (m^2/s) of the species, as

$$r_s = d_1\frac{Sc^{d_2}}{ku_*} \quad (3\text{-}54)$$

where d_1, d_2 are empirical parameters (d_1 ≅1.6 - 16.7, and d_2 = 0.4 - 0.8, with a suggested choice of d_1 = 5, d_2 = 0.66).

The canopy resistance is the resistance for gases in the vegetation layer. There are three main pathways for uptake/reaction of the pollutant within the vegetation or surface: (1) transfer through the stomatal pore and dissolution or reaction in the mesophyll cell; (2) reaction with or transfer through the leaf cuticle; (3) transfer into the ground/water surface. In the resistance model, these pathways are treated as three resistances in parallel. The canopy resistance r_c for a gaseous species may be parameterized (Yamartino et al., 1992) as:

$$r_c = [LAI/r_f + LAI/r_{cut} + 1/r_g]^{-1} \quad (3\text{-}55)$$

where LAI is the leaf area index (i.e., the ratio of leaf surface area divided by ground surface area), r_f is the internal foliage resistance, r_{cut} is the cuticle resistance, and r_g is the ground or water surface resistance. Values for r_f are discussed by O'Dell et al. (1977). The resistance r_{cut} is parameterized by Pleim et al. (1984).

For gaseous pollutants, solubility and reactivity are the major factors affecting surface resistance and net deposition velocity. For particles, the factor most strongly influencing the deposition velocity is the particle mass or, assuming similar densities, the particle size. Particles are transported toward the surface by turbulent diffusion, which for larger particles is enhanced by gravitational settling. Across the quasi-laminar surface layer very small particles (< 0.05 μm diameter) are transported primarily by Brownian diffusion, analogous to the molecular diffusion of gases. The larger particles possess inertia, which may enhance the flux through the quasi-laminar sublayer.

The downward pollutant flux is the sum of the turbulent diffusive flux and a flux due to gravitational settling, i.e.,

$$\mathbf{F(z) = F_d + V_g C = V_d C} \qquad (3\text{-}56)$$

where V_g is the gravitational settling velocity of the particle. Whereas in the formulation of the algorithm for gases the analogy with electrical resistance is straightforward, it is less so for particles. This is because at any height within the aerodynamic layer and surface layer the flux of trace gases is diffusive only and hence a function of the concentration gradient. Consequently, when equating the fluxes through each layer under the steady-state assumption, the deposition velocity may be cast in a form proportional to the inverse of a sum of resistances. Nevertheless, the electrical resistance analogy can still be employed for particles. The gravitational settling velocity is merely represented by the reciprocal of an additional resistance acting in parallel with the diffusive resistance.

As noted earlier, for particles, the resistance in the vegetation layer (r_c) is usually assumed to be zero, since particles that penetrate the surface layer are assumed to stick to the surface. The expression for deposition velocity in terms of the resistances, modified to include gravitational settling, is

$$\mathbf{V_d = (r_a + r_s + r_a r_s V_g)^{-1} + V_g} \qquad (3\text{-}57)$$

Therefore, the deposition velocity of particles may be viewed in terms of electrical resistance as the reciprocal of three resistances in series (r_a, r_s, and $r_a r_s V_g$) and one in parallel ($1/V_g$). The third resistance in series is denoted here as a virtual resistance in view of the fact that it is a mathematical artifact of the equation manipulation and not a physical resistance. Equation 3-57 is usually implemented with r_a (particles) equal to r_a (gases), in which r_a is computed by Equation 3-53, and the surface layer resistance is

$$r_s = (Sc^{-2/3} + 10^{-3/St})^{-1} (u*)^{-1} \quad (3\text{-}58)$$

where Sc is the Schmidt number based on D, the Brownian diffusivity of the particle in air, and St is the Stokes number, $St=V_g(u*)^2/gv$, where u* is the friction velocity, g is the gravitational constant and v is the air kinematic viscosity. The surface layer resistance incorporates the effects of both Brownian diffusion, through the Schmidt number, and inertial impaction effects, through the Stokes number.

The gravitational settling velocity V_g is a function of the particle size, shape and density. For spherical particles (Seinfeld, 1986),

$$V_g = \frac{d_p^2 g(\rho_p - \rho_a)C}{18\mu} \quad (3\text{-}59)$$

where d_p is the particle diameter (m), ρ_p is the particle density (g /m^3), ρ_a is density of the air (g /m^3), μ is the viscosity of air (g m^{-1}s^{-1}), and C is the slip correction factor

$$C = 1 + (2\lambda / d_p)[1.257 + 0.4\exp(-0.55 d_p / \lambda)] \quad (3\text{-}60)$$

where λ is the mean free path of air molecules (λ = 6.53 x 10^{-6} cm at 298K)

Figure 3-12 shows particle deposition velocities based on wind tunnel measurements. Deposition velocities are presented as a function of particle diameter, particle density, and surface roughness height. Particle deposition velocities exhibit a characteristic minimum as a function of particle size. For the smallest particles, deposition velocity increases as particle size decreases because diffusion by Brownian motion increases as particles get smaller. For the largest particles, gravitational settling becomes important as particles get larger so the deposition velocity increases as particles increase in size. A characteristic minimum in deposition velocity results in the range of 0.1 to 1.0 μm diameter where neither Brownian diffusion nor gravitational settling is strong enough to control removal.

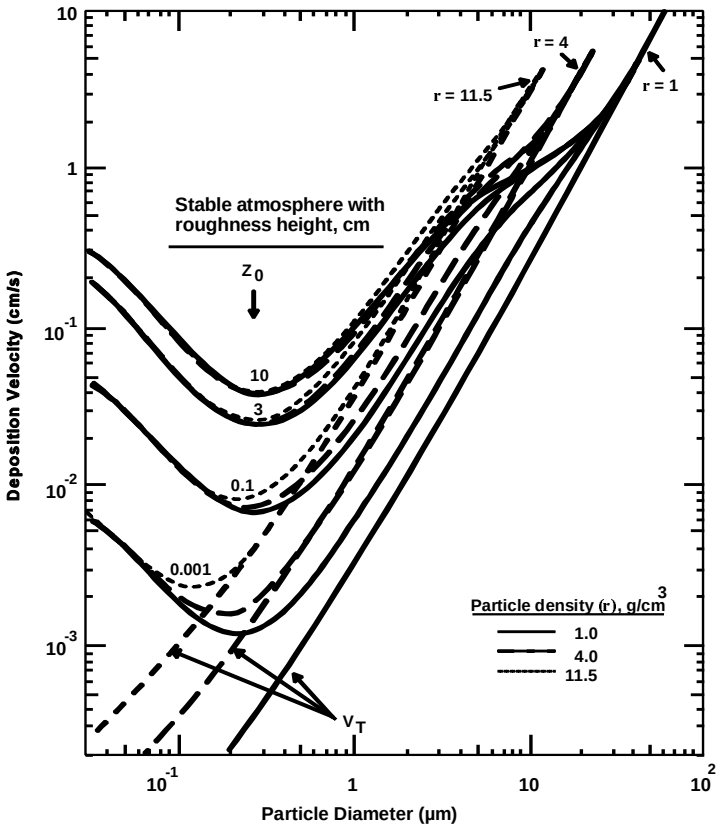

Figure 3-12. Extrapolations from correlations of wind-tunnel measured deposition velocities for z = 1 m, densities of 1, 4, and 11.5 g cm^{-3}. V_T represents terminal settling velocity.

Source: Sehmel (1980) as presented by Nicholson (1988).

It is possible to obtain a rapid estimate of the atmospheric lifetime of particles with respect to removal by dry deposition. If the aerosol can be assumed to have a uniform concentration between the ground and a height *h*, then the residence time relative to removal by dry deposition is h/V_d. For example, for a 1000 m atmospheric layer, and a particle deposition velocity of 0.1 cm/s, the estimated residence time is 11.5 days.

3.5.2 Field Studies of Dry Deposition

In spite of many field measurements and considerable progress since 1980 in our understanding of dry deposition processes and their quantification, uncertainties remain substantial. The problem is extremely complex involving a large multiplicity of factors, and their complex interactions, which influence dry deposition of atmospheric particles and their precursors (see, for example, a tabulation of some of these in Davidson and Wu, 1990). These factors relate to characteristics of the atmosphere, nature of the deposition surface, and properties of the depositing species. It is impossible in field studies to measure all the pertinent variables over large enough spatial and temporal domains. In essence, knowledge of dry deposition is limited by the inability to make the necessary measurements in other than special circumstances. This was a key statement of the NAPAP Workshop on Dry Deposition in Harpers Ferry, West Virginia (Hicks et al., 1986). The Workshop report also noted that there is presently a lack of fundamental knowledge concerning the chemical and biological processes influencing dry deposition, and there are serious hazards associated with scaling input information down from grid level to local, and scaling up the results of local measurements to broader domains. Information contained in the Workshop report and in subsequent research publications on the subject were reviewed by Davidson and Wu (1990). That review summarizes the results of a large number of field studies published since earlier reviews by McMahon and Denison (1979), Sehmel (1980), Hosker and Lindberg (1982) and Galloway et al. (1982). It also includes summaries of dry deposition processes, wind tunnel studies and empirical models, techniques for measuring deposition in the field, and comparisons of field data and model results. The summary presented in this section is based largely on Davidson and Wu (1990).

Many techniques have been used to measure dry deposition. They are generally grouped into two classes: surface analysis methods, which are based on examination of contaminant

accumulations on natural or surrogate surfaces, and atmospheric flux methods, which involve ambient measurements of the species of interest and other related variables. These methods provide the deposition flux out of which the deposition velocity is inferred. *Surface analysis methods* include foliar extraction (by washing individual leaves), throughfall and stemflow (wet measurements above and within the canopy), watershed mass balance, tracer techniques, snow sampling, collection on surrogate surfaces, etc. These methods may provide useful data on the flux of coarse particles, but fail to simulate the physical processes which control the deposition of sub-micron particles to natural surfaces, and to give meaningful data on trace gas deposition. Deposition on surrogate surfaces may not mimic that on natural surfaces. *Atmospheric flux methods* include micrometeorological methods (eddy correlation and vertical gradients), aerometric mass balance in a box over the depositing surface, tracer techniques, etc. Micrometeorological methods also include what has come to be known as the inferential approach in which measured concentrations are combined with specified or calculated deposition velocities based on meteorological data and surface information. This approach is used in long-term monitoring programs in which only simple measurements are possible at remote sites (e.g. weekly average species concentrations and routine meteorological measurements). For details of the various methods, see Davidson and Wu (1990) and the report from NAPAP Workshop on Dry Deposition (Hicks et al., 1986).

Estimates of flux in the surface layer have historically been inferred from measurements of the vertical gradients of mean quantities such as concentration or horizontal wind speed under conditions that the gradient-transport theory was assumed to be valid. Calculations are modified by corrections of departures from neutral stability. However, with fast response instruments it is possible to directly measure the correlation of fluctuations in velocity and transported quantities of interest such as pollutants, water vapor or heat. For direct measurement of flux, the eddy correlation method is widely used. In this case, pollutant flux and aerodynamic resistance can be measured with appropriate fast sensors with matched time response. A discussion of these methods may be found in Hubbe (1989).

Several limitation of the methods presently being implemented should be noted. For example, the aerometric mass balance technique is essentially inferential, relying heavily on the accurate measurements of air concentrations and on the evaluation of accurate deposition

velocities. The dominant limitations are probably those associated with the ability to evaluate appropriate deposition velocities. The knowledge on which any interpretive scheme for deposition can be based is quite limited. Most information on gas transfer either deals with average uptake in laboratory conditions (chambers, wind-tunnel, etc.), or is derived from short-term micrometerological measurements at selected field sites. Ongoing research programs are addressing these problems. However, a major task, confronting all attempts to monitor dry deposition, is to assess the magnitude of errors arising from the need to apply poorly-known relationships.

3.5.3 Measured Deposition Velocities

Measurements of dry deposition in the field and in chambers have primarily involved six categories of contaminants: sulfur species, nitrogen species, chloride species, ozone, trace elements and atmospheric particles. The results of many of these studies published between 1978 and 1987 are reviewed in Davidson and Wu (1990), which includes extensive tabulations of the studies and their results. Of the reported studies on sulfur species, 20 pertain to SO_2. They give deposition velocities ranging from nearly 0 to 3.4 cm/s. The variations are due to differences in seasonal and diurnal conditions, aerodynamic transfer, surface characteristics (especially stomatal resistance), measurement methods, etc. Daytime values are generally higher, as expected (lower aerodynamic and stomatal resistances). Micrometeorological methods were used in 16 studies whose average values of v_d gave a grand average of 0.95 ± 0.62 cm/s. Four studies provided an average value of 0.13 ± 0.09 cm/s for deposition velocity on snow. For particulate sulfur, 34 studies are included, with 10 also including particle size measurements. A graph also includes results of earlier studies, and gives values of v_d in the range 0.01 to 10 cm/s. Results for v_d in cm/s based on different methods are as follows: 0.55 ± 0.65 for micromet methods, 0.26 ± 0.25 for surrogate surface exposures, 0.23 ± 0.24 for foliar extraction, and 1.00 ± 0.41 for throughfall. Since the micromet method is believed to be more specific for submicron particles while the surrogate surface method is biased in favor of larger particles, the difference in the results of those methods is opposite to that expected. The surrogate surface and foliar extraction results are close, but each has a large variance. Throughfall values are

the largest probably partly because they include deposition of SO_2. Evidently, measurement methods themselves are an important variable because they do not measure the same thing.

Twenty two species are reported for nitrogen species, including NO_2, NO_x, HNO_3, NO_3^-, NH_3, and NH_4^+. The inferred values of v_d (cm/s) are: 0.012 to 0.5 for NO_2 (2 studies), -2.6 to 0.3 for NO_x (4 studies), 0 to 2.9 for HNO_3 (4 studies), 0.13 to 1.3 for NO_3^- (7 studies), 1.9 ± 1.55 for NH_3 (1 study), and 0.06 to 1.0 for NH_4^+ (4 studies). The zero value for nitric acid was for snow in a chamber study; otherwise, the values for nitric acid are the highest, indicating low surface resistance. The values for particulate nitrate are somewhat larger than for sulfate; this may reflect larger particle size associated with nitrate. Davidson and Wu (1990) report four studies for chloride-containing particles, giving values of 1.0 to 5.1 cm/s; and one study for HCl gas giving a value for HCl of 0.73 cm/s on dew. The highest values for chloride were in winter, related to road salt. Deposition velocities to dew were measured for a number of species including HNO_3, NO_2, SO_2, and aerosol $SO_4^=$ and NH_4^+ in southwest Pennsylvania (Pierson et al., 1986) and in the Los Angeles basin (Pierson et al., 1988; Pierson and Brachaczek, 1990). Low values were obtained, consistent with the high atmospheric stability required for dew formation. Based on 11 studies using micromet methods, v_d of ozone on vegetation ranged between nearly 0 and 1.5 cm/s (average of 15 values = 0.39 ± 0.21). Nighttime values were lower, but the day-night difference was less for ozone than for NO_2.

Results of 19 studies included measurements for 21 trace elements, with particle size data in 15 studies. For these data, crustal element enrichment factors (EF) were determined. Values of EF ≈ 1 indicate crustal sources, while EF > 1 (enriched) indicate non-crustal sources such as anthropogenic, natural combustion (volcanism, forest fires), biogenic, sea-spray, etc.. Large enrichment factors were found for Ag, As, Cd, Cu, In, Pb, Sb, Se and Zn. Ni and V were marginally enriched. Other elements were mainly soil-derived. v_d for these elements were generally higher (>1 cm/s), while they were generally less than 1 cm/s for the enriched elements (smaller, submicron particles). A figure including these as well as data of earlier studies is presented, showing a positive correlation between v_d and MMD (mass median diameter). For Pb, the values ranged between 0.1 and 1.0 cm/s. Friedlander et al. (1986) have used CO as a tracer for automobile emissions to estimate the deposition velocity for Pb, by comparing the ratio Pb/CO in ambient air to that in a tunnel.

They found the former to be lower, indicating deposition compared to its value in fresh emission (tunnel). Based on these data, they estimated v_d for Pb to be 0.26 cm/s, which is consistent with the range given above. Davidson and Wu (1990) also report the results of 5 other field studies with micromet measurements of dry deposition for submicron particles, and particle size measurements also. v_d was generally less than 1 cm/s, in general agreement with results for sulfate and the enriched trace elements.

Davidson and Wu (1990) have also presented results of comparisons between measured values of v_d with predicted values based on six model calculations. These results are from published studies with size distribution data for aerosol sulfate and trace elements. The measured values of v_d are for the full size range; the model value is the concentration-weighted average of the calculated values for all size classes. For sulfate, the predicted values were generally smaller than the measured values. Good agreement was, however, not expected because of differences in ambient conditions and surface conditions between values used in the model compared to the corresponding measured values. Similar comparisons for 24 trace elements were also tenuous: out of 11 of the 24 elements for which more than one or two data points only were available, the measured values were in the predicted range; for Al, Ca and Fe, the predictions were low, while for Zn, the predictions were too high. For the other 13 elements with sparse measured data, the agreement was generally much poorer.

3.6 WET DEPOSITION

3.6.1 Introduction

Although detailed physico-chemical models are needed to describe the details of in-cloud and below-cloud scavenging of particles, there has been a benefit in using comparatively simple formulations of precipitation scavenging that provide a convenient picture of the process as a whole. These simple methods are not designed to explain detailed variations in wet deposition with time or space, but they are useful in describing average deposition rates over large areas. Two alternative techniques have become popular. The first relates concentrations of material in precipitation to the quantity available in the air, thus describing the overall efficiency of precipitation as a removal path. By relating concentrations in precipitation to those in the air, dimensionless scavenging ratios can be determined. The second common method is based on

the first-order removal of airborne gases or particles as rain falls through the atmosphere. Concentrations in the air will decrease exponentially and a scavenging rate can then be determined.

Below-cloud scavenging rates for particles of about 3×10^{-5} s^{-1} appear to be typical; in-cloud scavenging leads to rates typically ten times larger (Hicks and Meyers, 1989). Hygroscopic particles are scavenged more readily than hydrophobic ones.

Based on the wet flux *W*, the wet deposition velocity may be defined as

$$V_w = \frac{W}{c(x,y,0,t)} \simeq \bar{\Lambda} h \tag{3-61}$$

where $\bar{\Lambda}$ is the vertically averaged scavenging rate. The last equality assumes that the pollutant is uniformly distributed between $z = 0$ and $z = h$. The wet deposition velocity V_w can be computed by

$$V_w = w_r p_o \tag{3-62}$$

where w_r is the washout ratio (i.e., the dimensionless ratio of the concentration of material in surface-level precipitation to the concentration of the material in surface-level air) and p_o is the precipitation intensity (mm hr^{-1}). For example, if $w_r = 10^6$ and $p_o = 1$ mm h^{-1}, then $V_w = 28$ cm s^{-1}, which gives, for $h = 1{,}000$ m, $\bar{\Lambda} = 2.8 \times 10^{-4}$ s^{-1}. Seinfeld (1986) provides a detailed discussion of precipitation scavenging of particles, including the calculation of collision efficiencies and scavenging rates.

Scavenging ratios relate concentrations in precipitation to those in air. Although such ratios depend on many factors, they provide a simple way to include wet deposition processes in air quality models. The washout (or "scavenging") ratio is

$$w_r = \frac{[c]_{rain}\rho_a}{[c]_{aerosol}} \quad (3\text{-}63)$$

with $[c]_{rain}$ in mg g^{-1}, $[c]_{aerosol}$ in mg m^{-3}, and ρ_a (=1,200 *g* m^{-3}), the density of air. The definition of this ratio presumes that the aerosol measured at ground level is vertically uniform and that there are no factors limiting the collection of aerosol by the droplets, such as solubility. Scavenging ratios of about 400 appear to be appropriate in the case of particles well mixed in the lower atmosphere but originating near the surface, while values of about 800 appear characteristic of material derived from the free troposphere (Hicks and Meyers, 1989).

3.6.2 Field Studies of Wet Deposition

Removal of accumulation mode aerosol particles from the atmosphere occurs largely by the precipitation process (e.g., Slinn, 1983). These particles are the dominant particles on which cloud droplets form (cloud condensation nuclei, CCN). Once a cloud droplet (of diameter of a few up to about 20 micrometers) is formed, it is much more susceptible to scavenging and removal in precipitation than is the original submicrometer particle. The fraction of aerosol particles incorporated in cloud droplets on cloud formation is the subject of active current research, which has been reviewed in Section 3.4.2.2.

The dominance of precipitation removal processes for accumulation mode particles results in high variability in temporal patterns of aerosol loadings, that may be attributed to the episodicity of precipitation events and synoptic scale meteorology that delivers air of differing origins to a given location (e.g., Waldman et al., 1990). This variability leads to difficulties in attempts to estimate mean residence times based on budget considerations (Junge, 1963; Schwartz, 1979). A unique approach to estimation of the mean residence time of accumulation mode aerosol particles was presented by measurement of the decay of atmospheric concentrations of ^{137}Ce at several mid-latitude surface stations in Europe and Asia in the weeks following the Chernobyl accident (Cambray et al., 1987); the ^{137}Ce was present largely in this size range. This study led to an estimate for the mean residence time of 7 days, consistent with other estimates. It may be noted, however, that this residence

time is applicable to particles in the free troposphere, where the ^{137}Ce was mainly present during the several week period. The mean residence time of accumulation mode particles in the boundary layer is expected to be somewhat less (Benkovitz et al., 1994).

Wet deposition measurements are made principally to meet three objectives: (1) to determine the regional spatial-temporal distribution and chemistry of wet deposition; (2) to study pathways and mechanisms of pollutant wet removal from the atmosphere; and, (3) to generate data for diagnostic evaluations of precipitation scavenging modules. The first of these objectives is best studied based on data of routine monitoring programs. These were reviewed in detail by NAPAP (Sisterson et al., 1991) and are not covered here. The focus here is on recent research field studies aimed at objectives (2) and (3) above.

A significant effort in NAPAP in the 1980s was devoted to development of wet removal characterizations that directly reflected the cloud physics, attachment, reaction, and precipitation processes (Hales, 1991). The PLUVIUS II models, prepared under the auspices of NAPAP, was a reactive storm model based on multi-phase material balance, and served as the basis for the development of the one-dimensional RADM Scavenging Module, RSM. A parallel activity in NAPAP was DOE's PRECP (Processing of Emissions by Clouds and Precipitation) field measurements program which comprised a series of six individual intensive field studies with the objective of systematically measuring scavenging characteristics for different classes of storm systems important to regional acid deposition. In these, studies, the emphasis was on *in situ* aircraft measurements. What follows is a brief review of such research field studies. It is based substantially on Hales (1991). In the context of precipitation scavenging studies, it is useful to bear in mind that pollutant particles, on average, undergo a number of repeated cycles in and out of non-precipitating clouds before finally being removed by precipitation.

In situ aircraft measurements in clouds and precipitation are of crucial importance in mechanistic/diagnostic studies. Current technology permits continuous aircraft measurements of NO, NO_2, NO_y, HNO_3, PAN, SO_2, O_3, H_2O_2, liquid water content (LWC), and size-segregated aerosol and cloud/rain droplet concentrations with quite high sensitivity and precision. In addition, filter samples and cloudwater samples can provide mass concentrations of the major ions in aerosols and droplets at a temporal resolution of a few minutes. Ground monitoring of precipitation in recent studies has included use of the

NAPAP-developed Computer-Controlled Automated Rain Sampler (CCARS) which is a combination rain gauge and sequential precipitation chemistry sampler, controlled and monitored by a programmable microprocessor. Such samplers permit capture of statistically valid footprints (multiple sequential event samples) of deposition during the course of a storm. Upper-air meteorological measurements with fine vertical resolution of wind components, temperature and moisture are also important. These can be made using radar profilers and doppler radars.

Field studies have been conducted in and below point-source plumes (meso-γ scale) and urban plumes (meso-β scale). In the former, precipitation scavenging of S and N compounds was found to be minimal (Granat and Soderland, 1975; Dana et al., 1976; Drewes and Hales, 1982), indicating low precipitation scavenging efficiency for SO_2 and NO_x from fresh plumes. Hales and Dana (1979) found appreciable removal of S and N compounds from the urban plume of St. Louis by summer convective storms. Patrinos and Brown (1984), Patrinos (1985) and Patrinos et al. (1989) found efficient scavenging of these compounds from the urban plumes of Philadelphia and Washington, DC by frontal storms. H_2O_2 data in rain showed considerable spatial variability in the plumes.

The major regional-scale field studies include OSCAR (Oxidation and Scavenging by April Rains, April 1981), PRECP (mid-1980s), and the DOE-FBS (Frontal Boundary Study). OSCAR (Chapman et al., 1987) included a nested array of ground level sampling (an extended regional precipitation chemistry network in northeastern United States, with an embedded high-density network in northeast Indiana) as well as three research aircraft. The focus was on scavenging by extratropical cyclonic storms. The aircraft made clear air measurements before and after frontal passage, as well as measurements within the storm, in the vicinity of the high-density network. Measurements were made during four storms. OSCAR data have been used for regional model development and evaluation.

The six PRECP studies, conducted between 1984 and 1988, were targeted at scavenging measurements in different types of storm systems. Three studies were focussed on convective storms (II, V, and VI) in summer, and the other three on extratropical cyclonic and frontal storms during other seasons; five were conducted east of the Mississippi River, and one in the Oklahoma-Kansas-Colorado area. All of them included two or more research aircraft, and all also included at least limited area precipitation chemistry networks (PRECP IV had three

multiscale networks ranging from a coastal "rain-band" network to a truly regional scale network). The network in PRECP VI was a highly-density network within an 80-km RADM grid cell, designated to provide information about regional sub-grid scale variability. Two of the studies were conducted jointly with other meteorology-focussed measurement programs; PRECPII with the NSF PRESTORM study, and PRECP IV with the NSF-NASA-NOAA Genesis of Atlantic Lows Experiment (GALE). Such synergism resulted in particularly strong meteorological data in these two studies. PRECP I was intended to be an exploratory study, but generated a database of which at least one storm has been extensively studied (Saylor, 1989). PRECP VI, on the other hand was designed as the grand finale aimed at generating a definitive database for evaluation of the RADM Scavenging Module, but failed to meet its main objective owing to the extreme drought of the summer of 1988.

Overall, the studies have developed a substantial database of mechanistic-diagnostic information suitable for diagnostic model studies. PRECP II definitively demonstrated the cloud venting phenomenon transporting boundary layer pollutants to considerable heights in the free troposphere (Dickerson et al., 1987). PRECP III provided a significant new mechanistic insight regarding scavenging in orographically enhanced storms, e.g., the observation of an unexpected entrainment mechanism that occurs as orographic lifting occurs, and which enhances chemical wet removal appreciably (Hales, 1991). PRECP V, focussed on studying vertical profiles of chemical species in and around convective storms, resulted in one study (Daum et al., 1990) which showed that while SO_2 was more concentrated in the lower parts of the ABL, H_2O_2 was concentrated near the top, underscoring the importance of mixing in facilitating aqueous-phase of SO_2 by H_2O_2. The same study also found that in the low-NO_x background, H_2O_2 was correlated with humidity.

The Frontal Boundary Study (DOE) was conducted in fall 1989 as part of a global study of the fate of energy-related pollutants. The focus was on pollutant redistribution and removal by stable frontal storms occurring subsequent to pollution episodes associated with high-pressure stagnation. Aircraft soundings ahead of, within, and following the passage of the front showed considerable spatial variability in precipitation amount and composition (Hales, 1991).

The data of the above studies constitute a substantial mechanistic-diagnostic database for model evaluation. In addition to these research studies, a number of research-grade precipitation chemistry networks were also operated in the 1980s. They include the Canadian CAPMON, and the U.S. MAP3S and UAPSP, as well as the shorter-term EPRI-OEN and the EPA-ME35. Applications of the research network measurements for source-receptor pathway studies are discussed by Hales et al. (1987).

Jaffrezo and Colin (1988) studied the wet removal of trace elements in a year-long study in Paris. They reported their results in terms of the scavenging ratio, along with corresponding information from a number of earlier studies (Table 3-14). The scavenging coefficient and the scavenging ratio, in common use in the Lagrangian models of the 1970s, represent highly lumped representations of the complex of processes involved in wet removal. They are empirical entities which, by themselves, contain little mechanistic information. While reporting their measurements of scavenging ratio during a year-long study in Paris, Jaffrezo and Colin (1988) included a table (Table 3-14) which summarized not only their own data but also those of other earlier studies. The various results are not directly comparable owing, at least partly, to differences in measurement methods. Of particular interest in their study is the interpretation of elemental composition data. They were able to separate the measured elements into three groups which differed in terms of their solubility and also, by the mechanisms of their scavenging. The measured concentrations in precipitation and in air were nearly proportional for the insoluble species Al, Si, and Fe; this was interpreted to imply that their scavenging was mostly a local mechanism (below-cloud impaction). At the other extreme, the local concentrations of the very soluble species Na and Cl in the two phases were least correlated, indicating a more complex and progressive process of enrichment of one medium relative to the other (in-cloud processes). The remaining soluble species ($SO_4^=$, K, Ca, Zn, and Mg) showed an intermediate behavior. Earlier data at the same site of the relationship between scavenging ratio and particle mass median diameter (MMD), which showed a minimum in the scavenging ratio for MMD = 1 to 2 μm (reported as Figure 6-1), were judged to be supportive of the above interpretation.

TABLE 3-14. SCAVENGING RATIOS (Dimensionless)[a]

Reference	n	G.M.	Med. (1)	S.D.	A.M.	A.M. (2)	G.M. (3)	G.M. (4)	A.M. (5)	A.M. (6)	G.M. (7)	A.M. (8)	A.M. (9)	A.M. (10)
Cl	78	2,941	2,917	4.73	7,710	600	350	1,400				2,300	4,100	
S	82	743	753	1.98	940	700			1,000					370
Na	81	444	530	3.17	744	560	360	2,100				2,900	5,500	490
K	82	951	970	2.30	1,325	620	300	2,000		548				
Mg	81	596	682	2.39	816	850	400			457				
Ca	82	1,048	1,097	2.49	1,579	1,890	320	1,100		352		2,100		
Zn	69	767	707	2.65	1,226		790		820	179	612	1,050	1,030	
Al	82	291	283	2.72	459		580	1,300			756	620	430	
Si	82	373	405	2.35	533									
Fe	82	184	194	2.51	267		390	600		253	468	890	270	2
Ti	9	305		1.30	378									
Mn	7	146		1.36	171		250	2,100	3,600	370	756	760		

1. Jaffrezo and Colin (1988).
2. Harrison and Pio (1983).
3. Arimoto et al. (1985).
4. Buat-Menard and Duce (1986).
5. Lindberg (1982).
6. Gatz (1977).
7. Chan et al. (1986).
8. Peirson et al. (1973).
9. Cawse (1981).
10. Savoie et al. (1987).

[a]G.M.=Geometric mean.
A.M.=Arithmetic mean.
Med.=Median.
S.D.=Geometric standard deviation.
[b]Non-sea sulfate.

3.6.3 Overview of Sulfur Dioxide and Nitrogen Oxide Wet Scavenging

Hales (1991) has presented a useful overview of our understanding of SO_2 and NO_x wet scavenging based on field measurements which is very pertinent here, and is recapped below. SO_x: SO_2 is emitted principally from point sources. It is moderately soluble in water, and its solubility decreases with increasing acidity of the solution. It is not efficiently scavenged from concentrated fresh plumes, but this efficiency improves as the plumes dilute. It is essentially insoluble in ice and cold snows, but tends to be more efficiently scavenged by wet slushy snow and snows composed of graupel formed by rimming of supercooled cloud water. Only a small fraction of the SO_2 emission is removed as unreacted S(IV) which constitutes about 20% of S in precipitation in the eastern U.S. in sold seasons (significantly in the form of hydroxymethane sulfonate ions), and virtually none in summer (high acidity of droplets). Sulfate removal is also small from fresh plumes (not much there), but increases substantially with plume dilution as more is formed in the plume. It is scavenged efficiently by clouds and rain. Roughly 1/3 of the S emitted annually in North America is believed to be removed by precipitation.

NO_x: Point sources are a relatively smaller contributor of NO_x, but still quite substantial. Both NO and NO_2 have low solubility in water. Virtually no NO_x is removed from fresh plumes. HNO_3 formed by gas-phase oxidation of NO_2 is very soluble in water and is the principal source of NO_3^- in precipitation. NO_3, N_2O_5, and HO_2NO_2 are also believed to be significant intermediates. Since all of the intermediates are secondary products, NO_x scavenging increases with plume dilution and oxidation. Mesoscale studies show much variation in the efficiency of wet scavenging of SO_x and NO_x, depending on storm type and history of plume chemistry. About 1/3 of the anthropogenic NO_x emissions in the U.S. are estimated to be removed by wet deposition. The distinct seasonal character of SO_x wet deposition is absent in the case of NO_x wet deposition. Some likely reasons are as follows: HNO_3 has a strong affinity for ice as well as liquid water; its formation has no direct dependence on H_2O_2 which peaks in summer; and, there are mechanisms for the formation of HNO_3 in low winter sunlight.

3.7 PHYSICAL AND CHEMICAL CONSIDERATIONS IN SELECTING A SIZE CUT-POINT FOR SEPARATING FINE AND COARSE PARTICULATE MATTER

Particulate matter is not a single pollutant but a mixture of many classes of pollutants that differ in sources; formation mechanisms; composition; size; and chemical, physical and biological properties. One of the most fundamental divisions is the natural separation into a fine particle mode and a coarse particle mode as shown in Figure 3-6. (The term "fine" and "coarse" are used in this section to refer to particles in the fine or coarse particle distribution or modes. It is understood that the two distribution overlap between 1 and 3 μm aerodynamic diameter, D_{ae}. Fine is also used to refer to particles with a upper cut point of 3.5, 2.5, 2.1, or 1.0 μm D_{ae}. Coarse is also used to refer to particles between 2.5 and 10 μm D_{ae} or particles collected by the high volume samples as well as the entire coarse mode.) Some of the many differences between fine and coarse particles are summarized in Table 3-15. Because of these many differences it may be advantageous to treat fine and coarse PM as separate pollutants.

As will be discussed in Chapter 5, fine and coarse particles have different sources. Therefore, in order to devise a cost effective control program it is necessary to know, as a minimum, the relative amount of fine and coarse particles in order to know what types of sources to target for control. Source apportionment analysis, i.e., studies of particle composition and other properties to determine the contributions of specific types of sources, is most effective if fine and coarse particles are collected and analyzed separately.

Fine and coarse particles may be anticipated to have different biological properties as well as different physical and chemical properties. As discussed later in Chapters 10 through 13, many of the current hypotheses for health effects at PM concentration levels near or below the current standard are increasingly focusing attention on components of fine particles. Most of the particle strong acidity, sulfate, transition metals, toxic elements, and all of the ultrafine particles are found in the fine particle mode or distribution. On the other hand, much of the airborne biological material, such as pollen, mold spores and insect parts, are found in the coarse particle mode or distribution. Because of the potential for different types of biological effects from fine and coarse particles, it may be useful to separate out relative contributions of each to observed or projected health risks and to balance controls for one or both sizes/types of particles accordingly.

TABLE 3-15. COMPARISON OF AMBIENT FINE AND COARSE MODE PARTICLES

	Fine	Coarse
Formed from:	Gases	Large solids/droplets
Formed by:	Chemical reaction Nucleation Condensation Coagulation Evaporation of fog and cloud droplets in which gases have dissolved and reacted	Mechanical disruption (crushing, grinding, abrasion of surfaces, etc.) Evaporation of sprays Suspension of dusts
Composed of:	Sulfate, $SO_4^=$ Nitrate, NO_3^- Ammonium, NH_4^+ Hydrogen ion, H^+ Elemental carbon, Organic compounds (e.g., PAHs, PNAs) Metals, (e.g., Pb, Cd, V, Ni, Cu, Zn, Mn, Fe) Particle-bound water	Resuspended dust (Soil dust, street dust) Coal and oil fly ash Oxides of crustal elements, (Si, Al, Ti, Fe) $CaCO_3$, NaCl, sea salt Pollen, mold, fungal spores Plant/animal fragments Tire wear debris
Solubility:	Largely soluble, hygroscopic and deliquescent	Largely insoluble and non-hygroscopic
Sources:	Combustion of coal, oil, gasoline, diesel fuel, wood Atmospheric transformation products of NO_x, SO_2, and organic compounds including biogenic organic species, e.g., terpenes High temperature processes, smelters, steel mills, etc.	Resuspension of industrial dust and soil tracked onto roads and streets Suspension from disturbed soil, e.g., farming, mining, unpaved roads Biological sources Construction and demolition, coal and oil combustion, ocean spray
Atmospheric half-life:	Days to weeks	Minutes to hours
Travel distance:	100s to 1000s of km	<1 to 10s of km

Source: Adapted from Wilson and Suh (1996).

Considerations of the relationships between the concentrations measured at a control site and the personal exposure of individuals, discussed in detail in Chapter 7, suggest that a central site monitor may serve as a useful indicator of community exposure to fine particles. A central monitor is a poor indicator of exposure to coarse particles and other PM components with localized sources. Thus for epidemiological or personal exposure studies it will be useful to have separate measurements of fine and coarse particles.

Visibility degradation is due primarily to fine particles since particles with diameters near the wavelengths of visible light (0.4 to 0.7 μm) are much more effective in scattering light on a unit mass basis than larger particles (Chapter 8). On the other hand soiling is more closely related to coarse particles (Chapter 9). Again, these differences provide additional reasons to treat fine and coarse particles separately.

3.7.1 Background

In 1979 EPA scientists, in a paper entitled "Size Considerations for Establishing a Standard for Inhalable Particles" recommended that total suspended particulate matter (TSP), as defined by the high volume sampler, be replaced by the fraction obtained with a sampler having a precise upper cut-point (originally 15 μm D_{ae}, but later changed to 10 μm D_{ae}); and that "a second particle size cut-point of $\leq$ 2.5 μm D_{ae} be incorporated in the air sampling devices" (Miller et al., 1979). This study found that "the existence of a bimodal distribution with fine and coarse modes has been clearly demonstrated by.... mass-size distribution studies and by number distribution studies. These size distribution studies suggest 1 to 3 μm D_{ae} as the most appropriate range for a cut-point for fine and coarse aerosols. However, practical considerations of reducing plugging of impactor orifices indicate that 2.5 μm D_{ae} is a more appropriate cut-point, especially for particle size fractionating devices such as the dichotomous sampler" (Miller et al., 1979).

The cut-point of 2.5 μm D_{ae}, which has been used in many studies since 1979, was chosen not because it was ideal but because it was the smallest cut-point deemed feasible for a dichotomous sampler at that time. Current technology has demonstrated the feasibility of dichotomous samplers with cut-points at 1 μm D_{ae}, or even lower if desired. Impactor and cyclone technology can also be used for cut-points below 2.5 μm D_{ae}. Therefore, it is appropriate at this time to review existing data on size distribution of ambient aerosols so